The Structure of Quark Stars

Eirik Samuel Berge

Physics
Submission date: August 2013
Supervisor: Jens Oluf Andersen, IFY

Norwegian University of Science and Technology
Department of Physics

Acknowledgements

First of all, I would like to thank professor Jens Oluf Andersen for being an excellent supervisor, and for giving me such an interesting project to work on. I am grateful for the time and effort he has dedicated to me.

I would also like to thank my fellow students for constructive discussions and for making the years spent at NTNU terrific.

Last, but not least, I want to thank my fiancée Stine Dahlen for being so caring and supportive, and my one year old daughter Kine Dahlen Berge for smiling at me each morning.

Abstract

In this thesis we will study the structure of quark stars using different models to mimic the interactions of quantum chromodynamics (QCD). We will first derive the pressure, energy density and particle number density to one-loop for free Dirac fermions from the grand partition function. Then we will derive the Tolman-Oppenheimer-Volkoff equation, which is used to describe the structure of spherically symmetric and static stars.

We will first study quark stars in the MIT bag model, where we assume that deconfined strange quark matter is absolutely stable. The strange quark matter hypothesis will also be discussed in the chapter concerning the MIT bag model. The results show that the maximum mass of a quark star described using the MIT bag model ranges from $1.6 M_\odot$ to $2.0 M_\odot$, with $M_\odot$ being the solar mass, depending on the chosen bag constant.

The last models we study are the two- and three-flavour linear sigma models with quark degrees of freedom. We calculate the thermodynamical potential in these models and extract an effective, density dependent bag constant which we use as a replacement for the MIT bag constant. Both of these models lead to unphysical results and cannot be used to study the structure of quark stars near the surface. We conclude that the these models can only be used in high density regions inside hybrid stars. The maximum stars found in the three-flavour linear sigma model with quarks reach high enough densities for strange quarks to appear.

Table of Contents

List of Tables

List of Figures

Notation and conventions

- We will use natural units with $\hbar = c = k_B = 1$ throughout this thesis unless otherwise stated.

- In Minkowski space the metric is $\eta^{\mu\nu} = \mathrm{diag}(1, -1, -1, -1)$.

- Space vectors will be written in boldface $\mathbf{x}$. Space-time vectors will be written as x or x^{μ}.

- Einstein's sum convention is implied unless otherwise stated.

- The Feynman slash-notation is defined as $\slashed{A} \equiv \gamma^{\mu} A_{\mu}$.

Chapter 1

Introduction

The birth of stars begins in *nebulae*; large, dense clouds made mostly of hydrogen. Gravitational forces pulls regions of the cloud together and form protostars. The protostar will slowly heat up by particle collisions and gravitational energy transforming into kinetic energy. When the core of the protostar is hot enough to burn hydrogen to helium, the star will reach an equilibrium where the pressure arising from the hydrogen and helium fusion counterbalances the gravitational pressure. It has now become a main sequence star, and will stay this way for the main part of its lifespan. How long the star will live, and what it will turn into after its death is believed to be determined solely by the star's initial mass. A heavy star lives shorter than a light one. When a star dies it becomes a compact star or a black hole, depending on the mass of the core at the time of death. A light star, with a less massive core than the Chandrasekhar limit, $M \approx 1.44 M_{\odot}$, will become a *white dwarf*. More massive stars but lighter than about $3 M_{\odot}$ will become *neutron stars*, and the most massive stars will collapse into singularities, or *black holes*. In this thesis we will study a certain type of neutron stars called *quark stars*.

1.1 Neutron stars

Neutron stars are the second densest objects in the universe and are only beaten by black holes. The typical radius of a neutron star is $10 \, \text{km}$, and with a mass of about $1.5 M_{\odot}$ we get the extreme density $\rho \approx 7 \cdot 10^{11} \, \text{kg/cm}^3$. This is even larger than the typical density of a heavy atomic nucleus, $\rho_0 \approx 2.5 \cdot 10^{11} \, \text{kg/cm}^3$[1]. However, the density inside the star is not constant, but depends highly on the distance to the center. Due to this, some neutron stars are believed to have a core made of quark matter which is surrounded by nuclear matter. Such a star is called a hybrid star. Recent measurements of the pulsar[1] PSR J0348+043 indicates a mass of $2.01 \pm 0.04 M_{\odot}$ [2], which is the highest measured mass of a neutron star so far. The pulsar is in orbit with a white dwarf of mass $0.172 \pm 0.003 M_{\odot}$, which makes the measurements of the pulsar mass more accurate. The second most massive star

---

[1]A pulsar is a rotating neutron star with a strong magnetic field that emits a beam of electromagnetic radiation.

Figure 1.1: The Helix Nebula lies 650 light-years away and is a dying star which eventually will become a white dwarf. Credit: NASA, JPL-Caltech

with an accurate measured mass is PSR J1614-2230 with a mass of $1.97 \pm 0.04 M_\odot$ [3]. Both of these pulsars are strong candidates for hybrid stars, and have led to new studies of quark matter in compact stars [4, 5, 6].

Neutron stars are considered as cold objects and are often studied at zero temperature, even though their actual temperatures can be up to 10^{11} K [1]. This might seem like a daring approximation, but 10^{11} K ~ 10MeV in natural units where $k_B = 1$, and is therefore negligible compared to the baryon chemical potential which, due to the star's high density, is of the order 10^3 MeV. Neutron stars also constantly cools down during its lifespan as a consequence of neutrino radiation. The neutrinos are made in weak processes known as β-decay and inverse β-decay, or electron capture.

1.2 Quark stars

A neutron star is produced when the gravitational force is so strong that the electron degeneracy pressure coming from Pauli's exclusion principle is not enough to counterbalance the gravitational pressure, and hence electrons merge with protons to form neutrons. If the gravitational pressure is strong enough, the neutrons might even break down into their constituent up and down quarks. Such stars are hypothetical and known as quark stars or strange stars. The term strange star is used because some of the up and down quarks can be converted into strange quarks. However, this might not be the only way for quark stars to be produced. If a hypothesis called the *strange quark matter hypothesis* is true, quark stars might be formed by converting an ordinary neutron star into a pure quark star by injecting a *strangelet* into the neutron star. The strange quark matter hypothesis will be discussed in section 6.2.2.

Since quark stars are almost like gigantic hadrons, we will make use of both general relativity and quantum field theory (QFT) as well as statistical mechanics when studying them. Neutron stars usually also have a huge magnetic field with $B \sim 10^{12}$ G, so electrodynamics certainly plays a role too[1]. Even weak interactions must be included to achieve equilibrium in the star. Due to the wide range of fields needed to understand quark stars, we will make several assumptions and start with a very simple model of a quark star and gradually build our way up to more realistic models. We will, however, neglect the influence of the magnetic field throughout this thesis, and always work in the zero-temperature limit.

Preliminaries

2.1   Euler-Lagrange equation

From classical mechanics we remember the Lagrangian defined as $L = T - V$, where T and V are the kinetic energy and potential energy respectively. In field theory, the Lagrangian density $\mathcal{L}$ is a more useful quantity and is related to the Lagrangian L by

$$L = \int d^3x \, \mathcal{L}. \tag{2.1}$$

$\mathcal{L}(\phi, \partial_\mu \phi)$ is a funciton of the fields ϕ and their derivatives $\partial_\mu \phi$. Furthermore, the time-space integral of $\mathcal{L}$,

$$S \equiv \int d^4x \, \mathcal{L}, \tag{2.2}$$

is called the action and is the most fundamental quantity in classical field theory. Using the priciple of least action, we can derive the well known Euler-Lagrange equations of motion. This principle states that when a physical system evolves from one given state to another one it does so along the path that minimises the action. This is the same as saying that $\delta S = 0$ when δS is an infinitesimal change in the action arising from an infinitesimal change in the fields, $\phi \to \phi + \delta \phi$. Using this, we get constraints on the fields,

$$
\begin{aligned}
0 &= \delta S \\
&= \int d^4x \left[\frac{\partial \mathcal{L}}{\partial \phi} \delta \phi + \frac{\partial \mathcal{L}}{\partial(\partial_\mu \phi)} \delta(\partial_\mu \phi) \right] \\
&= \int d^4x \left[\frac{\partial \mathcal{L}}{\partial \phi} \delta \phi - \partial_\mu \left(\frac{\partial \mathcal{L}}{\partial(\partial_\mu \phi)} \right) \delta \phi + \partial_\mu \left(\frac{\partial \mathcal{L}}{\partial(\partial_\mu \phi)} \delta \phi \right) \right] \\
&= \int d^4x \left[\frac{\partial \mathcal{L}}{\partial \phi} - \partial_\mu \left(\frac{\partial \mathcal{L}}{\partial(\partial_\mu \phi)} \right) \right] \delta \phi + \int_\Omega dS \, n_\mu \left[\left(\frac{\partial \mathcal{L}}{\partial(\partial_\mu \phi)} \delta \phi \right) \right].
\end{aligned} \tag{2.3}
$$

In the last line we used the divergence theorem to rewrite the volume integral to a surface integral over the surface Ω. The last term of this equation vanishes due to the fact that

$\delta\phi = 0$ on the surface of the time-space region. We know that $\delta\phi(\Omega) = 0$ because the initial and the final states are known. As $\delta\phi$ generally is different from zero when the system is in a state between the inital and final states, the only way for eq. (2.3) to hold is if

$$\frac{\partial \mathcal{L}}{\partial \phi} - \partial_\mu \left(\frac{\partial \mathcal{L}}{\partial(\partial_\mu \phi)} \right) = 0. \tag{2.4}$$

This is the Euler-Lagrange equations of motion.

2.2 Noether's theorem

Noether's theorem states that for every continuous symmetry in the Lagrangian there exists a corresponding conserved current [7]. A continuous transformation on the fields ϕ can be written in infinitesimal form as

$$\phi(x) \to \tilde{\phi}(x) = \phi(x) + \alpha\Delta\phi(x), \tag{2.5}$$

where α is some infinitesimal parameter and $\Delta\phi$ is some deformation of the field configuration. If the equations of motion are invariant under this transformation, we have a symmetry. This is the same as requiring that the Lagrangian is invariant under the transformation (2.5) up to a 4-divergence, because such a surface term will vanish in the action and leave the Euler-Lagrange equation invariant,

$$\mathcal{L} \to \mathcal{L} + \alpha\partial_\mu \mathcal{J}^\mu. \tag{2.6}$$

We can now perform the transformation (2.5) on the Lagrangian and compare the result with eq. (2.6),

$$\begin{aligned}
\mathcal{L}(\tilde{\phi}, \partial_\mu \tilde{\phi}) =& \mathcal{L}(\phi, \partial_\mu \phi) + \frac{\partial \mathcal{L}}{\partial \phi}(\alpha\Delta\phi) + \frac{\partial \mathcal{L}}{\partial(\partial_\mu \phi)}\partial_\mu(\alpha\Delta\phi) \\
=& \mathcal{L}(\phi, \partial_\mu \phi) + \alpha\partial_\mu \left(\frac{\partial \mathcal{L}}{\partial(\partial_\mu \phi)}\Delta\phi \right) + \alpha \left[\frac{\partial \mathcal{L}}{\partial \phi} - \partial_\mu \left(\frac{\partial \mathcal{L}}{\partial(\partial_\mu \phi)} \right) \right] \Delta\phi.
\end{aligned} \tag{2.7}$$

The third term is the Euler-Lagrange equation and is consequently zero. If we have a symmetry we therefore must have

$$\partial_\mu j^\mu(x) \equiv \partial_\mu \left[\left(\frac{\partial \mathcal{L}}{\partial(\partial_\mu \phi)}\Delta\phi \right) - \mathcal{J}^\mu \right] = 0. \tag{2.8}$$

This equation states that j^μ is a conserved current. Moreover, integrating this equations over $\mathbf{x}$ yelds

$$\int d^3x \left[\partial_0 j^0 - \boldsymbol{\nabla} \cdot \mathbf{j} \right] = 0, \tag{2.9}$$

which by the divergence theorem gives

$$\partial_0 \int d^3x \, j^0 = \int_\Omega dS \, \mathbf{n} \cdot \mathbf{j}. \tag{2.10}$$

In the limit $\mathbf{x} \to \infty$ we must have $\mathbf{j} \to 0$ as the current must be zero at infinity. Hence, the total charge

$$Q = \int j^0 d^3 x, \tag{2.11}$$

must be constant in time.

2.3 Grassmann numbers

Later in this thesis we will deal with fermionic fields. These fields anticommute and will therefore make some integrals impossible to calculate using real, commuting numbers. To calculate such integrals, we must represent these fields by anticommuting numbers known as Grassmann numbers. The fundamental feature of Grassmann numbers is of course that they anticommute, so for any two Grassmann numbers η and θ, we have

$$\eta\theta = -\theta\eta. \tag{2.12}$$

This implies that the square of a Grassmann number is zero, and the product of two such numbers will commute with another anticommuting number, ξ

$$\eta^2 = 0, \quad (\eta\theta)\xi = \xi(\eta\theta). \tag{2.13}$$

The integral of a general function f of a Grassmann variable η is defined as

$$\int d\eta f(\eta) = \int d\eta (A + B\eta). \tag{2.14}$$

Here we used that $f(\eta)$ can be expanded in a Taylor series and the only terms surviving is of order η or less according to eq. (2.13). We will demand that integrals over Grassmann numbers should be invariant under shifts of the integration variable, in the same way as ordinary functional integrals. If we now let $\eta \to \eta + \theta$ we get the condition

$$\int d\eta (A + B\eta) = \int d\eta (A + B\theta + B\eta). \tag{2.15}$$

As the linear term $B\eta$ is left unchanged and the constant term changed, we know that the integrals cannot depend on the constant term, but must be equal to B (times a constant which we set to 1),

$$\int d\eta (A + B\eta) = B. \tag{2.16}$$

So far we have only looked at integration over a single variable. If we deal with more than one integration variable, we must choose which integral we should perform first. The common convention for this is choosing

$$\int d\eta \int d\theta \, \theta\eta = \int d\eta \, d\theta \, (\theta\eta) = +1, \tag{2.17}$$

i.e. computing the inner integral first. When we start working with complex fermionic fields, we also need complex Grassmann numbers. We will define the complex conjugate of a product of Grassmann numbers to reverse the order of the product,

$$(\eta\theta)^* = \theta^*\eta^*. \tag{2.18}$$

To make sure that η and η^* are independent numbers, which must be the case if we integrate over both, we can define

$$\eta = \frac{\eta_1 + i\eta_2}{\sqrt{2}}, \quad \eta^* = \frac{\eta_1 - i\eta_2}{\sqrt{2}}. \tag{2.19}$$

Later we will encounter Gaussian integrals over complex fermionic fields. We will therefore investigate how such integrals are evaluated over complex Grassmann variables:

$$\int d\eta^* d\eta\, e^{-\eta^* a\eta} = \int d\eta^* d\eta\,(1 - \eta^* a\eta) = \int d\eta^* d\eta\,(1 + \eta\eta^* a) = a. \tag{2.20}$$

In the first equality we expanded the exponential and used $\eta^2 = 0$. The last equality is found by combining eqs. (2.16) and (2.17). We now generalise the integral to $2N$ variables and change a into an $N \times N$ Hermitian matrix A,

$$\prod_{i=1}^{N} \int d\eta_i^* d\eta_i\, e^{-\eta^* A\eta}. \tag{2.21}$$

η and η^* are now of course vectors with lenght N. As A is a Hermitian matrix it can be diagonalised, $A = U^\dagger \Lambda U$, and we can rewrite $\eta^* A\eta$ in terms of new, transformed Grassmann variables $\xi = U\eta$ and $\xi^* = \eta^* U^\dagger$:

$$\eta^* A\eta = \eta^* U^\dagger \Lambda U\eta = \xi^* U^\dagger U \Lambda U U^\dagger \xi \tag{2.22}$$
$$= \xi^* \Lambda \xi = \sum_i \xi_i^* \lambda_i \xi_i.$$

Here U is a unitary matrix composed of the eigenvectors of A as columns and $\Lambda_{ij} = \delta_{ij}\lambda_i$ (no summation over i here) is a diagonal matrix with the eigenvalues of A on the diagonal. The integrand in (2.21) expressed in the new variables is thus

$$e^{-\eta^* A\eta} = \prod_i e^{-\xi_i^* \lambda_i \xi_i} = \prod_i (1 - \xi_i^* \lambda_i \xi_i). \tag{2.23}$$

Now that we have rewritten the integrand, we must investigate how the integral changes under this unitary transformation. We have

$$\prod_{i=1}^{N} \eta_i = \frac{1}{N!}\epsilon^{ij\ldots k}\eta_i \eta_j \cdots \eta_k$$
$$= \frac{1}{N!}\epsilon^{ij\ldots k}U_{ii'}^\dagger \xi_{i'} U_{jj'}^\dagger \xi_{j'} \cdots U_{kk'}^\dagger \xi_{k'}$$
$$= \frac{1}{N!}\epsilon^{ij\ldots k}U_{ii'}^\dagger U_{jj'}^\dagger \cdots U_{k'}^\dagger \xi_{i'}\xi_{j'} \cdots \xi_{k'}, \tag{2.24}$$

and

$$\xi_{i'}\xi_{j'}\cdots\xi_{k'} = \epsilon^{i'j'\ldots k'}\prod_{i=1}^{N}\xi_i. \tag{2.25}$$

By using that

$$\det U^{\dagger} = \epsilon^{ij\ldots k}U_{1i}^{\dagger}U_{2j}^{\dagger}\cdots U_{Nk}^{\dagger}, \tag{2.26}$$

where we sum over all the indicies $i, j, ..., k$ from 1 to N, we find

$$\prod_{i=1}^{N}\eta_i = \frac{1}{N!}N!\det U^{\dagger}\prod_{i=1}^{N}\xi_i$$

$$= \det U^{\dagger}\prod_{i=1}^{N}\xi_i. \tag{2.27}$$

Following the same procedure we get[1]

$$\prod_{i=1}^{N}\eta_i^* = \det U\prod_{i=1}^{N}\xi_i^*. \tag{2.28}$$

We are now finally ready to calculate the integral (2.21):

$$\prod_{i}\int d\eta_i^* d\eta_i\, e^{-\eta^* A\eta} = \det U \det U^{\dagger}\prod_{i}\int d\xi_i^* d\xi_i\prod_{k}(1 + \lambda_k\xi_k\xi_k^*)$$

$$= \prod_{k}\lambda_k = \det A. \tag{2.29}$$

This result will be useful when calculating the partition function for an ideal gas of free fermions.

2.4 Path integral formalism

A fundamental task in quantum physics is to find the probability for a particle at position q_i at time t_i to be at position q_f at time t_f. From quantum mechanics we know that the answer to this is the transition amplitude

$$\langle q_f|\, e^{-iHT}\, |q_i\rangle, \tag{2.30}$$

where H is the hamiltonian and $T = t_f - t_i$ is the time it takes for the particle to move from its inital position to its final position. We are intrested in an integral form of this amplitude, so let us start by dividing the time T into N infinitesimal time intervals δt. Furthermore, we require that our states are normalised, $\langle q_f|\, q_i\rangle = \delta(q_f - q_i)$, where $\delta(x)$ is the Dirac

---

[1]The eqs. (2.27) and (2.28) actually shows that any functional integral over Grassmann numbers is invariant under unitary transformations: A general integrand $f(\eta)$ can be expressed as $\prod_i \eta_i \prod_i \eta_i^*$ which after the transformation gives rise to a factor $(\det U)(\det U^{\dagger}) = 1$ and transforms the variables $\eta_i \rightarrow \xi_i$. But since $\prod_i d\eta_i^* d\eta_i$ transform accordingly, the integral is unchanged.

delta function, and that $|q_a\rangle$ form a complete set of states, i.e. that $\int dq_a\,|q_a\rangle\langle q_a| = 1$. Our amplitude now reads

$$\langle q_f|\,\mathrm{e}^{-iHT}\,|q_i\rangle = \prod_{j=1}^{N-1}\int dq_j\,\langle q_f|\,\mathrm{e}^{-iH\delta t}\,|q_{N-1}\rangle$$

$$\times\,\langle q_{N-1}|\,\mathrm{e}^{-iH\delta t}\,|q_{N-2}\rangle\cdots\langle q_2|\,\mathrm{e}^{-iH\delta t}\,|q_1\rangle\langle q_1|\,\mathrm{e}^{-iH\delta t}\,|q_i\rangle. \quad (2.31)$$

Since δt is small, we can expand the exponentials to first order in δt, so that a single factor $\langle q_{j+1}|\,\mathrm{e}^{-iH\delta t}\,|q_j\rangle$ becomes

$$\langle q_{j+1}|\,\mathrm{e}^{-iH\delta t}\,|q_j\rangle = \langle q_{j+1}|\,q_j\rangle - i\delta t\,\langle q_{j+1}|\,H\,|q_j\rangle + \mathcal{O}(\delta t^2). \quad (2.32)$$

The first term is a delta function and can be rewritten as an integral:

$$\langle q_{j+1}|\,q_j\rangle = \int\frac{dp_j}{2\pi}\,\mathrm{e}^{ip_j(q_{j+1}-q_j)}. \quad (2.33)$$

The second term can be manipulated by inserting momentum eigenstates on the form $\int\frac{dp_j}{2\pi}\,|p_j\rangle\langle p_j| = 1$ and using $H = \frac{\hat{p}^2}{2m} - V(\hat{q})$:[2]

$$\langle q_{j+1}|\,H\,|q_j\rangle = \langle q_{j+1}|\int\frac{dp_j}{2\pi}\,|p_j\rangle\langle p_j|\left(\frac{\hat{p}^2}{2m} - V(\hat{q})\right)|q_j\rangle$$

$$= \int\frac{dp_j}{2\pi}\left(\frac{p_j^2}{2m} - V(q_j)\right)\langle q_{j+1}|\,p_j\rangle\langle p_j|\,q_j\rangle. \quad (2.34)$$

From quantum mechanics we know that the momentum eigenstate in the coordinate representation is a plane wave, that is $\langle q|\,p\rangle = \mathrm{e}^{ipq}$, so the product of bra-kets in the last line equals $\mathrm{e}^{ip_j(q_{j+1}-q_j)}$. Combining eqs. (2.33) and (2.34) we find

$$\langle q_{j+1}|\,\mathrm{e}^{-iH\delta t}\,|q_j\rangle = \int\frac{dp_j}{2\pi}\left[1 - i\delta t\left(\frac{p_j^2}{2m} - V(q_j)\right)\right]\mathrm{e}^{ip_j(q_{j+1}-q_j)} + \mathcal{O}(\delta t^2)$$

$$= \int\frac{dp_j}{2\pi}\,\mathrm{e}^{-i\delta t\left(p_j^2/2m - V(q_j)\right)}\mathrm{e}^{ip_j(q_{j+1}-q_j)} + \mathcal{O}(\delta t^2). \quad (2.35)$$

As we only write out δt to first order, we rewrote the parenthesis as an exponential. Next, we can simplify the rightmost exponential by setting $\Delta q_j = (q_{j+1} - q_j)/\delta t$:

$$\langle q_{j+1}|\,\mathrm{e}^{-iH\delta t}\,|q_j\rangle = \int\frac{dp_j}{2\pi}\,\mathrm{e}^{-i\delta t H(p_j,q_j)}\mathrm{e}^{i\delta t p_j\Delta q_j} + \mathcal{O}(\delta t^2). \quad (2.36)$$

The amplitude (2.31) now becomes

$$\langle q_f|\,\mathrm{e}^{-iHT}\,|q_i\rangle = \int\prod_{j=1}^{N-1}\frac{dq_j dp_j}{2\pi}dp_0\,\exp\left[\sum_{k=0}^{N-1}i\delta t[p_k\Delta q_k - H(p_k,q_k)]\right]$$

$$+\,\mathcal{O}(\delta t^2). \quad (2.37)$$

---

[2]Note the difference in inserting this factor of 1 left or right of H. If we inserted the integral before H we would get $V(q_{j+1})$ instead of $V(q_j)$. The difference of these two cases will however vanish when we take the continuum limit $N\to\infty$.

Now we take the continuum limit $N \to \infty$. The integral is then over all functions $q(t)$ and $p(t)$ that satisfy the boundary conditions. This can be written more elegantly by defining

$$\int \prod_{j=1}^{N-1} \frac{dq_j dp_j}{2\pi} dp_0 \equiv \int \mathcal{D}q \mathcal{D}p. \tag{2.38}$$

Moreover, we get $\sum_{k=0}^{N-1} \delta t \to \int_{t_i}^{t_f} dt$ and $\Delta q \to \dot{q}$. Eq. (2.37) now reduces to

$$\langle q_f | e^{-iHT} | q_i \rangle = \int \mathcal{D}q \mathcal{D}p \, \exp\left\{ i \int_{t_i}^{t_f} dt \, [p\dot{q} - H(p,q)] \right\}. \tag{2.39}$$

We can calculate the integral over $\mathcal{D}p$ using [15]

$$\int \frac{dp}{2\pi} e^{i\delta t(p\dot{q} - p^2/2m)} = \left(\frac{m}{2\pi i \delta t} \right)^{1/2} e^{i\delta t m \dot{q}^2/2}. \tag{2.40}$$

Since we have N such integrals, we get a total factor $\left(\frac{m}{2\pi i \delta t} \right)^{N/2}$, which we just absorb into $\mathcal{D}q$. The amplitude finally takes the form

$$\langle q_f | e^{-iHT} | q_i \rangle = \int \mathcal{D}q \, e^{i \int_{t_i}^{t_f} dt \, [\frac{1}{2} m \dot{q}^2 - V(q)]} = \int \mathcal{D}q \, e^{i \int_{t_i}^{t_f} dt \, L(q, \dot{q})}$$

$$= \int \mathcal{D}q \, e^{iS[q]}. \tag{2.41}$$

This is the path integral in quantum mechanics. In *quantum field theory* (QFT), the particles are not described as point particles at position $q(t)$, but insead as fields $\varphi(x) = \varphi(t, \mathbf{x})$. The action S is now, as mentioned in section 2.1, the space-time integral of the Lagrangian density $\mathcal{L}$, which in D spatial dimensions becomes

$$S[\varphi] = \int dt \int d^D x \, \mathcal{L}(\varphi, \partial_\mu \varphi). \tag{2.42}$$

$\mathcal{L}(\varphi, \partial_\mu \varphi)$ is the field theoretical analogue to the quantum mechanical Lagrangian $L(q, \dot{q})$, and the path integral in QFT simply becomes

$$Z \equiv \int \mathcal{D}\varphi \, e^{iS[\varphi]} = \int \mathcal{D}\varphi \, e^{i \int d^d x \, \mathcal{L}(\varphi, \partial_\mu \varphi)}. \tag{2.43}$$

In the next chapter we will make use of this result when deriving the path integral representation of the grand canonical partition function.

Chapter 3

Thermodynamics

In our study of quark stars, we need to know some thermodynamical quantities such as the pressure, energy density and particle density. The relation between the pressure and the energy density, known as the equation of state (EoS), is especially important. Why the EoS is so crucial will be clear when we study the Tolman-Oppenheimer-Volkoff (TOV) equation in chapter 5. These thermodynamical quantities can be found if we know the grand canonical partition function $\mathcal{Z}$ (from now on simply referred to as the partition function), which is a function used to describe a system in thermodynamical equilibrium. Actually, every thermodynamical quantity can be derived from $\mathcal{Z}$. This makes the partition function the most fundamental quantity in equilibrium statistical mechanics.

3.1 The grand canonical partition function

Assume that we have a system with a constant volume V which can exchange energy E and particles N with a heat reservoir at constant temperature T. This system can then be described as a *grand canonical ensemble*, and the partition function describing the system is [10]

$$\mathcal{Z} = \mathrm{Tr}\, \mathrm{e}^{-\beta(H - \mu_i \hat{Q}_i)}. \tag{3.1}$$

Here H is the Hamiltonian, $\beta = 1/T$ is the inverse temperature and μ_i is the chemical potential corresponging to the conserved charge Q_i. In principle, Q_i can be any conserved charge that is Hermitian and commutes with H and Q_j, and not only the particle number like here. This is the quantum mechanical version of the partition function. However, we will use a field theoretical approach and use the path integral formalism to calculate the thermodynamical functions we need. We can start by rewriting eq. (3.1), replacing the trace with a sum over states:

$$\mathcal{Z} = \sum_n \langle n | \mathrm{e}^{-\beta(H - \mu_i \hat{Q}_i)} | n \rangle. \tag{3.2}$$

Comparing this equation to eq. (2.41) in the previous section, we see that the partition function is very similar to the transition amplitude in quantum mechanics. If we absorb

$\mu_i \hat{Q}_i$ into H and set $\beta = iT$ (here T is time, and not temperature), the exponentials in the two expressions are identical. Let us see what happens with eq. (2.41) if we set the initial and final states equal and *Wick rotate* the integration contour, i.e. change the time t to imaginary time $\tau = it$. We also for simplicity set $t_i = 0$ and $t_f = T = -i\beta$, implying that τ ranges from 0 to β:

$$\langle n | e^{-iHT} | n \rangle = \int\limits_{q(0)=q(\beta)} \mathcal{D}q \, \exp\left\{ \int_0^\beta d\tau \left[-\frac{1}{2} m \left(\frac{dq}{d\tau} \right)^2 - V(q) \right] \right\}$$

$$= \int\limits_{q(0)=q(\beta)} \mathcal{D}q \, \exp\left\{ -\int_0^\beta d\tau \, L_E(q, \dot{q}) \right\}. \tag{3.3}$$

Here L_E is the Euclidean Lagrangian corresponding to the Hamiltonian H in Euclidean time τ. The boundary conditions $q(0) = q(\beta)$ appears because we require the particle to return to its initial state after a time β when $|q_i\rangle = |q_f\rangle = |n\rangle$. The only difference between eq. (3.2) and eq. (3.3) is now the sum over n, which simply means that we have a set of particles and need to integrate over all paths $q_a(t)$ for every particle a. We are now ready to write down the path integral version of the partition function in field theory. The result is as follows:

$$\mathcal{Z} = \int\limits_{BC} \mathcal{D}\varphi \, e^{-\int_0^\beta d\tau \int d^D x \, \mathcal{L}_E(\varphi)}. \tag{3.4}$$

BC is the Boundary Conditions, which are periodic, $\varphi(x, 0) = \varphi(x, \beta)$, for bosons and antiperiodic, $\varphi(x, 0) = -\varphi(x, \beta)$, for fermions, see appendix A.1. The integral is written in compact notation; φ is a collection of all the fields present, so $\mathcal{D}\varphi = \mathcal{D}\varphi_1 \mathcal{D}\varphi_2 \cdots \mathcal{D}\varphi_n$ and $\mathcal{L}_E(\varphi)$ is a function of all the fields φ_a. $\mathcal{L}_E$ is the Euclidean Lagrangian density corresponding to the shifted hamiltonian density $\mathcal{H} = \mathcal{H}_0 - \mu_i \rho_i$ given by

$$\mathcal{H} = \pi_i \dot{\varphi}^i - \mathcal{L}_0 - \mu_i \rho_i = \frac{\partial \mathcal{L}_0}{\partial \dot{\varphi}^i} \dot{\varphi}^i - \mathcal{L}_0 - \mu_i \rho_i. \tag{3.5}$$

Here, ρ_i is the conserved charge density corresponding to j^0 in eq. (2.11). We sum over repeated indices, so if the Lagrangian depends on more than one field, we get seperate contributions from each field φ^i. Eq. (3.4) will be our starting point for calculating the thermodynamical functions in the next chapter.

3.2 Relations between $\mathcal{Z}$ and thermodynamical quantities

We will not derive the relations between the different thermodynamical functions and the partition function. For a detailed derivation of these, see [8]. The functions we need when studying a quark star is the pressure p, the energy density ϵ and the number density ρ.

These functions are given by the following expressions in the infinite volume limit:

$$p = \frac{1}{\beta} \frac{\partial \ln \mathcal{Z}}{\partial V}, \tag{3.6}$$

$$\rho = \frac{1}{\beta V} \frac{\partial \ln \mathcal{Z}}{\partial \mu}, \tag{3.7}$$

$$S = \frac{\partial (T \ln \mathcal{Z})}{\partial T}, \tag{3.8}$$

$$\epsilon = \mu \rho + TS - \frac{1}{V} \frac{\partial \ln \mathcal{Z}}{\partial \beta}, \tag{3.9}$$

$$\Omega = - \int p \, dV. \tag{3.10}$$

$\beta = 1/T$ is again the inverse temperature, μ is the chemical potential, S is the entropy and Ω is the Landau potential. In the introduction we mentioned that we would model the quark star as zero temperature objects. In the next chapter, when we calculate the pressure etc. from an ideal Fermi gas, we will take the zero-temperature limit and obtain the results for a cold quark star of finite chemical potential.

Ideal Fermi gas

Our first model of a quark star will be very simple. We will neglect any interactions between the quarks and describe the quark star using the EoS for a free gas of fermions at $T = 0$. In this chapter we will calculate the thermodynamical quantities we need to study the star within this model. We are especially interested in the pressure p, the energy density ϵ and the particle density ρ. With these three functions alone, we can to a great extent determine the structure of a quark star.

4.1   The partition function

As the partition function $\mathcal{Z}$ can be used to calculate all the thermodynamical quantities we need, we will in this section find $\mathcal{Z}$ for an ideal gas of fermions. To do so, we see from the path integral version of the partition function, eq. (3.4), that we need to know the Euclidean Lagrangian for this system. The Lagrangian for free Dirac fermions[1] is

$$\mathcal{L}_0 = \bar{\psi} \left(i \slashed{\partial} - m \right) \psi. \tag{4.1}$$

ψ and $\bar{\psi} = \psi^\dagger \gamma^0$ are treated as independent variables, and thus yields one corresponding equation of motion each.

$\mathcal{L}_0$ is invariant under the global phase transformation

$$\psi \to \mathrm{e}^{i\alpha} \psi \tag{4.2a}$$

$$\bar{\psi} \to \mathrm{e}^{-i\alpha} \bar{\psi}, \tag{4.2b}$$

where α is a constant in the interval $[0, 2\pi)$. This is a U(1) symmetry, which according to Noether's theorem gives rise to a conserved quantity. The conserved quantity can be found

---

[1] A *Dirac* fermion is simply a fermion which is not its own antiparticle. So all fermions in the standard model except possibly the neutrinos are Dirac fermions. Fermions that are their own antiparticle are called Majorana fermions after Ettore Majorana. Dark matter have also recently been hypothesised as a Majorana fermion [11].

from eq. (2.8) with $\mathcal{J}^\mu = 0$,

$$\partial_\mu j^\mu = \partial_\mu \left(\frac{\partial \mathcal{L}_0}{\partial(\partial_\mu \psi^i)} \Delta \psi^i \right) = 0. \tag{4.3}$$

As there are no terms like $\partial_\mu \bar{\psi}$ in $\mathcal{L}_0$, the only contribution to j^μ comes from ψ. Now, using $\Delta \psi = i\alpha \psi$ for small α, we get

$$j^\mu = \bar{\psi} \gamma^\mu \psi. \tag{4.4}$$

As mentioned in the previous chapter, the conserved charge density is the zeroth component of j^μ. With $\rho = \bar{\psi} \gamma^0 \psi$, we can now calculate the Hamiltonian density from eqs. (3.5) and (4.1):

$$\mathcal{H} = \bar{\psi} \left(i\gamma^i \partial_i + m - \mu \gamma^0 \right) \psi. \tag{4.5}$$

It is easy to check that the Lagrangian density corresponding to this Hamiltonian density is $\mathcal{L}_0 + \bar{\psi} \mu \gamma^0 \psi$,

$$\mathcal{L} = \bar{\psi} \left(i\gamma^\mu \partial_\mu - m + \mu \gamma^0 \right) \psi. \tag{4.6}$$

This Lagrangian is in Minkowski space, but the Lagrangian in eq. (3.4) is as mentioned earlier the Euclidean Lagrangian. We must therefore perform a Wick rotation on $\mathcal{L}$, i.e. switch to imaginary time:

$$\mathcal{L}_E(\tau) = -\mathcal{L}(t \to -i\tau) = \bar{\psi} \left(\gamma^0 \partial_\tau - i\gamma^i \partial_i + m - \mu \gamma^0 \right) \psi. \tag{4.7}$$

Inserting this expression into (3.4) we get

$$\mathcal{Z} = \int_{BC} \mathcal{D}\bar{\psi} \mathcal{D}\psi \, e^{- \int_0^\beta d\tau \int d^3x \, \bar{\psi} \left(-\gamma^0 \partial_\tau + i\gamma^i \partial_i - m + \mu \gamma^0 \right) \psi}. \tag{4.8}$$

As $\bar{\psi}$ and ψ are fermion fields, the boundary conditions are antiperiodic,

$$\psi(0, \mathbf{x}) = -\psi(\beta, \mathbf{x}) \tag{4.9a}$$

$$\bar{\psi}(0, \mathbf{x}) = -\bar{\psi}(\beta, \mathbf{x}). \tag{4.9b}$$

The integral is easier to solve in $(\omega_n, \mathbf{p},)$ space than in $(\tau, \mathbf{x})$ space, so we Fourier transform the fields and write

$$\psi(\mathbf{x}, \tau) = \frac{1}{\sqrt{V}} \sum_{n=-\infty}^{\infty} \sum_{\mathbf{p}} e^{i(\mathbf{p} \cdot \mathbf{x} + \omega_n \tau)} \tilde{\psi}(\mathbf{p}). \tag{4.10}$$

ω_n are the Matsubara frequencies and must be equal $(2n+1)\pi T$ since the conditions in (4.9) must hold for all $\mathbf{x}$. After this transformation we can make the replacement

$$\bar{\psi} \left(-\gamma^0 \partial_\tau + i\gamma^i \partial_i - m + \mu \gamma^0 \right) \psi \to \bar{\psi} \left(-i\gamma^0 \omega_n - \boldsymbol{\gamma} \cdot \mathbf{p} - m + \mu \gamma^0 \right) \psi. \tag{4.11}$$

Now the exponentials in $\bar{\psi}$ and ψ will cancel so that all the $\mathbf{x}$ and τ dependence vanish. The integral over τ and $\mathbf{x}$ is then trivial and contributes with a factor βV. We are thus left with[2]

$$\mathcal{Z} = \prod_{n,\mathbf{p}} \int_{BC} \mathcal{D}\bar{\psi}\mathcal{D}\psi \, e^{\bar{\psi}D\psi}, \tag{4.12}$$

where

$$D = -\beta\gamma^0 \left(\mu - i\omega_n - \gamma^0\boldsymbol{\gamma}\cdot\mathbf{p} - m\gamma^0\right). \tag{4.13}$$

As free fermionic fields anticommute due to the Pauli exclusion principle, we can treat $\bar{\psi}$ and ψ as Grassmann variables. The integral in eq. (4.12) is then a Gaussian integral over Grassman variables, which we discussed in section 2.3. This is actually the same integral as in eq. (2.29), so we find

$$\mathcal{Z} = \prod_{n,\mathbf{p}} \det D. \tag{4.14}$$

The thermodynamical functions are related to the partition function through $\ln \mathcal{Z}$,

$$\ln \mathcal{Z} = \sum_{n,\mathbf{p}} \ln \det \left[-\beta \left(\mu - i\omega_n - \gamma^0\boldsymbol{\gamma}\cdot\mathbf{p} - m\gamma^0\right)\right]. \tag{4.15}$$

Using the Dirac representation of the γ matrices, we have

$$\gamma^0 = \begin{pmatrix} I & 0 \\ 0 & -I \end{pmatrix}, \tag{4.16}$$

$$\gamma^0\boldsymbol{\gamma}\cdot\mathbf{p} = \begin{pmatrix} 0 & \boldsymbol{\sigma}\cdot\mathbf{p} \\ \boldsymbol{\sigma}\cdot\mathbf{p} & 0 \end{pmatrix}, \tag{4.17}$$

where $\boldsymbol{\sigma} = (\sigma_1, \sigma_2, \sigma_3)$ denote the Pauli matrices. Each element in the matrices are thus 2×2-matrices themselves. The matrix D written out explicitly is

$$D = -\beta \begin{pmatrix} \mu - i\omega_n - m & -\boldsymbol{\sigma}\cdot\mathbf{p} \\ \boldsymbol{\sigma}\cdot\mathbf{p} & -\mu + i\omega_n - m \end{pmatrix}. \tag{4.18}$$

The determinant can be evaluated in the same way as the determinant of a 2×2-matrix, but here we must square the result since each elements counts twice,

$$\det D = \beta^4 \left\{-(\mu - i\omega_n)^2 + m^2 + \det\left[(\boldsymbol{\sigma}\cdot\mathbf{p})^2\right]\right\}^2. \tag{4.19}$$

Using the anticommutation relation for the Pauli-matrices, $\{\sigma_i, \sigma_j\} = 2\delta_{ij}I$, we get

$$(\boldsymbol{\sigma}\cdot\mathbf{p})^2 = p_i\sigma_i p_j\sigma_j = (2\delta_{ij}I - \sigma_j\sigma_i)p_i p_j = 2\mathbf{p}^2 - (\boldsymbol{\sigma}\cdot\mathbf{p})^2$$

$$\Rightarrow (\boldsymbol{\sigma}\cdot\mathbf{p})^2 = \mathbf{p}^2 \tag{4.20}$$

---

[2]Here ψ and $\bar{\psi}$ are the Fourier transformed fields $\tilde{\psi}(\mathbf{p})$ and $\tilde{\bar{\psi}}(\mathbf{p})$ respectively.

Now we insert eqs. (4.19) and (4.20) into eq. (4.15) and set $m^2 + \mathbf{p}^2 = E_p^2$:

$$
\begin{aligned}
\ln \mathcal{Z} &= \sum_{n,\mathbf{p}} \ln \left\{ \beta^4 \left[(\mu - i\omega_n)^2 - E_p^2 \right]^2 \right\} \\
&= 2 \sum_{n,\mathbf{p}} \ln \left[\beta^2 (\mu - i\omega_n + E_p)(\mu - i\omega_n - E_p) \right] \\
&= 2 \sum_{n,\mathbf{p}} \ln \left[\beta(\mu - i\omega_n + E_p) \right] + \ln \left[\beta(\mu - i\omega_n - E_p) \right].
\end{aligned}
\tag{4.21}
$$

This expression can be further rewritten, using that $\sum_n \omega_n = \sum_n (-\omega_n)$ because $\omega_n = (2n+1)\pi T$ and the sum over n goes from $-\infty$ to $+\infty$:

$$
\begin{aligned}
2 \sum_{n=-\infty}^{\infty} \ln \left[\beta(\mu - i\omega_n \pm E_p) \right] &= \sum_{n=-\infty}^{\infty} \ln \left[\beta(\mu - i\omega_n \pm E_p) \right] + \ln \left[\beta(\mu + i\omega_n \pm E_p) \right] \\
&= \sum_{n=-\infty}^{\infty} \ln \left[\beta^2 (\omega_n^2 + (\mu \pm E_p)^2) \right].
\end{aligned}
\tag{4.22}
$$

If we now take the continuum limit, $\sum_{\mathbf{p}} \to V \int \frac{d^3 p}{(2\pi)^3}$, we get

$$
\ln \mathcal{Z} = V \sum_n \int \frac{d^3 p}{(2\pi)^3} \left\{ \ln \left[\beta^2 (\omega_n^2 + (\mu + E_p)^2) \right] + \ln \left[\beta^2 (\omega_n^2 + (\mu - E_p)^2) \right] \right\}.
\tag{4.23}
$$

To proceed, we have to evaluate the sum over n. These sums are the so-called Matsubara sums, and can be evaluated using contour integration. Let us take a closer look at these sums:

$$
\sigma \equiv \sum_{n=-\infty}^{\infty} \ln \left[\beta^2 (\omega_n^2 + a^2) \right],
\tag{4.24}
$$

where $a = E_p \pm \mu$. Differentiating σ with respect to a^2 gives

$$
\frac{d\sigma}{da^2} = \sum_{n=-\infty}^{\infty} \frac{\beta^2}{\beta^2 (\omega_n^2 + a^2)} = - \sum_{n=-\infty}^{\infty} \frac{1}{(i\omega_n)^2 - a^2}.
\tag{4.25}
$$

This sum can be rewritten as a contour integral using the identity

$$
\sum_{n=-\infty}^{\infty} \frac{1}{(i\omega_n)^2 - a^2} = \frac{1}{2\pi i} \oint_{\mathcal{C}} \frac{1}{z^2 - a^2} h(z) dz,
\tag{4.26}
$$

where $h(z)$ is some function with simple poles and residue one at $z = i\omega_n$, and $\mathcal{C}$ is the contour enclosing the poles of $h(z)$ [12]. A suitable function is $h(z) = \frac{\beta}{2} \tanh \frac{\beta z}{2}$. We can change the integration contour $\mathcal{C}$ to enclose the simple poles $z = \pm a$ instead of $z = i\omega_n$, as shown in Fig. 4.1.
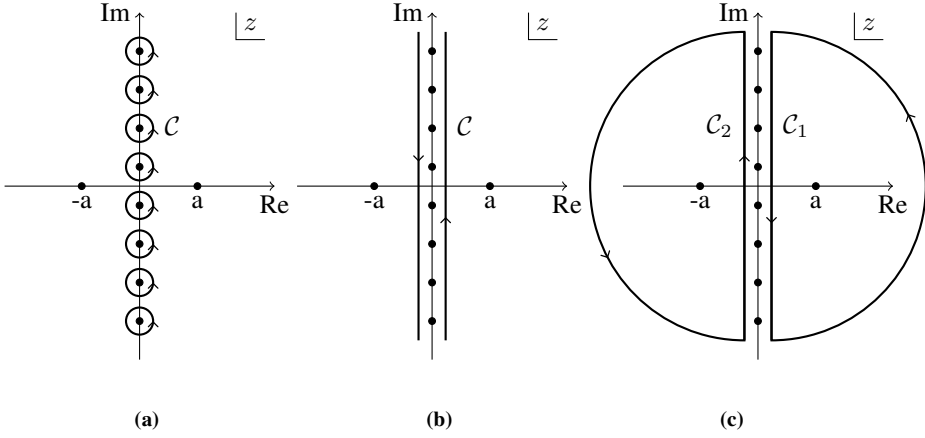
Figure 4.1: Deforming the contour from enclosing the poles $z = i\omega_n$ to enclosing the poles $z = \pm a$

The contribution from the semicircles in figure (c) vanish as the radius of the semicircles goes to infinity. Hence, after changing the contour, the integral in eq. (4.26) becomes

$$\frac{1}{2\pi i} \oint_{\mathcal{C}} \frac{1}{z^2 - a^2} h(z) dz = -\frac{\beta}{2} \sum_{z = \pm a} \operatorname{Res} \frac{1}{z^2 - a^2} \tanh \frac{\beta z}{2}. \tag{4.27}$$

The (-)sign on the right-hand-side arises when we switch the integration direction as showed in Figure 4.1b and Figure 4.1c. The residues are now easy to calculate and we find

$$\frac{d\sigma}{da^2} = \frac{\beta}{2} \left(\frac{\tanh \frac{\beta a}{2}}{2a} - \frac{\tanh \frac{\beta a}{2}}{-2a} \right)$$

$$= \frac{\beta}{2a} \tanh \frac{\beta a}{2}. \tag{4.28}$$

Now we can find σ by integrating over a^2 and making the substitution $u = \cosh \frac{\beta a}{2}$,

$$\sigma = \frac{\beta}{2} \int \frac{\tanh \frac{\beta a}{2}}{a} da^2 = 2 \int \frac{1}{u} du = 2 \ln \left(\cosh \frac{\beta a}{2} \right) + C$$

$$= 2 \ln \left(1 + e^{-\beta a} \right) + \beta a + C'. \tag{4.29}$$

Remembering that $a = E_p \pm \mu$ and omitting terms that do not depend on β, we insert eq. (4.29) into eq. (4.23) and get

$$\ln \mathcal{Z} = 2V \int \frac{d^3 p}{(2\pi)^3} \left[\beta E_p + \ln \left(1 + e^{-\beta(E_p - \mu)} \right) + \ln \left(1 + e^{-\beta(E_p + \mu)} \right) \right]. \tag{4.30}$$

From this expression we can calculate all the thermodynamical quantities we need, so we do not need to rewrite this any further. The first term is a divergent vacuum term, and the two others are contributions from particles (second term) and antiparticles (third term). We will see that the term coming from antiparticles will not contribute to any of the thermodynamical quantities at zero temperature and positive chemical potential.

4.2 The thermodynamical quantities

The thermodynamical relations are given by eqs. (3.6) to (3.9). The pressure becomes

$$p = \frac{2}{\beta} \int \frac{d^3 p}{(2\pi)^3} \left[\beta E_p + \ln \left(1 + e^{-\beta(E_p - \mu)} \right) + \ln \left(1 + e^{-\beta(E_p + \mu)} \right) \right], \qquad (4.31)$$

which in the zero-temperature limit reduces to

$$\frac{2 \cdot 4\pi}{(2\pi)^3} \int dp \, p^2 \left[\theta(\mu - E_p)(\mu - E_p) \right] + 2 \int \frac{d^3 p}{(2\pi)^3} \, E_p. \qquad (4.32)$$

Here we used that

$$\lim_{T \to 0} T \ln \left(1 + e^{-(E_p \pm \mu)/T} \right) = \begin{cases} 0 & , \quad E_p \pm \mu > 0 \\ -(E_p \pm \mu) & , \quad E_p \pm \mu < 0 \end{cases}, \qquad (4.33)$$

which is the Heaviside step function multiplied with $-(E_p \pm \mu)$. The contribution from antiparticles in eq. (4.32) is zero because $E_p + \mu$ is always larger than zero. The heavyside step function $\theta(\mu - E_p)$ is zero when the energy is larger than the chemical potential. Let us therefore introduce the Fermi momentum p_F which is the largest occupied momentum, corresponding to the energy state $E_p = \mu$. The first integral in eq. (4.32) will thus vanish for momentum larger than p_F. We then have $\mu = \sqrt{p_F^2 + m^2} = m\sqrt{x_F^2 + 1}$, where $x_F = \frac{p_F}{m}$. The divergent vacuum term of eq. (4.32) can be calculated using dimensional regularisation, changing the dimension of the integral from $d = 3$ to $d = 3 - 2\epsilon$ where ϵ is an infinitesimal number. In the limit $\epsilon \to 0$ we obtain the physical result. To make sure the action, and thus the Lagrangian still have the same dimension as before, we also have to multiply the vacuum integral by the renormalisation scale $\left(\frac{e^\gamma}{4\pi} \right)^\epsilon \Lambda^{2\epsilon}$ with $[\Lambda] = \text{MeV}$. The factor $\left(\frac{e^\gamma}{4\pi} \right)^\epsilon$ is added for later convenience.[3] Now

$$p = \frac{1}{\pi^2} \int_0^{p_F} dp \, p^2 \left[\mu - E_p \right] + 2 \left(\frac{e^\gamma}{4\pi} \right)^\epsilon \Lambda^{2\epsilon} \int \frac{d^{3-2\epsilon} p}{(2\pi)^{3-2\epsilon}} \, E_p$$

$$\equiv I_1 + I_2. \qquad (4.34)$$

Let us start by integrating I_1:

$$I_1 = \frac{1}{\pi^2} \int_0^{p_F} dp \, p^2 \left[\mu - E_p \right]$$

$$= \frac{m^4}{\pi^2} \int_0^{x_F} dx \, x^2 \left[\sqrt{x_F^2 + 1} - \sqrt{x^2 + 1} \right]$$

$$= \frac{m^4}{24\pi^2} \left[\left(2x_F^3 - 3x_F \right) \sqrt{x_F^2 + 1} + 3 \sinh^{-1} x_F \right]$$

$$= \frac{1}{24\pi^2} \left[\mu \left(2\mu^2 - 5m^2 \right) \sqrt{\mu^2 - m^2} + 3m^4 \ln \left(\frac{\mu + \sqrt{\mu^2 - m^2}}{m} \right) \right]. \qquad (4.35)$$

---

[3]When we multiply the renormalisation scale Λ by the factor $\left(\frac{e^\gamma}{4\pi} \right)^\epsilon$, we work in the $\overline{\text{MS}}$ scheme. In the renormalisation procedure we then absorb the constant terms $\gamma + \ln 4\pi$ in addition to the divergent $\frac{1}{\epsilon}$ arising from dimensional regularisation. If we multiply only by Λ instead, we work in the MS scheme where solely the divergent terms are absorbed.

Here we used the relations $m^2 x_f^2 = \mu^2 - m^2$ and $\sinh^{-1} x = \ln\left(x + \sqrt{x^2 + 1}\right)$. We next integrate I_2, using that the surface area of the unit sphere in d dimensions is $\frac{2\pi^{d/2}}{\Gamma(d/2)}$, where $\Gamma(z)$ is Euler's gamma function:

$$
\begin{aligned}
I_2 &= 2\left(\frac{\mathrm{e}^\gamma}{4\pi}\right)^\epsilon \Lambda^{2\epsilon} \int \frac{d^{3-2\epsilon}p}{(2\pi)^{3-2\epsilon}} E_p \\
&= 4\left(\frac{\mathrm{e}^\gamma}{4\pi}\right)^\epsilon \frac{\pi^{3/2-\epsilon}\Lambda^{2\epsilon}}{(2\pi)^{3-2\epsilon}\Gamma\left(\frac{3}{2}-\epsilon\right)} \int_0^\infty dp\, p^{2-2\epsilon} \sqrt{p^2 + m^2},
\end{aligned}
\tag{4.36}
$$

and performing the momentum integral gives

$$
\begin{aligned}
I_2 &= \frac{4\left(\mathrm{e}^\gamma \Lambda^2\right)^\epsilon}{(4\pi)^{3/2}\Gamma\left(\frac{3}{2}-\epsilon\right)} \frac{m^4 \Gamma\left(\frac{3}{2}-\epsilon\right)\Gamma(-2+\epsilon)}{2m^{2\epsilon}\Gamma\left(-\frac{1}{2}\right)} \\
&= \frac{m^4}{4\pi^{3/2}}\left(\mathrm{e}^\gamma \frac{\Lambda^2}{m^2}\right)^\epsilon \frac{\Gamma(-2+\epsilon)}{\Gamma\left(-\frac{1}{2}\right)}.
\end{aligned}
\tag{4.37}
$$

Using the identities $\Gamma(1/2) = \sqrt{\pi}$, $z\Gamma(z) = \Gamma(z+1)$ and $\Gamma(\epsilon) = \frac{1}{\epsilon} - \gamma + \mathcal{O}(\epsilon)$, where $\gamma \approx 0.577$ is the Euler-Mascheroni constant, we can expand I_2 in orders of ϵ,

$$
\begin{aligned}
I_2 &= \frac{m^4}{4\pi^{3/2}}\left(\mathrm{e}^\gamma \frac{\Lambda^2}{m^2}\right)^\epsilon \frac{\Gamma(-2+\epsilon)}{\Gamma\left(-\frac{1}{2}\right)} \\
&= \frac{m^4}{4\pi^{3/2}}\left[1 + \epsilon\left(\gamma + \ln\frac{\Lambda^2}{m^2}\right) + \mathcal{O}(\epsilon^2)\right] \frac{\Gamma(\epsilon)}{-2\sqrt{\pi}(-2+\epsilon)(-1+\epsilon)} \\
&= \frac{-m^4}{8\pi^2}\left[1 + \epsilon\left(\gamma + \ln\frac{\Lambda^2}{m^2}\right) + \mathcal{O}(\epsilon^2)\right]\left[\frac{1}{\epsilon} - \gamma + \mathcal{O}(\epsilon)\right]\frac{1}{2}\left(1 - \frac{\epsilon^2 - 3\epsilon}{2} + \mathcal{O}(\epsilon^2)\right) \\
&= \frac{-m^4}{16\pi^2}\left[\frac{1}{\epsilon} + \ln\frac{\Lambda^2}{m^2} + \frac{3}{2} + \mathcal{O}(\epsilon)\right].
\end{aligned}
\tag{4.38}
$$

Dropping terms of order ϵ, our final expression for the pressure reads

$$
\begin{aligned}
p &= \frac{1}{24\pi^2}\left[\mu\left(2\mu^2 - 5m^2\right)\sqrt{\mu^2 - m^2} + 3m^4 \ln\left(\frac{\mu + \sqrt{\mu^2 - m^2}}{m}\right)\right] \\
&\quad - \frac{m^4}{16\pi^2}\left(\frac{1}{\epsilon} + \ln\frac{\Lambda^2}{m^2} + \frac{3}{2}\right).
\end{aligned}
\tag{4.39}
$$

We have split the pressure into two parts; one density-dependent part and one vacuum part. More interestingly, we get a negative pressure in vacuum ($\mu = 0$). In chapter 6 we will extract the vacuum term from the pressure and add it to an effective bag pressure, which we will use to mimic quantum chromodynamics (QCD) interactions.

As $\mathcal{Z}$ is proportional to V, we found $p = \frac{\ln\mathcal{Z}}{\beta V}$. From eq. (3.7) we then get $\rho = \frac{\partial p}{\partial\mu}$,

which is straightforward to calculate using eq. (4.34). The particle density is thus

$$
\begin{aligned}
\rho = \frac{\partial p}{\partial \mu} &= \frac{1}{\pi^2} \int_0^{x_F} dx\, x^2 \\
&= \frac{m^3}{3\pi^2} x_F^3 \\
&= \frac{1}{3\pi^2} \left(\mu^2 - m^2\right)^{3/2}.
\end{aligned}
\tag{4.40}
$$

We see from this expression that no particles are present as long as $\mu \leq m$ i.e. the vacuum persists until the chemical potential of a particle is larger than its mass. The energy density is given by eq. (3.9). However, it is easy to verify that the term TS is zero when $T = 0$, so we are left with

$$
\begin{aligned}
\epsilon &= \mu\rho - \frac{1}{V} \frac{\partial \ln \mathcal{Z}}{\partial \beta} \\
&= \mu\rho - \frac{1}{\pi^2} \int dp\, p^2 \left[E_p + \frac{-(E_p - \mu)e^{-\beta(E_p - \mu)}}{1 + e^{-\beta(E_p - \mu)}} \right].
\end{aligned}
\tag{4.41}
$$

In the zero-temperature limit this reduces to

$$
\epsilon = \frac{\mu}{3\pi^2} \left(\mu^2 - m^2\right)^{3/2} - \frac{1}{\pi^2} \int dp\, p^2 (\mu - E_p)\theta(\mu - E_p) - \frac{1}{\pi^2} \int dp\, p^2 E_p.
\tag{4.42}
$$

Here we used that

$$
\lim_{T \to 0} \frac{e^{-(E_p - \mu)/T}}{1 + e^{-(E_p - \mu)/T}} = \begin{cases} 0 & , \quad E_p \pm \mu > 0 \\ 1 & , \quad E_p \pm \mu < 0 \end{cases},
\tag{4.43}
$$

which is just another representation of the Heaviside step function. We recognise the integrals in eq. (4.42) as I_1 and I_2, so the final expression for the energy density is

$$
\begin{aligned}
\epsilon &= \mu\rho - p \\
&= \frac{1}{24\pi^2} \left[\mu \left(6\mu^2 - 3m^2\right) \sqrt{\mu^2 - m^2} - 3m^4 \ln \left(\frac{\mu + \sqrt{\mu^2 - m^2}}{m} \right) \right] \\
&\quad + \frac{m^4}{16\pi^2} \left(\frac{1}{\epsilon} + \ln \frac{\Lambda^2}{m^2} + \frac{3}{2} \right).
\end{aligned}
\tag{4.44}
$$

With the pressure and energy density determined, we can find the equation of state, $\epsilon(p)$. We cannot find the EoS analytically from the general expressions (4.39) and (4.44), but both are parameterised by μ, so we can find out how they are related numerically. However, if we look at the ultrarelativistic limit where $m^2/\mu^2 \ll 1$, the expressions (4.39), (4.40) and (4.44) simplify to

$$
p \to \frac{\mu^4}{12\pi^2},
\tag{4.45}
$$

$$
\rho \to \frac{\mu^3}{3\pi^2},
\tag{4.46}
$$

$$
\epsilon \to \frac{\mu^4}{4\pi^2},
\tag{4.47}
$$

and we obtain the simple EoS $\epsilon = 3p$. As quark stars are extremely dense objects, taking the ultrarelativistic limit will be a good approximation to the more general expressions (4.39), (4.40) and (4.44). Our effort and work for finding the pressure, number density and energy density will be made useful in the section 5.2.2, where we solve the TOV equation using the ultrarelativistic EoS $\epsilon = 3p$.

Chapter 5

The Tolman-Oppenheimer-Volkoff equation

Due to the extreme density of the quark star, the gravitational field is so strong that general relativity plays a central role in the physics describing them. However, as we in this thesis focus on particle physics and use quantum field theory to study the star, a detailed derivation of the Tolman-Oppenheimer-Volkoff (TOV) equation is not our main concern. We will thus assume that the reader is familiar with the basics of general relativity and derive the TOV equation accordingly. For a detailed introduction to general relativity we refer to e.g. [13] or [14].

5.1 Deriving the TOV equation

The TOV equation is derived under the following assumptions:

1. The star is spherically symmetric and the gravitational field is static and isotropic. We can then write the metric as

$$ds^2 = A(r)dt^2 - B(r)dr^2 - r^2 \left(d\theta^2 + \sin^2\theta d\phi^2 \right). \tag{5.1}$$

2. Matter constitutes a perfect fluid. The energy-momentum tensor is then [15]

$$T_{\mu\nu} = (\epsilon + p)u_\mu u_\nu - pg_{\mu\nu}, \tag{5.2}$$

where p, ϵ and u_μ are the pressure, energy density and four-velocity of the fluid respectively, and $g_{\mu\nu}$ is the metric tensor.

3. The system is in hydrostatic equilibrium, i.e. the fluid is at rest or moving with a constant velocity. This implies that $\mathbf{u}$ and the time derivatives of p, ϵ and $g_{\mu\nu}$ are zero.

In addition, $g_{\mu\nu}$ is related to $T_{\mu\nu}$ and the Ricci tensor $R_{\mu\nu}$ by the Einstein's field equations,

$$R_{\mu\nu} - \frac{1}{2}g_{\mu\nu}R = 8\pi G T_{\mu\nu}. \tag{5.3}$$

Here, $R \equiv g^{\mu\nu}R_{\mu\nu}$ is the Ricci scalar, or curvature scalar, and G is the gravitational constant. Assumption 2 and 3 imply that only the diagonal components of the energy-momentum tensor are nonzero,

$$T = \begin{pmatrix} \epsilon A & 0 & 0 & 0 \\ 0 & pB & 0 & 0 \\ 0 & 0 & pr^2 & 0 \\ 0 & 0 & 0 & pr^2\sin\theta \end{pmatrix}. \tag{5.4}$$

Here we also used that $g^{\mu\nu}u_\mu u_\nu = 1$, and since $\mathbf{u} = 0$ we must have $u_0 u_0 = \left(g^{00}\right)^{-1} = A$. It follows from the last assumption that the only nonzero components of the Ricci tensor is on the diagonal. These four components can be found using the definition of the Ricci tensor [15]:

$$R_{\mu\nu} = \partial_\alpha \Gamma^\alpha_{\mu\nu} - \partial_\nu \Gamma^\alpha_{\mu\alpha} + \Gamma^\alpha_{\mu\nu}\Gamma^\beta_{\alpha\beta} - \Gamma^\beta_{\nu\alpha}\Gamma^\alpha_{\mu\beta}, \tag{5.5}$$

where $\Gamma^\mu_{\nu\alpha}$ are the Christoffel symbols defined as

$$\Gamma^\mu_{\nu\alpha} = \frac{1}{2}g^{\mu\beta}\left(\partial_\nu g_{\beta\alpha} + \partial_\alpha g_{\nu\beta} - \partial_\beta g_{\nu\alpha}\right). \tag{5.6}$$

The calculation of these components is quite involved, so I will not go through the details here. After some tensor calculations the various components read

$$R_{00} = \frac{A''}{2B} - \frac{A'}{4B}\left(\frac{A'}{A} + \frac{B'}{B}\right) + \frac{A'}{rB} \tag{5.7}$$

$$R_{11} = -\frac{A''}{2A} + \frac{A'}{4A}\left(\frac{A'}{A} + \frac{B'}{B}\right) + \frac{B'}{rB} \tag{5.8}$$

$$R_{22} = 1 - \frac{r}{2B}\left(\frac{A'}{A} - \frac{B'}{B}\right) - \frac{1}{B} \tag{5.9}$$

$$R_{33} = \sin^2\theta R_{22}, \tag{5.10}$$

where the prime denotes differentiation with respect to r. We will use these equations together with eq. (5.3) to find the unknown functions $A(r)$ and $B(r)$. Let us start by isolating $B(r)$ by writing out a sum of the eqs. (5.7) to (5.10):

$$\frac{R_{00}}{2A} + \frac{R_{11}}{2B} + \frac{R_{22}}{r^2} = \frac{B'}{rB^2} - \frac{1}{r^2 B} + \frac{1}{r^2}. \tag{5.11}$$

We also notice that the left hand side of this equation can be rewritten in the same form as Einstein's field equations,

$$\frac{R_{00}}{2A} + \frac{R_{11}}{2B} + \frac{R_{22}}{2r^2} + \frac{R_{33}}{2r^2\sin^2\theta} = \frac{R_{00}}{A} - \frac{1}{2}R$$

$$= \frac{1}{A}\left(R_{00} - \frac{1}{2}g_{00}R\right)$$

$$= 8\pi\epsilon G. \tag{5.12}$$

The last equality we recognised as eq. (5.3) with $\mu = \nu = 0$ and $T_{00} = \epsilon A$. Now, setting the right hand side of eq. (5.11) and eq. (5.12) equal, we get an equation for $B(r)$:

$$8\pi\epsilon G = \frac{B'}{rB^2} - \frac{1}{r^2 B} + \frac{1}{r^2}. \qquad (5.13)$$

This yields

$$1 - 8\pi r^2 \epsilon G = \frac{1}{B} - \frac{B'r}{B^2}$$
$$= \left(\frac{r}{B}\right)'. \qquad (5.14)$$

Furthermore, the mass inside a sphere of radius r is[1]

$$M(r) = \int_0^r 4\pi \tilde{r}^2 \epsilon(\tilde{r}) \, d\tilde{r}, \qquad (5.15)$$

so integrating eq. (5.14) gives

$$B(r) = \left(1 - \frac{2GM(r)}{r}\right)^{-1}. \qquad (5.16)$$

To determine $A(r)$, we need the equation for energy and momentum conservation,

$$0 = T^{\mu\nu}_{;\mu} \equiv \partial_\mu T^{\mu\nu} + \Gamma^\alpha_{\mu\alpha} T^{\mu\nu} + \Gamma^\nu_{\alpha\mu} T^{\mu\alpha}$$
$$= \frac{1}{\sqrt{-g}} \partial_\mu \left(\sqrt{-g} T^{\mu\nu}\right) + \Gamma^\nu_{\alpha\mu} T^{\mu\alpha}. \qquad (5.17)$$

Here we used the relation $\Gamma^\alpha_{\mu\alpha} = \frac{1}{\sqrt{-g}} \partial_\mu \sqrt{-g}$ derived in Appendix A.2. Inserting the energy-momentum tensor for perfect fluids, eq. (5.2), yields

$$0 = -\partial_\mu \left(p g^{\mu\nu}\right) - \frac{p g^{\mu\nu}}{\sqrt{-g}} \partial_\mu \sqrt{-g} + \Gamma^\nu_{\alpha\mu} \left[(\epsilon + p) u^\mu u^\alpha - p g^{\mu\alpha}\right]. \qquad (5.18)$$

Note that we used assumption 3 here by setting $u^\mu \partial_\mu \sqrt{-g} = 0$ and $\partial_\mu(\epsilon + p) u^\mu u^\nu = 0$. This equation must hold for each index ν. If we multiply both sides by $g_{\nu\beta}$ and set $\nu = 1$, our equation reduces to (see appendix A.3 for a derivation)

$$p' = -\frac{1}{2}(p + \epsilon)\frac{A'}{A}, \qquad (5.19)$$

or

$$\frac{A'}{A} = -\frac{2p'}{p + \epsilon}. \qquad (5.20)$$

---

[1]Note that $\epsilon(r)$ is only a function of r, or else the star would not be spherically symmetric and assumption 1 would be violated.

Since R_{22} only depends on A through A'/A, we can eliminate the A dependence from eq. (5.9). We can also eliminate B from R_{22} by using eq. (5.16) and

$$\frac{B'}{B^2} = -\left(1 - \frac{2GM}{r}\right)^{-2}\left(-\frac{2G}{r}4\pi r^2\epsilon + \frac{2GM}{r^2}\right)\left(1 - \frac{2GM}{r}\right)^2$$

$$= 2G\left(4\pi r\epsilon + \frac{M}{r^2}\right). \tag{5.21}$$

R_{22} can now be written as

$$R_{22} = 1 + \left(\frac{rp'}{p+\epsilon} - 1\right)\left(1 - \frac{2GM}{r}\right) + G\left(4\pi r^2\epsilon + \frac{M}{r}\right). \tag{5.22}$$

Furthermore, multiplying eq. (5.3) by $g^{\mu\nu}$, we get

$$R - \frac{4}{2}R = 8\pi G T^{\mu}_{\mu}, \tag{5.23}$$

where we used $g_{\mu\nu}g^{\mu\nu} = \delta^{\mu}_{\mu} = 4$. Evaluating the trace, we obtain

$$\Rightarrow R = -8\pi G(\epsilon - 3p). \tag{5.24}$$

Using this result and eq. (5.3), we can also express R_{22} as

$$R_{22} = \frac{1}{2}g_{22}R + 8\pi G T_{22}$$

$$= 4\pi G r^2(\epsilon - 3p) + 8\pi G p r^2$$

$$= 4\pi G r^2(\epsilon - p). \tag{5.25}$$

Combining eq. (5.22) and eq. (5.25) gives

$$4\pi G r^2(\epsilon - p) = 1 + \left(\frac{rp'}{p+\epsilon} - 1\right)\left(1 - \frac{2GM}{r}\right) + G\left(4\pi r^2\epsilon + \frac{M}{r}\right). \tag{5.26}$$

The $4\pi G r^2\epsilon$ terms cancels, and by rearranging we find

$$\frac{rp'}{p+\epsilon} - 1 = -\frac{4\pi G r^2 p + 1 - \frac{GM}{r}}{1 - \frac{2GM}{r}}. \tag{5.27}$$

Finally, isolating $p'(r)$ on the left hand side yields

$$p'(r) = -\left[\frac{p+\epsilon}{r}\right]\frac{4\pi G r^2 p + 1 - \frac{GM}{r} - 1 + \frac{2GM}{r}}{1 - \frac{2GM}{r}}$$

$$= -\frac{G}{r}[p(r) + \epsilon(r)]\frac{4\pi r^4 p(r) + M(r)}{r - 2GM(r)}, \tag{5.28}$$

which is the Tolman-Oppenheimer-Volkoff equation. The importance of the EoS becomes clear now, as we can use it to eliminate ϵ in favour of p.

5.2   Solving the TOV equation

In this thesis we will solve the TOV equation numerically using Mathematica [16]. As the TOV equation is a differential equation containing two unknown functions, $p(r)$ and $M(r)$, we have to couple it with another equation involving one or both of these functions. We already know that $M'(r) = 4\pi r^2 \epsilon$ from eq. (5.15) and can thus use this as the second equation. Up until now we have used natural units where all quantities are expressed in units of MeV. When describing a quark star, however, it is disconvenient to express the mass in MeV and radius in $(\text{MeV})^{-1}$. Hence, we will not use natural units when solving the TOV equation, but rather express the mass in terms of solar masses $M_\odot$ and radius as km. Furthermore, numerical calculations are easier to perform using dimensionless variables. We therefore introduce the dimensionless variables $\tilde{M}(r) \equiv \frac{M(r)}{M_\odot}$, $\tilde{p} \equiv \frac{p(r)}{\epsilon_0}$ and $\tilde{\epsilon}(r) \equiv \frac{\epsilon(r)}{\epsilon_0}$ for the mass, pressure and energy density respectively. Here ϵ_0 is some free parameter with dimension energy density. The two coupled equations can now be written as

$$\frac{d\tilde{p}}{dr} = -\frac{R_0}{r} \left[\tilde{p}(r) + \tilde{\epsilon}(r) \right] \frac{\tilde{M}(r) + \alpha r^3 \tilde{p}(r)}{r - 2R_0 \tilde{M}(r)} \tag{5.29}$$

$$\frac{d\tilde{M}}{dr} = \alpha r^2 \tilde{\epsilon}(r), \tag{5.30}$$

where we introduced the constant $R_0 = \frac{GM_\odot}{c^2} = 1.477$ km and $\alpha = \frac{4\pi\epsilon_0}{M_\odot c^2}$. Because ϵ_0 is a free parameter, so is α. Both eqs. (5.29) and (5.30) are written in dimension km^{-1} since $[\alpha] = \text{km}^{-3}$.

5.2.1   Finding the mass-radius relation

To solve the TOV equation we need two initial conditions in addition to the EoS. One of these is intuitive; the mass at the center of the star must be zero, $m(0) = 0$. The second initial condition is $p(0) = p_c$, where p_c is the pressure at the center. Because we do not know central pressure, the solution of the TOV equation will be parameterised by p_c. Varying p_c will thus give different masses and radii of the star. With Mathematica we can solve coupled differential equations using the built-in function NDSolve. Solving the TOV equation gives $p(r)$ and $m(r)$, where r is the distance to the center of the star. The radius R of the star is defined as the distance to the center where the pressure becomes zero, $p(R) = 0$, and the mass of the star is defined as $M \equiv M(R)$. If we solve the coupled eqs. (5.29) and (5.30) for successive values p_c, we can find approximations of the radius and mass of the star as functions of p_c. These functions can be used to find a relation between the mass of a star and its radius. The procedure for doing this is as follows:

1. Make a loop that goes from $i = 1$ to $i = N$.

2. Solve the coupled eqs. for $p_c = p_{c,i}$, and find the radius and mass of the star corresponding to this central pressure. Now, make two arrays with $N \times 2$ components; one for saving mass values, and one for saving values of the radius. R and $\tilde{M}$ is written in component $[i, 2]$ of its corresponding array, and p_c is written in component $[i, 2]$.

3. Increase p_c by a small amount, say $p_c = p_{c,i} + \frac{p_{c,\max} - p_{c,\min}}{N-1}$, where $p_{c,\min} \equiv p_{c,1}$ and $p_{c,\max} \equiv p_{c,N}$ are the smallest and largest central pressures the TOV eq. is solved for. Also increase i by one and close the loop.

4. Use the built-in Mathematica function `Interpolation` on the two arrays. This will give approximations of the mass and radius as functions of the central pressure.

5. Finally, plot the mass as function of radius using e.g. Mathematicas `ParametricPlot`.

A full Mathematica code where this procedure is included can be found in Appendix B.

5.2.2 Ideal Fermi gas revisited

In the previous chapter we found the pressure, energy density and particle density for an ideal Fermi gas and saw that the EoS in the ultrarelativistic regime is $\epsilon = 3p$. When studying a quark star, we have to take into account that quarks have some additional properties other than half integer spin. First of all, there are several different quark *flavours*, each with a unique mass m_f and chemical potential μ_f. The flavour of a quark simply tells us what type of quark it is, e.g. up (u) or down (d) quark. We therefore have to sum eqs. (4.45) to (4.47) over all flavours f. Another important property to account for is the colour charge, which is a property assigned to quarks and gluons to explain why quarks never have been observed as free particles.[2] Quarks carries one out of three types of colours, and antiquarks carries one out of three anticolours, which simply is negative colourcharge. To account for all the different colours the quarks can have, we have to multiply the eqs. (4.45) to (4.47) by the number of colours $N_c = 3$. For quarks, the pressure, particle density and energy density thus becomes

$$p = \frac{N_c}{12\pi^2} \sum_f \mu_f^4, \tag{5.31}$$

$$\rho = \frac{N_c}{3\pi^2} \sum_f \mu_f^3, \tag{5.32}$$

$$\epsilon = \frac{N_c}{4\pi^2} \sum_f \mu_f^4 = 3p. \tag{5.33}$$

We now solve the TOV equation using this EoS. The result is shown in Fig. 5.1. We see that the pressure never becomes zero, and that the mass diverges as the radius of the star goes to infinity. Since all compact stars obviously have finite radii and finite mass, these results are unphysical.

---

[2]It is believed that only colour singlet states can exist as free particles [17], however, there is still ongoing a lot of research in the field of colour confinement, see e.g. [18]. Baryons are made up of three quarks with different colour. The three colours combined will neutralise and make the baryon colourless. Mesons consists of one quark and one antiquark. The antiquark carries the anticolour corresponding to the quark's colour, making the meson colourless as well.
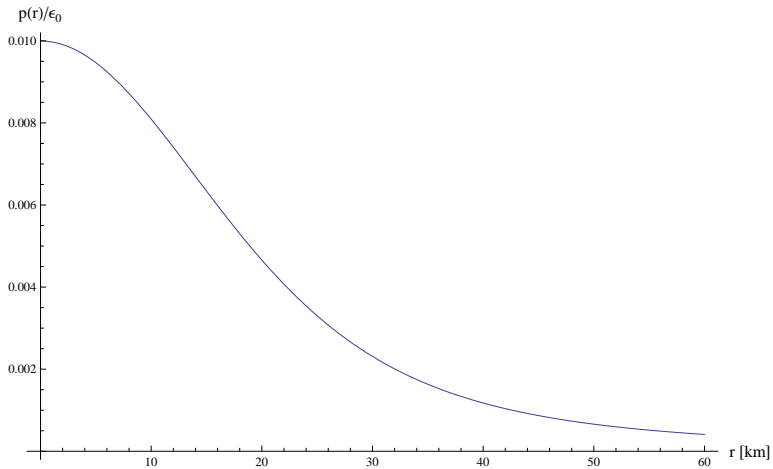
(a) Pressure distribution inside the star.
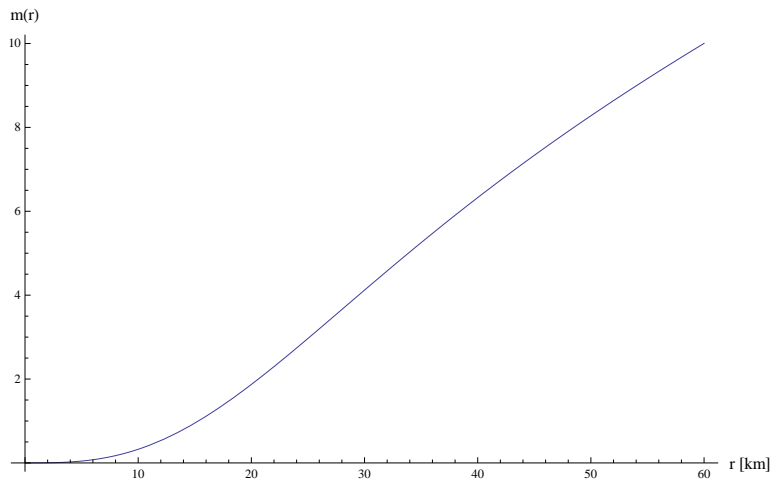
(b) Mass distribution in terms of solar masses

Figure 5.1: A quark star described using the EoS for an ultrarelativistic ideal Fermi gas.

Chapter 6

Effective Bag models

So far we have treated the quarks as free particles. However, we saw in the previous chapter that neglecting quark interactions gave unphysical results, as we got no constraints on the mass of the star and an infinite radius. Now it is time to introduce interactions between the particles. This can be done in several different ways, but in this thesis we will restrict ourselves to using *bag models* and a quark-meson model. The first bag model was invented at MIT by Chodos et al. in 1974 [19]. Later, several other bag models have been used to describe quark confinement and asymptotic freedom. We will first briefly consider the original bag model proposed by Chodos et al., and later, we will consider a quark-meson model.

6.1 Equilibrium requirements

When stars are born they are almost exclusively made out of hydrogen and helium. This makes stars globally electrically neutral objects. The electrical neutrality is also assumed to be valid after the star's death, as there would be an energy penalty for the quark star to carry charge after the supernova event. We therefore implement the charge neutrality condition for quark stars by demanding

$$0 = \sum_f Q_f \rho_f - e\rho_e, \tag{6.1}$$

where Q_f is the electrical charge of quark flavour f, ρ_e is the electron number density and e is the elementary charge. Note that we also demand *local* charge neutrality with eq. (6.1). In addition to the required charge neutrality, neutron stars must be in chemical equilibrium with respect to β-decay and electron capture mentioned in the introduction. This balances the amount of protons, electrons and neutrons in the star via the weak processes

$$n \rightarrow p + e + \bar{\nu}_e, \tag{6.2a}$$

$$p + e \rightarrow n + \nu_e. \tag{6.2b}$$

After the phase transition to quark matter, the corresponding processes for three-flavour quark matter read [1]

$$d \leftrightarrow u + e + \bar{\nu}_e, \tag{6.3a}$$

$$s \leftrightarrow u + e + \bar{\nu}_e, \tag{6.3b}$$

$$s + u \leftrightarrow d + u. \tag{6.3c}$$

We will assume that the neutrinos and anti-neutrinos leave the star without further interactions, i.e. that $\mu_{\nu_e} = \mu_{\bar{\nu}_e} = 0$. This might, however, be a daring approximation due to the uncertainty of the neutrino mean free path (MFP) in compact stars. Studies indicate a MFP in neutron stars of the order $10 - 100 \, \text{m}$ [20, 21], which is a few times lower than the radii of compact stars. Ignoring the effects this might have, we get the following relations between the quark and electron chemical potentials

$$\mu_d = \mu_e + \mu_u, \tag{6.4a}$$

$$\mu_s = \mu_e + \mu_u, \tag{6.4b}$$

$$\mu_s = \mu_d. \tag{6.4c}$$

Moreover, we can use eqs. (6.1) and (6.4) to express all the chemical potentials in terms of a single chemical potential μ. In this thesis, we will mostly set $\mu = \mu_B$, where $\mu_B \equiv \sum_f \mu_f$ for three flavours and $\mu_B \equiv \mu_u + 2\mu_d$ for two flavours, is the baryon chemical potential. We thus use μ_B as the only independent chemical potential. These relations can generally not be found analytically, but as a starting point we can express the quark chemical potentials in terms of two independent chemical potentials, μ_e and μ_B, as follows

$$\mu_u = \frac{1}{3}\mu_B - \frac{2}{3}\mu_e, \tag{6.5a}$$

$$\mu_d = \mu_s = \frac{1}{3}\mu_B + \frac{1}{3}\mu_e. \tag{6.5b}$$

As an example of an analytic relation between the quark chemical potentials, we have for three flavours, in the ultra relativistic regime, $\mu_u = \mu_d = \mu_s = \frac{1}{3}\mu_B$ and $\mu_e = 0$.

6.2 MIT bag model

The phenomenon that quarks are never found isolated is called quark confinement. One model which tries to describe quark confinement and asymptotic freedom is the MIT Bag Model. This is a simple model which imposes that quarks move freely inside a finite region with a constant energy per unit volume B, called the bag constant. This finite region, which visually can be thought of as a bag, will restrict further stretching as this will cost energy proportional to the bag constant. The bag will thus also act as an external pressure in addition to the internal energy density, providing an energy difference between the inside and outside of the bag. We can now directly write down the pressure and energy

density from eqs. (5.31) and (5.33)

$$p = N_c \sum_f \frac{\mu_f^4}{12\pi^2} - B, \tag{6.6}$$

$$\epsilon(p) = 3N_c \sum_f \frac{\mu_f^4}{12\pi^2} + B = 3p + 4B. \tag{6.7}$$

Using eq. (6.7) as equation of state, the coupled equations from section 5.2 become

$$\frac{d\tilde{p}}{dr} = -4R_0 \left[\frac{\tilde{p}(r) + \tilde{B}}{r} \right] \left[\frac{\tilde{M}(r) + \alpha r^3 \tilde{p}(r)}{r - 2R_0 \tilde{M}(r)} \right], \tag{6.8}$$

$$\frac{d\tilde{M}}{dr} = \alpha r^2 \left[3\tilde{p}(r) + 4\tilde{B} \right], \tag{6.9}$$

where $\tilde{B} = \frac{B}{\epsilon_0}$.

6.2.1 The bag window

Before we can solve these equations, we need to know what values B can take. Ordinary nuclear matter (matter made out of neutrons and protons) is seen in nature, but two-flavour deconfined quark matter is not. We can use this to find a minimum value of B. The most stable nuclei is ^{56}Fe, with an energy per nucleon of about $930\,\text{MeV}$ [22]. Hence, at zero external pressure, $p = 0$, the energy E per nucleon number A for two-flavour deconfined quark matter must be larger than $930\,\text{MeV}$, i.e.

$$\left. \frac{E}{A} \right|_{N_f=2} = \frac{\epsilon(0)}{\rho_B} > 930\,\text{MeV}, \tag{6.10}$$

where $\rho_B \equiv \frac{1}{3} \sum_f \rho_f$ is the baryon number density and N_f is the number of flavours. For simplicity we shall now assume that all the quarks are massless (ultrarelativistic regime) and that no electrons are present. We will then have $\rho_d = 2\rho_u$ to satisfy the charge neutrality condition, which in turn implies that $\mu_d = 2^{1/3}\mu_u$. The energy density and baryon number density can now be found using eqs. (4.46) and (6.7), and reads

$$\rho_B = \frac{\mu_u^3}{\pi^2}, \tag{6.11}$$

$$\epsilon(0) = 4B. \tag{6.12}$$

Moreover, from eq. (6.6) the bag constant at zero external pressure and equal chemical potentials becomes

$$B = \frac{\left(1 + 2^{4/3}\right)\mu_u^4}{4\pi^2}. \tag{6.13}$$

Combining eqs. (6.10) – (6.13), we have

$$\left. \frac{E}{A} \right|_{N_f=2} = \left(4\pi^2\right)^{1/4} \left(1 + 2^{4/3}\right)^{3/4} B^{1/4} > 930\,\text{MeV}, \tag{6.14}$$

i.e. $B^{1/4} > 144.4$ MeV.

Following the same procedure as above for three flavour quark matter, still assuming massless quarks, we find $\rho_u = \rho_d = \rho_s$ and thus $\mu_u = \mu_d = \mu_s \equiv \mu$. Hence, for $N_f = 3$, eqs. (6.11) – (6.13) reads

$$\rho_B = \frac{\mu^3}{\pi^2}, \tag{6.15}$$

$$\epsilon(0) = 4B, \tag{6.16}$$

$$B = \frac{3\mu^4}{4\pi^2}. \tag{6.17}$$

We now obtain the energy per nucleon

$$\left.\frac{E}{A}\right|_{N_f=3} = \left(4\pi^2\right)^{1/4} 3^{3/4} B^{1/4}. \tag{6.18}$$

As $\left(4\pi^2\right)^{1/4} 3^{3/4} \approx 5.714 < 6.441 \approx \left(4\pi^2\right)^{1/4}\left(1 + 2^{4/3}\right)^{3/4}$, the energy per nucleon is lower for three flavour deconfined quark matter than for two flavours. This is also expected from the Pauli exclusion principle, as adding a particle species while keeping the total number of particles constant makes new low-energy eigenstates available, reducing the total energy of the system. Thus, if the bag constant is slightly larger than 144.4 MeV, but low enough for three-flavour deconfined quark matter to have a lower energy per baryon than ^{56}Fe, deconfined quark matter would be absolutely stable for three flavours at zero external pressure. The upper limit of the bag constant for this to be the case is found using

$$\left.\frac{E}{A}\right|_{N_f=3} < 930 \text{ MeV}, \tag{6.19}$$

which yields

$$B^{1/4} < 162.8 \text{ MeV}. \tag{6.20}$$

6.2.2 Strange quark matter hypothesis

The hypothesis that three flavour quark matter, or *strange quark matter*, is absolutely stable were suggested by Bodmer [23] and Witten [24] and is called the *strange quark matter hypothesis*. It would be realised if the bag constant is in the interval 144.4 MeV $< B^{1/4} <$ 162.8 MeV. The phase transition from ordinary nuclei to strange quark matter will, however, require a huge amount of energy because a large number of the u and d quarks in the nucleons must simultaneously be converted into s quarks via the weak interaction. As this is practically impossible, the observation of ordinary nuclei does not rule out the strange quark matter hypothesis. In order for strange matter to exist, it must thus be created in some other way. Assuming that the hypothesis is true, if a neutron star is hit by a large enough *strangelet* (a "lump" of strange quark matter), the conversion from u and d quarks to s quarks would increase the size of the strangelet. Thus, we would not need the large amount of simultaneous conversions described above. This process would not reverse, as this would require simultaneous conversions of the s quarks in the strangelet via the weak

interaction. Hence, the strangelet would successively convert the whole neutron star into a pure quark star.

If the strange quark matter hypothesis is true, a quark star can in theory have less mass than neutron stars, because a pure quark star will then be bound by the strong force, and not gravitationally bound like ordinary neutron stars are. A quark star will also have a smaller radius than a neutron star with equal mass and can possibly rotate faster than allowed for a neutron star. Two possible quark star candidates discussed in the literature are SAX J1808.4-3658 and RX J1856.5-3754 [25, 26, 27]. They seem to have a smaller radius than allowed by an ordinary neutron star.

Strangelets could e.g. be created in the early universe during the QCD phase transition, via heavy ion collisions, or in the core of neutron stars. However, if strangelets are in fact stable, and there is enough large strangelets to convert neutron stars into quarks stars, all neutron stars would eventually be converted into quark stars. This implies that the observation of a single pure neutron star would rule out the strange quark matter hypothesis. Bauswein et al. [28] discussed that there may not be enough strangelets around to convert all neutron stars into quark stars, and that more compact quark stars could coexist with neutron stars even if the strange quark matter hypothesis is wrong. For a detailed discussion of strange quark matter, see Weber [26] or Glendenning [22]. Weber et. al. also discuss the possibility of quark stars with a crust of nuclear matter in [29].

6.2.3 Mass-radius relation

Solving the coupled eqs. (6.8) and (6.9) by following the procedure described in section 5.2.1, we get a plot for the relation between the mass and radius of the quark star. The result is shown in Fig. 6.1. The central pressure is smallest in the lowest and leftmost point, and increases along the curve from there. We see that including the bag-constant to the ideal Fermi gas EoS gave us finite radii and masses of the star. The maximum masses and corresponding radii are listed in Table 6.1.

$B^{1/4}$ [MeV]	$M_{\max}$ [$M_\odot$]	R [km]
145	2.00	10.9
155	1.75	9.57
162	1.61	8.76

Table 6.1: Maximum masses with corresponding radii for different values of B.

In the next section we will extract a density dependent bag pressure from a quark-meson model. This bag pressure will give us a different EoS than those we have studied so far.
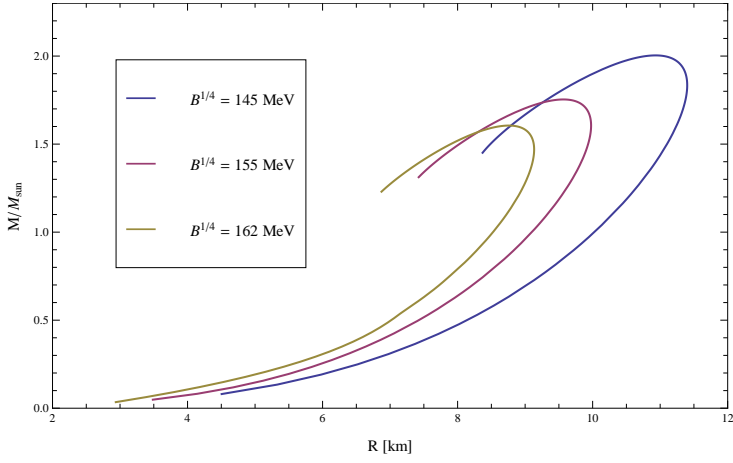
Figure 6.1: The mass - radius relation when using the MIT bag model with different values for B.

6.3 Two-flavour quark-meson model

In 1960, Gell-Mann and Lévy proposed the linear sigma model (LSM), which tries to describe the strong interaction at low energies [30]. At low energies, i.e. long distances, the degrees of freedom are the baryons and mesons, and at the time the LSM was developed, it was believed that the strong interactions were between hadrons [9]. Hence, the LSM originally describes interactions amongst mesons, but can be coupled to quarks by the Yukawa interaction. The Lagrangian of the LSM with two quark flavours (quark-meson model, or LSMq) is

$$\mathcal{L} = \text{Tr}\left[(\partial_\mu \Phi)^2\right] + m^2 \text{Tr}\left[\Phi^2\right] + \frac{\lambda}{3}\text{Tr}\left[\Phi^2\right]^2 - \frac{1}{2}h\text{Tr}\left[\Phi^\dagger + \Phi\right]$$
$$+ \bar{q}[i\slashed{\partial} + \mu_f\gamma^0]q - g\bar{q}[\sigma + \gamma^5\boldsymbol{\tau}\cdot\boldsymbol{\pi}]q, \tag{6.21}$$

where $\Phi = \frac{1}{2}(\sigma + \boldsymbol{\tau}\cdot\boldsymbol{\pi})$ is a linear combination of the sigma field (or $f_0(500)$ [31]), and the three pions π^-, π^0 and π^+. Moreover, $\boldsymbol{\tau}$ are the Pauli matrices and $\bar{q}$ and q denotes the quark fields. The first line of the Lagrangian, (6.21), is the ordinary LSM. The first term on the second line is the quark term, describing free quarks with a chemical potential μ_f, and the last term is the Yukawa interaction term. If $h = 0$ this Lagrangian is invariant under $SU(2)_L \times SU(2)_R \times U(1)_B \times U(1)_A$ [32], while $h \neq 0$ explicitly breaks chiral symmetry, reducing the symmetry to $SU(2)_V \times U(1)_B \times U(1)_A$.

6.3.1 The thermodynamical potential

The meson part of eq. (6.21) written in terms of the sigma and pion fields is

$$\mathcal{L}_{\text{meson}} = \frac{1}{2}[(\partial_\mu\sigma)^2 + (\partial_\mu\boldsymbol{\pi})^2] + \frac{1}{2}m^2(\sigma^2 + \boldsymbol{\pi}^2) + \frac{\lambda}{24}(\sigma^4 + \boldsymbol{\pi}^4) + \frac{\lambda}{12}\sigma^2\boldsymbol{\pi}^2 - h\sigma$$
$$= \frac{1}{2}[(\partial_\mu\sigma)^2 + (\partial_\mu\boldsymbol{\pi})^2] + V(\sigma, \boldsymbol{\pi}). \tag{6.22}$$

If the mass parameter m^2 is negative, the tree-level potential[1] $V(\sigma, \boldsymbol{\pi})$ have a minimum. With no loss of generality, we can choose the minimum of the potential to point in the direction of σ, orthogonal to π_i. If we then expand σ around the classical vacuum expectation value $\langle \sigma \rangle_0 = v$,

$$\sigma \to v + \tilde{\sigma}, \tag{6.23}$$

where $\tilde{\sigma}$ is quantum fluctuations, we have $\langle \tilde{\sigma} \rangle_0 = \langle \boldsymbol{\pi} \rangle_0 = 0$, and the expression for V in vacuum becomes

$$V_0 = \frac{1}{2}m^2v^2 + \frac{\lambda}{24}v^4 - hv. \tag{6.24}$$

The value of v that minimises V_0 is equal to the pion decay constant (divided by $\sqrt{2}$, depending on convention), $f_\pi = 93\,\mathrm{MeV}$, which is measured experimentally [31].[2] We thus get a relation between the coupling constant λ, the negative mass parameter m^2 and the symmetry breaking term h,

$$\lambda = \frac{6}{f_\pi^3}(h - f_\pi m^2). \tag{6.25}$$

By taking the second derivative of $V(\sigma, \boldsymbol{\pi})$ in eq. (6.22) with respect to σ or π^i and inserting their expectation values, we get the tree-level masses squared for the sigma and pion fields respectively,

$$m_\sigma^2 = \left.\frac{\partial^2 V(\sigma, \boldsymbol{\pi})}{\partial \sigma^2}\right|_{\sigma = \langle \sigma \rangle, \pi = \langle \pi \rangle} = m^2 + \frac{\lambda}{2}\langle \sigma \rangle^2 + \frac{\lambda}{6}\langle \boldsymbol{\pi} \rangle^2, \tag{6.26}$$

$$m_{\pi_i}^2 = \left.\frac{\partial^2 V(\sigma, \boldsymbol{\pi})}{\partial \pi_i^2}\right|_{\sigma = \langle \sigma \rangle, \pi = \langle \pi \rangle} = m^2 + \frac{\lambda}{6}\langle \sigma \rangle^2 + \frac{\lambda}{2}\langle \boldsymbol{\pi} \rangle^2. \tag{6.27}$$

In the vacuum eqs. (6.26) and (6.27) read

$$m_\sigma^2 = m^2 + \frac{\lambda}{2}v^2, \tag{6.28}$$

$$m_{\pi_i}^2 = m^2 + \frac{\lambda}{6}v^2. \tag{6.29}$$

In the vacuum minimum, $v = f_\pi$, and we see from eq. (6.25) that $h = f_\pi m_\pi^2$. Note that the pion becomes massless when $h = 0$, i.e. when chiral symmetry is not explicitly broken. As mentioned earlier, when $h = 0$, $\mathcal{L}_{\mathrm{meson}}$ is invariant under $SU(2) \times SU(2) \cong SO(4)$ [33]. However, as the vector $(v, 0, 0, 0)$ is only symmetric under rotations of the last three indices, the symmetry is broken down to $SO(3)$ by the nonzero vacuum minimum. As $SO(4)$ got $4(4-1)/2 = 6$ generators while $SO(3)$ only got $3(3-1)/2 = 3$ generators, this leads to three broken generators, which according to Goldstone's theorem yields three massless particles [34]. Thus, the three pions are recognised as the massless goldstone bosons. The bare mass m^2 and the bare coupling constant λ in eqs. (6.28) and (6.29) are

---

[1]Here, the potential actually is an energy density, which is easily seen as $\mathcal{L}$ in (6.21) is the Lagrangian density.
[2]An explanation of this non-intuitive equality, can be found in [9], p. 341–342.

given by the sigma and pion masses as

$$m^2 = -\frac{1}{2}(m_\sigma^2 - 3m_\pi^2), \tag{6.30}$$

$$\lambda = \frac{3}{f_\pi^2}(m_\sigma^2 - m_\pi^2). \tag{6.31}$$

We have now determined the constants we need in the tree-level vacuum potential (6.24), so it is time to include the contribution from the quarks. In section 4.2 we calculated the pressure from free Dirac fermions to one-loop. If these fermions are quarks we just multiply eq. (4.39) by the number of colours, N_c, and sum over all the flavours involved. The contribution from the quarks to the thermodynamical potential is given by eq. (3.10) which reduces to $V_q = -p$. We can rewrite V_q as a function of v and the chemical potential μ_f. To find $V_q(v)$, we read from the Lagrangian (6.21) that the quark mass-term is $g\sigma = gv$ if we neglect the quantum fluctuations of the meson fields. Combining eq. (4.39) and (6.24) and adding electrons we obtain the thermodynamical potential,

$$V = \frac{1}{2}m^2 v^2 + \frac{\lambda}{24}v^4 - hv - \frac{\mu_e^4}{12\pi^2} + \frac{N_c N_f}{16\pi^2}m_q^4\left(\frac{1}{\epsilon} + \ln\frac{\Lambda^2}{m_q^2} + \frac{3}{2}\right)$$
$$- \frac{N_c}{24\pi^2}\sum_f\left[\left(2\mu_f^2 - 5m_q^2\right)\mu_f\sqrt{\mu_f^2 - m_q^2} + 3m_q^4\ln\left(\frac{\sqrt{\mu_f^2 - m_q^2} + \mu_f}{m_q}\right)\right], \tag{6.32}$$

where N_f is the number of flavours. Note that we neglected the electron mass, which is more than justified, as $m_e = 0.51\,\mathrm{MeV}$ while $\mu_f \sim 10^2\,\mathrm{MeV}$. For simplicity, we only included the one-loop contribution from the quarks. This potential is divergent due to the $1/\epsilon$ term coming from the sea quarks.[3] This divergence is removed by renormalising the coupling constant by taking $\lambda \to \lambda + \delta\lambda$ in the Lagrangian (6.21). Choosing

$$\delta\lambda = \frac{-3N_c N_f g^4}{2\pi^2\epsilon}, \tag{6.33}$$

will remove the divergence. We are now left with a convergent potential which can be written as a function of the vacuum expectation value v and the chemical potentials μ_f,

$$V = \frac{1}{2}m^2 v^2 + \frac{\lambda}{24}v^4 - hv - \frac{\mu_e^4}{12\pi^2} + \frac{N_c N_f}{16\pi^2}m_q^4\left(\ln\frac{\Lambda^2}{m_q^2} + \frac{3}{2}\right)$$
$$- \frac{N_c}{24\pi^2}\sum_f\left[\left(2\mu_f^2 - 5m_q^2\right)\mu_f\sqrt{\mu_f^2 - m_q^2} + 3m_q^4\ln\left(\frac{\sqrt{\mu_f^2 - m_q^2} + \mu_f}{m_q}\right)\right]. \tag{6.34}$$

---

[3]Sea quarks are virtual quarks in hadrons and do not contribute to any quantum numbers.

The renormalisation scale Λ can be determined by requiring that the minimum of the potential (6.34) in vacuum, $\mu = 0$, remains at $v = f_\pi = 93\,\text{MeV}$:

$$0 = 4\left(\ln\frac{\Lambda^2}{(gf_\pi)^2} + \frac{3}{2}\right) + f_\pi\left(\frac{-2}{f_\pi}\right)$$

$$= \ln\frac{\Lambda^2}{(gf_\pi)^2} + 1. \tag{6.35}$$

The Yukawa coupling constant g is fixed by the vacuum constituent quark mass $\tilde{m}_q$ by $g = \tilde{m}_q/f_\pi$. We will set $\tilde{m}_q = 300\,\text{MeV}$ throughout this thesis. This yields

$$\Lambda = 182\text{MeV}. \tag{6.36}$$

Let us take a look at the potential in the simple case of equal chemical potentials and no electrons present. Then, $\mu_u = \mu_d \equiv \mu$ and $\mu_e = 0$. This will obviously break charge neutrality since two down quarks are needed to neutralise one up quark. We will set $m_\sigma = 800\,\text{MeV}$ throughout this thesis unless otherwise stated. The pion mass will be fixed at either $0\,\text{MeV}$ (chiral limit) or $138\,\text{MeV}$ (physical point). Fig. 6.2 shows the potential (6.34) for different values of the quark chemical potential in the chiral limit (Fig. 6.2a) and at the physical point (Fig. 6.2b). In the chiral limit the global minimum jumps to $v = 0$ for chemical potentials larger than a critical value $\mu = \mu_c$. The metastable state which in vacuum is centered around $v = f_\pi$ thus disappears for $\mu > \mu_c$ and a new metastable state is occur at $v = 0$. This is a first order phase transition [35]. The critical value of the chemical potential is $\mu_c = 322.137\,\text{MeV}$. When $h \neq 0$, the minimum goes continuously to zero when increasing μ as shown in Fig. 6.2b. The phase transition is now a crossover, as the minimum never reaches zero. Hence, the stable state is always located at $v > 0$.

6.3.2 The two-flavour effective bag pressure

In section 6.2 we saw how the MIT bag constant could be used to mimic QCD interactions. We will adopt the same idea in this section, but now the bag pressure will appear more naturally. Since we already have a nonzero energy density in the vacuum from eq. (6.34), we can use the vacuum part of this potential as a bag pressure. However, as we saw in Fig. 6.2, the location of the minimum of $V(v)$ varies with μ, and the bag pressure must always be evaluated in the minimum of the thermodynamical potential, as this is the only physically stable configuration. Hence, we obtain the bag pressure

$$B(v_0) = \frac{1}{2}m^2v_0^2 + \frac{\lambda}{24}v_0^4 - hv_0 + \frac{N_cN_f}{16\pi^2}m_q^4\left(\ln\frac{\Lambda^2}{m_q^2} + \frac{3}{2}\right), \tag{6.37}$$

where v_0 is the value of v that minimises $V(v)$ for some baryon chemical potential μ_B. In this way, the bag pressure is indirectly dependent on μ_B and thus also all the thermodynamical functions. It is important to remember that the quark masses m_q is also a function of v, $m_q = gv$. In addition to this complication, we have to satisfy the charge neutrality condition (6.1) and the equilibrium condition (6.5) at every minimum. Moreover, the
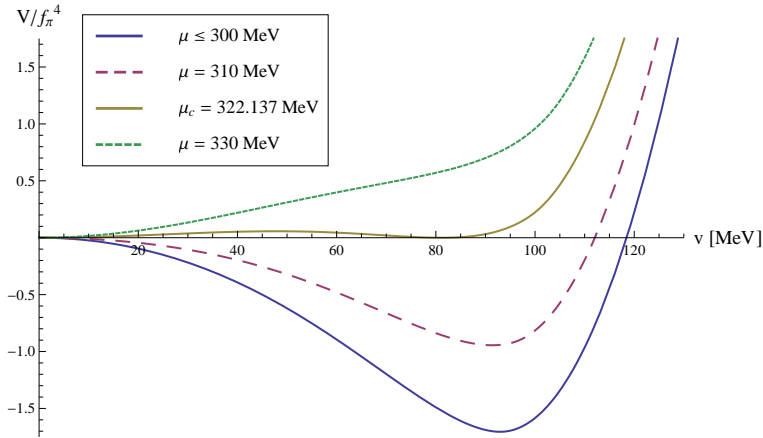
(a) We have a first order phase transition at $\mu = 322.137$ MeV in the chiral limit.
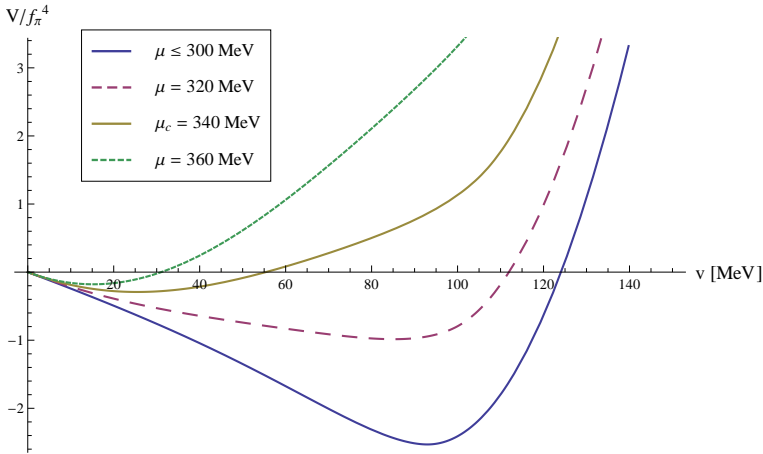
(b) The phase transition is a crossover at the physical point.

Figure 6.2: The normalised thermodynamical potential V/f_π^4 for different values of μ and m_π.

charge neutrality condition is dependent of v through the quark masses which appear in ρ_f. In other words, we must solve the coupled equations

$$\frac{\partial V(v)}{\partial v} = 0, \tag{6.38a}$$

$$2\left[\mu_u^2 - m_q(v)^2\right]^{3/2} - \left[\mu_d^2 - m_q(v)^2\right]^{3/2} - \mu_e^3 = 0 \tag{6.38b}$$

simultaneously to find the minimum of the potential and the last independent chemical potential μ_e. The procedure for finding the bag pressure as a function of e.g. the baryon number density ρ_B is similar to that described in section 5.2.1.

1. Choose a starting value for the baryon chemical potential $\mu_B = \mu_{B,\min}$. To avoid numerical problems, this value should be close to the largest value of μ_B that still describes the vacuum, $\rho_B = 0$.[4]

2. Make a loop that goes from $i = 1$ to $i = N$.

3. Solve the coupled equations (6.38). Calculate $B(v_0)$ and insert the value in component $(i, 2)$ of and $N \times 2$ array. In component $(i, 1)$ we insert the baryon number density.

4. Increase μ by a small amount, say $\mu_B = \mu_{B,i} + \frac{\mu_{B,\max} - \mu_{B,\min}}{N-1}$, where $\mu_{B,\min} \equiv \mu_{B,1}$ and $\mu_{B,\max} \equiv \mu_{B,N}$ are the smalles and largest physically relevant chemical potentials. Choosing $\mu_{B,\max}$ in the range $1500 - 1800\,\mathrm{MeV}$ should hold. Increase i by one and close the loop.

5. Use the built-in Mathematica function `Interpolation` on the array. This will produce an approximation of the function $B(\rho_B)$.

But how shall we normalise the bag pressure in the vacuum? For simplicity, we can rewrite B slightly by subtracting the non-normalised vacuum value,

$$B(v_0) \rightarrow B(v_0) - B(f_\pi). \tag{6.39}$$

This will only change the normalisation of B by giving the actual vacuum value B_{vac} of the bag pressure when solving the inequality equivalent to (6.14) for the two-flavour quark-meson model. In the MIT bag model we chose the bag constant in such a way that strange quark matter is absolutely stable at zero pressure while two-flavour deconfined quark matter is unstable. We will do the equivalent here, but now it cannot be done analytically, as B is not an analytic function of any thermodynamical quantity. However, to find the upper limit of B_{vac} for strange quark matter to be absolutely stable, we need to know the thermodynamical potential for three flavours. Nevertheless, for structural purposes of this thesis, we will simply state the interval of which B_{vac} can take values from here, and paste the Mathematica code used to find the interval in App. B. The result is

$$27.1\,\mathrm{MeV} < B_{\mathrm{vac}}^{1/4} < 48.2\,\mathrm{MeV}. \tag{6.40}$$

---

[4]If you choose the starting value at e.g. $\mu_B = 0$ so that the next value of μ_B is less than what is required for ρ_B to be positive, you end up with an array which might contain slightly different values for B_{eff} at the same point, $v = f_\pi$. This is due to the uncertainties numerical calculations involve.

This is the bag-window for the most general systems we will discuss in this thesis. In these systems, electrons are included and the quarks have nonzero masses. Moreover, the up and down quarks have equal masses, m_q, and the strange quark have a mass $m_s \neq m_q$. This in turn implies that for three flavours, $\mu_u \neq \mu_d = \mu_s \neq \mu_e$ and for two flavours, $\mu_u \neq \mu_d \neq \mu_e$. Including the vacuum renormalisation of B, we can write the effective bag pressure B_{eff} as

$$B_{\text{eff}}(v_0) = B(v_0) - B(f_\pi) + B_{\text{vac}}. \tag{6.41}$$

Note that we model the compact star as a pure quark star, with no quark confinement, even though we require that two-flavour quark matter is unstable with respect to hadronic matter at zero pressure. However, at high enough pressures, two-flavour deconfined quark matter will take over as the stable state. We will come back to some of the problems in this model later.

Fig. 6.3 shows the two-flavour effective bag pressure, with a chosen vacuum normalisation of $B_{\text{vac}} = (40 \, \text{MeV})^4$, as a function of dimensionless baryon number density ρ_B/ρ_0. The nuclear matter saturation density ρ_0 is the number density of the ground state of nuclear matter at a fixed proton ratio [36]. We will set $\rho_0 = 0.17 \, (\text{fm})^{-3} = 1.306 \cdot 10^6 \, (\text{MeV})^3$, which is the normal nuclear density. We know from Fig. 6.2a that in the chiral limit, the minimum at $v > 0$ disappears for values of μ_B above a certain certain limit, and a new global minimum appears at $v = 0$. The consequence of this, is that several thermodynamical functions become discontinuous in the chiral limit, as we can see from B_{eff} and ρ_B in figure 6.3a. The consequence of this is that the interface between the two phases is sharp. Moreover, the density of the phase on one side of the interface is different from the density of the phase on the other side of the interface. Furthermore, the potential has two extrema in the chiral limit (in addition to the one at $v = 0$) when the chemical potential is close to the critical value at which the phase transition occurs. One must therefore be careful that the bag pressure and the thermodynamical functions are evaluated at the minimum of the thermodynamical potential, and not the local maximum. At the physical point, none of these issues are a problem, as the minimum v_0 goes continuously to zero as μ_B increases, and there is always only one extremum. The dashed line is the limiting value of B_{eff} as $\mu_B \to \infty$.

6.3.3 Mass-radius relation

It is time to finally calculate the mass-radius relation we obtain using this model of quark matter. For this we need the EoS, which is easy to find numerically using the procedure described in the previous section. The only adjustments we must do, is swapping B_{eff} with $\epsilon + B_{\text{eff}}$, and ρ_B with $p - B_{\text{eff}}$, in accordance with eqs. (6.6) and (6.7). Fig. 6.4 shows a plot of the EoS for the two-flavour quark-meson model compared to the MIT bag model EoS. Both the pressure and the energy density are normalised by ϵ_0; the energy density parameter introduced in section 5.2. The curve is very steep around $p = 0$. This is due to the rapid increase in the bag pressure at low densities seen in Fig. 6.3b. For high pressures (or equivalently, high densities), B_{eff} is approximately constant, and the two-flavour quark-meson EoS approaches to the ordinary MIT bag model EoS, $\epsilon = 3p + 4B$. To use this EoS in the TOV equation, we have to tell the program that the pressure is a function of r, that

(a) Chiral limit.

(b) Physical point. The dashed line is the asymptote of B_{eff}, which equals $(B_{\text{vac}} - B(f_\pi))^{1/4}$.
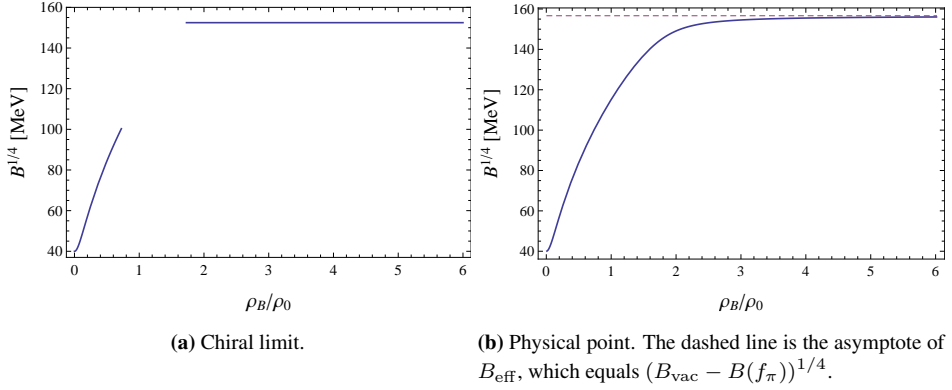
Figure 6.3: The effective bag pressure as a function of the baryon number density divided by the nuclear saturation density $\rho_0 = 0.17(\text{fm})^{-3} = 1.306 \cdot 10^6 (\text{MeV})^3$ at the physical point and in the chiral limit.
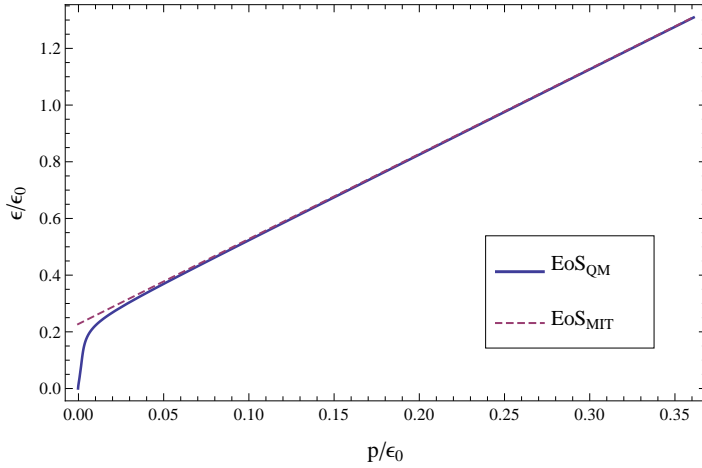
Figure 6.4: The EoS for the quark-meson model and the MIT bag model compared. For the quark-meson model the bag-pressure is normalised to $40\,(\text{MeV})^4$ in the vacuum, while the MIT bag constant is the limiting value of B_{eff} as μ_B goes to infinity, $B_{\text{MIT}} = B_{\text{vac}} - B(f_\pi) \approx (156.7\,\text{MeV})^4$.

$B_{\text{vac}}^{1/4}$ [MeV]	M_{max} [$M_{\odot}$]	R [km]
28	1.77	11.1
35	1.77	10.8
48	1.76	10.3

Table 6.2: Maximum masses with corresponding radii for different values of B_{vac}
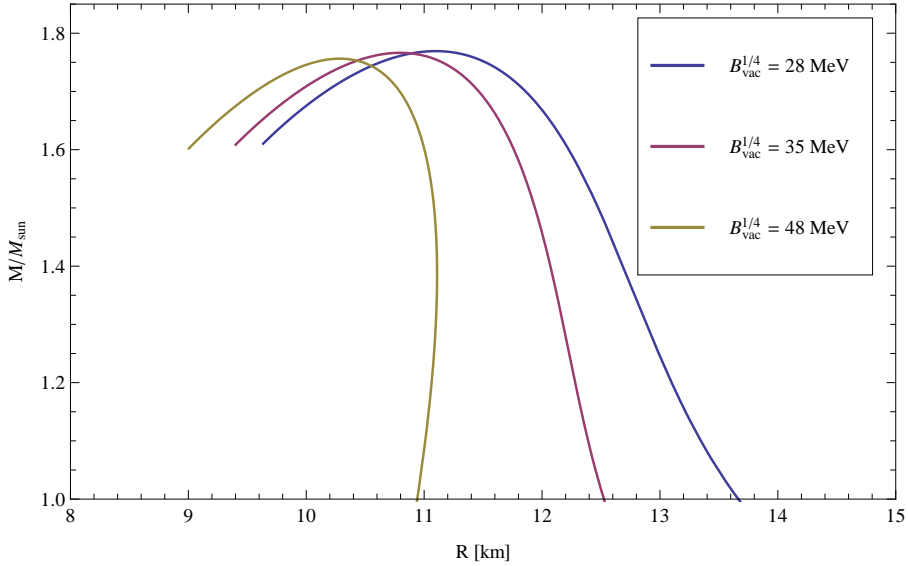
Figure 6.5: The mass-radius relation using the two-flavour quark-meson EoS with different normalisations of the effective bag pressure. Maximum masses with corresponding radii is shown in Table 6.2.

is $\epsilon(p) = \epsilon(p(r))$. In Mathematica, this can be done using the `With` command. Exactly how this is done is shown in Appendix B. The mass-radius relation obtained by using the two-flavour quark-meson EoS is shown in Fig. 6.5, and the maximum masses obtained for the different vacuum normalisations of the bag pressure is written in Table 6.2. We see that the maximum masses are less dependent on the vacuum renormalisation in the quark-meson model than in the MIT bag model, see Table 6.1 and Fig. 6.1. For a vacuum normalisation close to the lowest values in the bag intervals, the MIT bag model clearly predicts a greater maximum mass than the quark-meson model. However, for vacuum normalisations around the midpoint of the bag intervals, the two models predict a very similar maximum mass. When we choose the vacuum normalisation close to the largest values in the bag intervals, the quark-meson model predicts the largest maximum mass. We also note that the quark-meson model predicts a larger radius of the maximum-mass star for all three vacuum normalisations.

6.4 Three-flavour quark-meson model

The Lagrangian for the three-flavour quark-meson model is [37]

$$\mathcal{L} = \mathcal{L}_{\text{meson}} + \mathcal{L}_{\text{quark}} + \mathcal{L}_{\text{Yukawa}}, \tag{6.42}$$

where

$$\begin{aligned} \mathcal{L}_{\text{meson}} &= \text{Tr}\left[\left(\partial_\mu \Phi^\dagger\right)\left(\partial_\mu \Phi\right)\right] - m^2 \text{Tr}\left[\Phi^\dagger \Phi\right] - \lambda_1 \left[\text{Tr}\left(\Phi^\dagger \Phi\right)\right]^2 \\ &\quad - \lambda_2 \text{Tr}\left[\left(\Phi^\dagger \Phi\right)^2\right] + \text{Tr}\left[H\left(\Phi^\dagger + \Phi\right)\right], \end{aligned} \tag{6.43}$$

$$\mathcal{L}_{\text{quark}} = \bar{q}\left(i\slashed{\partial} + \mu_f \gamma^0\right) q, \tag{6.44}$$

$$\mathcal{L}_{\text{Yukawa}} = -g\bar{q}\, T_a(\sigma_a + i\gamma^5 \pi_a) q. \tag{6.45}$$

If $H = 0$, this Lagrangian is symmetric under $SU(3)_V \times SU(3)_A \times U(1)_B \times U(1)_A$. Here, $\Phi = T_a \Phi_a = T_a(\sigma_a + i\pi_a)$ is a complex 3×3-matrix and $T_a = \lambda_a/2$ with $a = 0, 1, ..., 8$ are the nine generators of the $U(3)$ symmetry, where λ_a are the eight Gell-Mann matrices and $\lambda_0 = \sqrt{\frac{2}{3}}I$. Moreover, σ_a are the scalar fields and π_a are the pseudoscalar meson nonet. $q = (u, d, s)$ is a column vector denoting the quark fields and $H = T_a h_a$ is a term for explicitly breaking chiral symmetry, corresponding to h in the two-flavour quark-meson model. The $U(3)$ algebra which T_a obey, is given by

$$[T_a, T_b] = if_{abc}T_c, \qquad \{T_a, T_b\} = d_{abc}T_c, \tag{6.46}$$

with f_{abc} and d_{abc} being the antisymmetric and symmetric structure constants of the $SU(3)$ group respectively. When one of the indices in the structure constants is zero, we have the identities

$$f_{ab0} = 0, \qquad d_{ab0} = \sqrt{\frac{2}{3}}\delta_{ab}. \tag{6.47}$$

The generators are normalised to $\text{Tr}\left[T_a T_b\right] = \delta_{ab}/2$. In analogy with the two-flavour quark-meson model, a nonzero vacuum expectation value $\langle\Phi\rangle$ of the field Φ spontaneously breaks the chiral symmetry [38]. Because of this, only the diagonal of H is nonzero. As λ_a has nonzero elements off the diagonal for $a \neq 0, 3, 8$, and all λ_a are independent, the only surviving components are h_0, h_3 and h_8. These components correspond to the vacuum expectation values $\langle\sigma\rangle_0 \equiv v_0$, $\langle\sigma\rangle_3 \equiv v_3$ and $\langle\sigma\rangle_8 \equiv v_8$ of the scalar fields. We will again assume that the mass, m_q, of the u and d quarks are equal. This is the equivalent of assuming isospin symmetri $SU(2)_V$, and since the current quark masses of the u and d quarks differ only by a few MeV, this is a good approximation. However, the strange quark mass, m_s is different from the light quark mass m_q. The term for explicitly breaking isospin symmetry is h_3. Assuming isospin symmetry, we must thus have $h_0 \neq 0$, $h_3 = 0$ and $h_8 \neq 0$ (or equivalently, swap h with $\langle\sigma\rangle$). The $SU(3)_V$ symmetry now breaks down to $SU(2)_V$ isospin symmetry.

The scalar fields v_0 and v_8 are a mixture of strange and non-strange parts. However, it is more convenient to separate the strangeness into a non-strange part v_x and a strange part v_y. This is done by the orthogonal basis transformation [37]

$$\begin{pmatrix} v_x \\ v_y \end{pmatrix} = \frac{1}{\sqrt{3}} \begin{pmatrix} \sqrt{2} & 1 \\ 1 & -\sqrt{2} \end{pmatrix} \begin{pmatrix} v_0 \\ v_8 \end{pmatrix}. \tag{6.48}$$

With this transformation, we can find the quark masses in terms of the expectation values v_x and v_y. The quark-mass term is

$$gT_a \langle \sigma_a \rangle = \frac{1}{2}(\lambda_0 v_0 + \lambda_8 v_8), \tag{6.49}$$

where

$$\lambda_8 = \frac{1}{\sqrt{3}} \begin{pmatrix} 1 & 0 & 0 \\ 0 & 1 & 0 \\ 0 & 0 & -2 \end{pmatrix}. \tag{6.50}$$

After transforming v_0 and v_8 and inserting λ_0 and λ_8, we obtain

$$\frac{g}{2}\bar{q}\, T_a \langle \sigma_a \rangle\, q = \frac{g}{2}(v_x u^2 + v_x d^2 + \sqrt{2}v_y s^2), \tag{6.51}$$

so the quark masses read

$$m_q = \frac{g}{2}v_x, \tag{6.52a}$$

$$m_s = \frac{g}{\sqrt{2}}v_y. \tag{6.52b}$$

6.4.1 The thermodynamical potential

In Appendix A.4, we show that the tree-level meson potential in the three-flavour quark-meson model reads

$$U(\sigma_a, \pi_a) = \frac{1}{2}m^2 \left(\sigma_a^2 + \pi_a^2 \right) + \frac{\lambda_1}{4} \left(\sigma_a^2 \sigma_b^2 + 2\sigma_a^2 \pi_b^2 + \pi_a^2 \pi_b^2 \right) - h_a \sigma_a$$
$$+ \frac{\lambda_2}{8}(\sigma_a - i\pi_a)(\sigma_b + i\pi_b)(\sigma_c - i\pi_c)(\sigma_d + i\pi_d)\mathcal{F}_{abcd}, \tag{6.53}$$

where the tensor $\mathcal{F}_{abcd}$ is defined as

$$\mathcal{F}_{abcd} \equiv [if_{abe}(if_{cde} + d_{cde}) + if_{ace}(-if_{bde} + d_{bde}) + d_{ade}(if_{bce} + d_{bce})]. \tag{6.54}$$

Written in terms of the vacuum expectation values v_x and v_y, the classical (tree-level) meson potential is

$$U(v_x, v_y) = \frac{1}{2}m^2 \left(v_x^2 + v_y^2 \right) + \frac{\lambda_1}{2}v_x^2 v_y^2 + \frac{1}{8}\left(2\lambda_1 + \lambda_2 \right) v_x^4$$
$$+ \frac{1}{8}(2\lambda_1 + 2\lambda_2)v_y^4 - h_x v_x - h_y v_y, \tag{6.55}$$

where h_0 and h_8 have been transformed into h_x and h_y according to eq. (6.48). The complete thermodynamical potential is again achieved by adding the one-loop quark potential

$V_q = -p$ to the meson potential,

$$
\begin{aligned}
V(v_x, v_y) =& \frac{1}{2}m^2\left(v_x^2 + v_y^2\right) + \frac{\lambda_1}{2}v_x^2 v_y^2 + \frac{1}{8}\left(2\lambda_1 + \lambda_2\right)v_x^4 + \frac{1}{8}(2\lambda_1 + 2\lambda_2)v_y^4 \\
& - h_x v_x - h_y v_y - \frac{\mu_e^4}{12\pi^2} + \frac{N_c}{16\pi^2}\sum_f m_f^4\left(\frac{1}{\epsilon} + \ln\frac{\Lambda^2}{m_f^2} + \frac{3}{2}\right) \\
& - \frac{N_c}{24\pi^2}\sum_f\left[\left(2\mu_f^2 - 5m_f^2\right)\mu_f\sqrt{\mu_f^2 - m_f^2} + 3m_f^4 \ln\left(\frac{\sqrt{\mu_f^2 - m_f^2} + \mu_f}{m_f}\right)\right].
\end{aligned}
\tag{6.56}
$$

To eliminate the divergent $1/\epsilon$-term, we must renormalise the coupling constants. The divergent term reads

$$
\begin{aligned}
\frac{N_c}{16\pi^2\epsilon}\sum_f m_f^4 &= \frac{N_c}{16\pi^2\epsilon}\left(2m_q^4 + m_s^4\right) \\
&= \frac{N_c g^4}{16\pi^2\epsilon}\left(\frac{1}{8}v_x^4 + \frac{1}{4}v_y^4\right),
\end{aligned}
\tag{6.57}
$$

which is similar to the term involving λ_2. Thus, by making the substitution $\lambda_2 \to \lambda_2 + \delta\lambda_2$ with

$$
\delta\lambda_2 = -\frac{N_c g^4}{16\pi^2\epsilon},
\tag{6.58}
$$

the divergences are cancelled. We thus end up with the finite, renormalised thermodynamical potential

$$
\begin{aligned}
V(v_x, v_y) =& \frac{1}{2}m^2\left(v_x^2 + v_y^2\right) + \frac{\lambda_1}{2}v_x^2 v_y^2 + \frac{1}{8}\left(2\lambda_1 + \lambda_2\right)v_x^4 + \frac{1}{8}(2\lambda_1 + 2\lambda_2)v_y^4 \\
& - h_x v_x - h_y v_y - \frac{\mu_e^4}{12\pi^2} + \frac{N_c}{16\pi^2}\sum_f m_f^4\left(\ln\frac{\Lambda^2}{m_f^2} + \frac{3}{2}\right) \\
& - \frac{N_c}{24\pi^2}\sum_f\left[\left(2\mu_f^2 - 5m_f^2\right)\mu_f\sqrt{\mu_f^2 - m_f^2} + 3m_f^4 \ln\left(\frac{\sqrt{\mu_f^2 - m_f^2} + \mu_f}{m_f}\right)\right].
\end{aligned}
\tag{6.59}
$$

In the next section we discuss how to fix the parameters in $V(v_x, v_y)$.

6.4.2 Parameter fitting

The mesonic part of the thermodynamical potential has five parameters, m^2, λ_1, λ_2, h_x and h_y, which must be fixed by five experimentally measured quantities. In analogy with the two-flavour quark-meson model, we will use the sigma mass m_σ, the pion mass m_π and the pion decay constant f_π as three of these quantities. For the two other experimentally measured quantities, we choose the kaon mass m_K, and the kaon decay constant f_K. In addition we must fix the Yukawa-coupling g which occurs in the quark masses, and the

values $\tilde{v}_x$ and $\tilde{v}_y$ of v_x and v_y which minimises the potential in the nonstrange and strange directions respectively, i.e.

$$\left.\frac{\partial U(v_x, v_y)}{\partial v_x}\right|_{v_x=\tilde{v}_x, v_y=\tilde{v}_y} = \left.\frac{\partial U(v_x, v_y)}{\partial v_y}\right|_{v_x=\tilde{v}_x, v_y=\tilde{v}_y} = 0. \tag{6.60}$$

In Ref. [39] the authors show that $\tilde{v}_x$ and $\tilde{v}_y$ is related to the decay constant f_a of the pseudoscalar meson nonet by

$$f_a = d_{aab}\tilde{v}_b, \tag{6.61}$$

where the summation is over the index b, but not over a. The pion and kaon decay constants are given by

$$f_\pi \equiv f_1 = d_{11a}\tilde{v}_a = \sqrt{\frac{2}{3}}\tilde{v}_0 + \frac{1}{\sqrt{3}}\tilde{v}_8, \tag{6.62}$$

$$f_K \equiv f_4 = d_{44a}\tilde{v}_a = \sqrt{\frac{2}{3}}\tilde{v}_0 - \frac{1}{2\sqrt{3}}\tilde{v}_8. \tag{6.63}$$

Here we used the relations (6.47) and (A.24). Using these relations, we can express $\tilde{v}_0$, $\tilde{v}_8$, $\tilde{v}_x$ and $\tilde{v}_y$ in terms of f_π and f_K as follows

$$\tilde{v}_0 = \frac{f_\pi + 2f_K}{\sqrt{6}}, \qquad \tilde{v}_8 = \frac{2}{\sqrt{3}}(f_\pi - f_K), \tag{6.64}$$

$$\tilde{v}_x = f_\pi, \qquad \tilde{v}_y = \frac{1}{\sqrt{2}}(2f_K - f_\pi). \tag{6.65}$$

For simplicity, we will use $\tilde{v}_0$ and $\tilde{v}_8$ when fixing the parameters involved in the thermodynamical potential. The mass matrices identified with the scalar and pseudoscalar meson nonets are defined as

$$\left(M_\sigma^2\right)_{kl} \equiv \left.\frac{\partial^2 U(\sigma_a, \pi_a)}{\partial \sigma_k \partial \sigma_l}\right|_{\sigma_a=\tilde{v}_a, \pi_a=0}, \tag{6.66}$$

$$\left(M_\pi^2\right)_{kl} \equiv \left.\frac{\partial^2 U(\sigma_a, \pi_a)}{\partial \pi_k \partial \pi_l}\right|_{\sigma_a=\tilde{v}_a, \pi_a=0}. \tag{6.67}$$

Since only the expectation value of σ_a is nonzero, terms proportional to π_a vanish in $\left(M_\sigma^2\right)_{kl}$. As explained in Appendix A.4, the last term of eq. (6.53) can be simplified by noting that the only contributing term from $\mathcal{F}_{abcd}$ is $d_{ade}d_{bce}$. Furthermore, since d_{abc} is symmetric under permutations of the indices, we find

$$\frac{\partial}{\partial \sigma_k}(\sigma_a\sigma_b\sigma_c\sigma_d)d_{ade}d_{bce} = 4\sigma_a\sigma_b\sigma_c d_{abe}d_{cke}. \tag{6.68}$$

When taking the derivative of this with respect to σ_l, we must be more careful. Now it does matter if the index l is in d_{abe} or d_{cke}, because we do not sum over k. We thus find

$$\frac{\lambda_2}{8}\frac{\partial^2}{\partial \sigma_k \partial \sigma_l}(\sigma_a\sigma_b\sigma_c\sigma_d)d_{ade}d_{bce} = \frac{\lambda_2}{2}\sigma_a\sigma_b\mathcal{G}_{abkl}, \tag{6.69}$$

where

$$\mathcal{G}_{abkl} \equiv d_{abe}d_{kle} + 2d_{ake}d_{ble}. \tag{6.70}$$

Furthermore, we have

$$\frac{\partial^2}{\partial\sigma_k\partial\sigma_l}\left(\frac{\lambda_1}{4}\sigma_a^2\sigma_b^2\right) = \frac{\partial}{\partial\sigma_k}\left(\lambda_1\sigma_a^2\sigma_l\right)$$
$$= \lambda_1\sigma_a^2\delta_{kl} + 2\lambda_1\sigma_k\sigma_l, \tag{6.71}$$

and

$$\frac{\partial^2}{\partial\sigma_k\partial\sigma_l}\left(\frac{1}{2}m^2\sigma_a^2\right) = m^2\delta_{kl}. \tag{6.72}$$

Combining all the contributions to the scalar mass matrix, we obtain

$$\left(M_\sigma^2\right)_{kl} = m^2\delta_{kl} + \lambda_1\tilde{v}_a^2\delta_{kl} + 2\lambda_1\tilde{v}_k\tilde{v}_l + \frac{\lambda_2}{2}\tilde{v}_a\tilde{v}_b\mathcal{G}_{abkl}. \tag{6.73}$$

When calculating $\left(M_\pi^2\right)_{kl}$, the only terms contributing are terms proportional to $\pi_a\pi_b$. Our argument that the only term contributing from $\mathcal{F}_{abcd}$ is $d_{ade}d_{bce}$ is not valid for the pseudoscalar mass matrix. Now, terms of the form $\sigma_a\sigma_b\pi_c\pi_d f_{ace}f_{bde}$ also contribute as the indices of the scalar fields are not both in the same structure constant. The contributing terms proportional to λ_2 become (see the end of Appendix A.4 for details)

$$\frac{\lambda_2}{4}\sigma_a\sigma_b\pi_c\pi_d\mathcal{H}_{abcd}, \tag{6.74}$$

where

$$\mathcal{H}_{abcd} = f_{ace}f_{bde} + f_{ade}f_{bce} + d_{abe}d_{cde}. \tag{6.75}$$

Differentiating eq. (6.74) with respect to $\pi_k\pi_l$ yields

$$\frac{\lambda_2}{4}\sigma_a\sigma_b\left(\mathcal{H}_{abkl} + \mathcal{H}_{ablk}\right) = \frac{\lambda_2}{2}\sigma_a\sigma_b\mathcal{H}_{abkl}. \tag{6.76}$$

Furthermore, we have

$$\frac{\partial^2}{\partial\pi_k\partial\pi_l}\left(\frac{1}{2}m^2\pi_a^2 + \frac{\lambda_1}{2}\sigma_a^2\pi_b^2\right) = m^2\delta_{kl} + \lambda_1\sigma_a^2\delta_{kl}. \tag{6.77}$$

Hence, the pseudoscalar mass matrix is

$$\left(M_\pi^2\right)_{kl} = m^2\delta_{kl} + \lambda_1\tilde{v}_a^2\delta_{kl} + \frac{\lambda_2}{2}\tilde{v}_a\tilde{v}_b\mathcal{H}_{abkl}. \tag{6.78}$$

In general, the mass matrices $\left(M_\pi^2\right)_{kl}$ and $\left(M_\sigma^2\right)_{kl}$ are not diagonal. This implies that the fields σ_a and π_a are not mass eigenstates [39]. Nevertheless, the mass matrices are symmetric and real, so they can be diagonalised by an orthogonal transformation,

$$\tilde{\sigma}_i = O_{ia}^{(\sigma)}\sigma_a, \tag{6.79a}$$

$$\tilde{\pi}_i = O_{ia}^{(\pi)}\pi_a, \tag{6.79b}$$

$$\left(\tilde{M}_{\sigma,\pi}^2\right)_i = O_{ai}^{(\sigma,\pi)}\left(M_{\sigma,\pi}^2\right)_{ab}O_{bi}^{(\sigma,\pi)}. \tag{6.79c}$$

In Appendix A.5, we calculate the nonzero components of the scalar mass matrix and find

$$\left(M_\sigma^2\right)_{00} = m^2 + \lambda_1 \left(3\tilde{v}_0^2 + \tilde{v}_8^2\right) + \lambda_2 \left(\tilde{v}_0^2 + \tilde{v}_8^2\right), \tag{6.80a}$$

$$\left(M_\sigma^2\right)_{11} = \left(M_\sigma^2\right)_{22} = \left(M_\sigma^2\right)_{33}$$
$$= m^2 + \lambda_1 \left(\tilde{v}_0^2 + \tilde{v}_8^2\right) + \lambda_2 \left(\tilde{v}_0^2 + \frac{1}{2}\tilde{v}_8^2 + \sqrt{2}\tilde{v}_0\tilde{v}_8\right), \tag{6.80b}$$

$$\left(M_\sigma^2\right)_{44} = \left(M_\sigma^2\right)_{55} = \left(M_\sigma^2\right)_{66} = \left(M_\sigma^2\right)_{77}$$
$$= m^2 + \lambda_1 \left(\tilde{v}_0^2 + \tilde{v}_8^2\right) + \lambda_2 \left(\tilde{v}_0^2 + \frac{1}{2}\tilde{v}_8^2 - \frac{1}{\sqrt{2}}\tilde{v}_0\tilde{v}_8\right), \tag{6.80c}$$

$$\left(M_\sigma^2\right)_{88} = m^2 + \lambda_1 \left(\tilde{v}_0^2 + 3\tilde{v}_8^2\right) + \lambda_2 \left(\tilde{v}_0^2 + \frac{3}{2}\tilde{v}_8^2 - \sqrt{2}\tilde{v}_0\tilde{v}_8\right), \tag{6.80d}$$

$$\left(M_\sigma^2\right)_{08} = \left(M_\sigma^2\right)_{80} = 2\lambda_1\tilde{v}_0\tilde{v}_8 + \lambda_2 \left(-\frac{1}{\sqrt{2}}\tilde{v}_8^2 + 2\tilde{v}_0\tilde{v}_8\right). \tag{6.80e}$$

The mass, m_σ, of the sigma meson is defined as the zeroth component of the diagonalised matrix $\left(\tilde{M}_\sigma^2\right)$,

$$m_\sigma^2 \equiv \left(\tilde{M}_\sigma^2\right)_0 = O_{a0}^{(\sigma)} \left(M_\sigma^2\right)_{ab} O_{b0}^{(\sigma)}. \tag{6.81}$$

We define $O_{00}^{(\sigma)} \equiv \cos\theta_\sigma$ and $O_{80}^{(\sigma)} \equiv \sin\theta_\sigma$. Since the only nonzero components off the diagonal of $\left(M_\sigma^2\right)$ is component (08) and (80), we have $O_{i0} = 0$ for $i \neq 0, 8$. The sigma mass is thus given by

$$m_\sigma^2 = O_{00}^{(\sigma)} \left[\left(M_\sigma^2\right)_{00} O_{00}^{(\sigma)} + \left(M_\sigma^2\right)_{08} O_{80}^{(\sigma)}\right] + O_{80}^{(\sigma)} \left[\left(M_\sigma^2\right)_{80} O_{00}^{(\sigma)} + \left(M_\sigma^2\right)_{88} O_{80}^{(\sigma)}\right]$$
$$= \left(M_\sigma^2\right)_{00} \cos^2\theta_\sigma + \left(M_\sigma^2\right)_{88} \sin^2\theta_\sigma + 2\left(M_\sigma^2\right)_{08} \cos\theta_\sigma \sin\theta_\sigma. \tag{6.82}$$

To find θ_σ, we use the eigenvector equation

$$\left[\left(M_\sigma^2\right) - \lambda_0\right] O_{a0} = \mathbf{0}, \tag{6.83}$$

where λ_0 is the egeinvalue of $\left(M_\sigma^2\right)$, corresponding to the eigenvector O_{a0}. This gives

$$\left[\left(M_\sigma^2\right)_{00} - \lambda_0\right] \cos\theta_\sigma = -\left(M_\sigma^2\right)_{08} \sin\theta_\sigma, \tag{6.84a}$$

$$\left[\left(M_\sigma^2\right)_{88} - \lambda_0\right] \sin\theta_\sigma = -\left(M_\sigma^2\right)_{08} \cos\theta_\sigma. \tag{6.84b}$$

From these eqs., we obtain the relations

$$\sin\theta_\sigma = -\frac{\left(M_\sigma^2\right)_{00} - \lambda_0}{\left(M_\sigma^2\right)_{08}} \cos\theta_\sigma, \tag{6.85a}$$

$$\sin\theta_\sigma = -\frac{\left(M_\sigma^2\right)_{08}}{\left(M_\sigma^2\right)_{88} - \lambda_0} \cos\theta_\sigma, \tag{6.85b}$$

$$\sin^2\theta_\sigma = \frac{\left(M_\sigma^2\right)_{00} - \lambda_0}{\left(M_\sigma^2\right)_{88} - \lambda_0} \cos^2\theta_\sigma. \tag{6.85c}$$

Hence, θ_σ is determined by the equation

$$
\begin{aligned}
\tan 2\theta_\sigma &= \frac{2\sin\theta_\sigma \cos\theta_\sigma}{\cos^2\theta_\sigma - \sin^2\theta_\sigma} \\
&= \frac{-2\left(M_\sigma^2\right)_{08}}{\left(M_\sigma^2\right)_{88} - \lambda_0 - \left(M_\sigma^2\right)_{00} + \lambda_0} \\
&= \frac{2\left(M_\sigma^2\right)_{08}}{\left(M_\sigma^2\right)_{00} - \left(M_\sigma^2\right)_{88}}.
\end{aligned}
\tag{6.86}
$$

Eq. (6.82) is one of the three equations needed to determine m^2, λ_1 and λ_2. The two other equations are found from the pseudoscalar mass matrix. In Appendix A.5, we calculate the nonzero components of $\left(M_\pi^2\right)$ and find

$$
\left(M_\pi^2\right)_{00} = m^2 + \lambda_1\left(\tilde{v}_0^2 + \tilde{v}_8^2\right) + \frac{\lambda_2}{3}\left(\tilde{v}_0^2 + \tilde{v}_8^2\right),
\tag{6.87a}
$$

$$
\begin{aligned}
\left(M_\pi^2\right)_{11} &= \left(M_\pi^2\right)_{22} = \left(M_\pi^2\right)_{33} \\
&= m^2 + \lambda_1\left(\tilde{v}_0^2 + \tilde{v}_8^2\right) + \frac{\lambda_2}{3}\left(\tilde{v}_0^2 + \frac{1}{2}\tilde{v}_8^2 + \sqrt{2}\tilde{v}_0\tilde{v}_8\right),
\end{aligned}
\tag{6.87b}
$$

$$
\begin{aligned}
\left(M_\pi^2\right)_{44} &= \left(M_\pi^2\right)_{55} = \left(M_\pi^2\right)_{66} = \left(M_\pi^2\right)_{77} \\
&= m^2 + \lambda_1\left(\tilde{v}_0^2 + \tilde{v}_8^2\right) + \frac{\lambda_2}{3}\left(\tilde{v}_0^2 + \frac{7}{2}\tilde{v}_8^2 - \frac{\sqrt{2}}{2}\tilde{v}_0\tilde{v}_8\right),
\end{aligned}
\tag{6.87c}
$$

$$
\left(M_\pi^2\right)_{88} = m^2 + \lambda_1\left(\tilde{v}_0^2 + \tilde{v}_8^2\right) + \frac{\lambda_2}{3}\left(\tilde{v}_0^2 + \frac{3}{2}\tilde{v}_8^2 - \sqrt{2}\tilde{v}_0\tilde{v}_8\right),
\tag{6.87d}
$$

$$
\left(M_\pi^2\right)_{08} = \left(M_\pi^2\right)_{80} = -\frac{\lambda_2}{3}\left(\tilde{v}_8^2 - 2\tilde{v}_0\tilde{v}_8\right).
\tag{6.87e}
$$

The pion mass and kaon mass are related to the pseudoscalar mass matrix by $m_\pi^2 \equiv \left(M_\pi^2\right)_{11}$ and $m_K^2 = \left(M_\pi^2\right)_{44}$ respectively. Hence, the final two equations needed to determine m^2, λ_1 and λ_2 are

$$
m_\pi^2 = m^2 + \lambda_1\left(\tilde{v}_0^2 + \tilde{v}_8^2\right) + \frac{\lambda_2}{3}\left(\tilde{v}_0^2 + \frac{1}{2}\tilde{v}_8^2 + \sqrt{2}\tilde{v}_0\tilde{v}_8\right),
\tag{6.88}
$$

$$
m_K^2 = m^2 + \lambda_1\left(\tilde{v}_0^2 + \tilde{v}_8^2\right) + \frac{\lambda_2}{3}\left(\tilde{v}_0^2 + \frac{7}{2}\tilde{v}_8^2 - \frac{\sqrt{2}}{2}\tilde{v}_0\tilde{v}_8\right).
\tag{6.89}
$$

If we subtract eq. (6.88) from eq. (6.89), we get an analytically solvable equation for λ_2,

$$
m_K^2 - m_\pi^2 = \frac{\lambda_2}{3}\left(3\tilde{v}_8^2 - \frac{3\sqrt{2}}{2}\tilde{v}_0\tilde{v}_8\right).
\tag{6.90}
$$

Solving this equations for λ_2 and inserting eqs. (6.64) yields

$$
\begin{aligned}
\lambda_2 &= \frac{m_K^2 - m_\pi^2}{\tilde{v}_8^2 - \frac{\sqrt{2}}{2}\tilde{v}_0\tilde{v}_8} \\
&= \frac{m_K^2 - m_\pi^2}{(2f_K - f_\pi)(f_K - f_\pi)}.
\end{aligned}
\tag{6.91}
$$

The coupling constant λ_1 and the mass parameter m^2 can in general not be solved analytically, but are related to each other from eqs. (6.88) and (6.89). Moreover, λ_1 is fixed by the value of the sigma meson mass through eq. (6.82). Knowing λ_2 and the relation between m^2 and λ_1, we find the explicit symmetry breaking terms h_x and h_y analytically from eqs. (6.60),

$$h_x = f_\pi m_\pi^2, \tag{6.92}$$

$$h_y = \frac{1}{\sqrt{2}} \left(2 f_K m_K^2 - f_\pi m_\pi^2\right). \tag{6.93}$$

Note that h_x is identical to the explicit symmetry breaking term for two flavours, h.

We can now find numerical values for all the parameters in the meson potential. Using the experimental values

$$f_\pi = 93 \,\text{MeV}, \qquad m_\pi = 138 \,\text{MeV}, \tag{6.94}$$

$$f_K = 113 \,\text{MeV}, \qquad m_K = 496 \,\text{MeV}, \tag{6.95}$$

$$m_\sigma = 800 \,\text{MeV}, \tag{6.96}$$

we get

$$\lambda_1 = -6.19, \qquad \lambda_2 = 85.3, \tag{6.97}$$

$$h_x = (121.0 \,\text{MeV})^3, \qquad h_y = (336.4 \,\text{MeV})^3, \tag{6.98}$$

$$m^2 = -(491.7 \,\text{MeV})^2. \tag{6.99}$$

In analogy with the two-flavour quark-meson model, the Yukawa coupling constant g is fixed from the constituent quark mass of the u and d quarks,

$$g = \frac{2\tilde{m}_q}{\tilde{v}_x} = 6.45. \tag{6.100}$$

The only parameter that is not yet fixed is the renormalisation scale Λ from the quark contribution to V. In the two-flavour quark-meson model we fixed the renormalisation scale by requiring that the minimum of the thermodynamical potential in vacuum is located at $v = f_\pi$. The corresponding requirement in the three-flavour quark-meson model is that eqs. (6.60) should still be valid if we swap $U(v_x, v_y)$ by $V(v_x, v_y)$ and set $\mu_f = 0$. This is, however, impossible to accomplish solely by fixing Λ, since the values of Λ that minimises the potential in the nonstrange and strange directions are not equal. We minimise the vacuum part of $V(v_x, v_y)$ in the nonstrange direction by solving

$$\left.\frac{\partial V(v_x, v_y)}{\partial v_x}\right|_{\mu_f=0, v_x=\tilde{v}_x, v_y=\tilde{v}_y} = 0. \tag{6.101}$$

This yields the same renormalisation scale as in the two-flavour quark-meson model, because the strange-part of the potential vanishes when differentiating with respect to v_x.

The value of Λ which minimises the potential in the nonstrange direction is therefore $\Lambda = 182\,\text{MeV} \equiv \Lambda_x$. When minimising $V(v_x, v_y)$ in the strange direction, i.e. solving

$$\frac{\partial V(v_x, v_y)}{\partial v_y}\bigg|_{\mu_f=0,\,v_x=\tilde{v}_x,\,v_y=\tilde{v}_y} = 0, \tag{6.102}$$

we obtain

$$\Lambda = 260\,\text{MeV} \equiv \Lambda_y. \tag{6.103}$$

Since the renormalisation scale can only have one value, we choose the average value

$$\Lambda \equiv \frac{2\Lambda_x + \Lambda_y}{3} \approx 208\,\text{MeV}, \tag{6.104}$$

where the nonstrange part counts twice; once for the u quark and once for the d quark. Now that we have all the parameters fixed, it is time to look at the three-flavour effective bag pressure.

6.4.3   The three-flavour effective bag pressure

In section 6.3.2 we showed how to extract an effective bag pressure from the two-flavour thermodynamical potential. We will follow the same procedure here, but now the thermodynamical quantities are functions of two variables instead of one variable. Extracting the vacuum part of the thermodynamical potential, the non-normalised bag pressure becomes

$$B(\bar{v}_x, \bar{v}_y) = \frac{1}{2}m^2 \left(\bar{v}_x^2 + \bar{v}_y^2\right) + \frac{\lambda_1}{2}\bar{v}_x^2\bar{v}_y^2 + \frac{1}{8}\left(2\lambda_1 + \lambda_2\right)\bar{v}_x^4 + \frac{1}{8}(2\lambda_1 + 2\lambda_2)\bar{v}_y^4$$
$$- h_x\bar{v}_x - h_y\bar{v}_y + \frac{N_c}{16\pi^2}\sum_f m_f^4 \left(\ln\frac{\Lambda^2}{m_f^2} + \frac{3}{2}\right), \tag{6.105}$$

where $\bar{v}_x$ and $\bar{v}_y$ are the values of v_x and v_y that minimise $V(v_x, v_y)$ for a given chemical potential μ_B. It is important to remember that the quark masses are dependent on $\bar{v}_x$ or $\bar{v}_y$ by eqs. (6.52). To determine $\bar{v}_x$, $\bar{v}_y$ and the chemical potential μ_e, we must solve three coupled equations simultaneously for a chosen baryon chemical potential μ_B. These equations are

$$\frac{\partial V(v_x, v_y)}{\partial v_x} = 0, \qquad \frac{\partial V(v_x, v_y)}{\partial v_y} = 0, \tag{6.106a}$$

$$2\left[\mu_u^2 - m_q(v_x)^2\right]^{3/2} - \left[\mu_d^2 - m_q(v_x)^2\right]^{3/2} - \left[\mu_d^2 - m_s(v_y)^2\right]^{3/2} - \mu_e^3 = 0. \tag{6.106b}$$

Note that we replaced μ_s by μ_d, according to eq. (6.4c). When we know μ_B and μ_e the quark chemical potentials μ_f are given by eqs. (6.5). We will normalise the three-flavour bag pressure in the same manner as done for the two-flavour bag pressure. Hence, we define

$$B_{\text{eff}}(\bar{v}_x, \bar{v}_y) = B(\bar{v}_x, \bar{v}_y) - B(\tilde{v}_x, \tilde{v}_y) + B_{\text{vac}}, \tag{6.107}$$

where $\tilde{v}_x$ and $\tilde{v}_y$ are given in eqs. (6.65), and B_{vac} takes values from the bag-window (6.40). To find the effective bag pressure as a function of ρ_B, we follow the exact same procedure as given in section 6.3.2,

1. Choose a starting value for the baryon chemical potential $\mu_B = \mu_{B,\min}$. To avoid numerical problems, this value should be close to the largest value of μ_B that still describes the vacuum, $\rho_B = 0$. For the set of parameter values used here (found in the previous section), $\mu_{B,\min} \approx 860\,\mathrm{MeV}$ is a fitting starting value.

2. Make a loop that goes from $i = 1$ to $i = N$.

3. Solve the coupled equations (6.106). Calculate $B_{\mathrm{eff}}(v_0)$ and insert the value in component $(i, 2)$ of and $N \times 2$ array. In component $(i, 1)$ we insert the baryon number density.

4. Increase μ by a small amount, say $\mu_B = \mu_{B,i} + \frac{\mu_{B,\max} - \mu_{B,\min}}{N-1}$, where $\mu_{B,\min} \equiv \mu_{B,1}$ and $\mu_{B,\max} \equiv \mu_{B,N}$ are the smalles and largest physically relevant chemical potentials. Choosing $\mu_{B,\max}$ in the range $1500 - 1800\,\mathrm{MeV}$ should hold. Increase i by one and close the loop.

5. Use the built-in Mathematica function `Interpolation` on the array. This will produce an approximation of the function $B_{\mathrm{eff}}(\rho_B)$.

We have plotted the effective bag pressures for both two and three flavours as functions of the baryon number density in Fig. 6.6. Again, we chose to normalise the bag pressure at $B_{\mathrm{vac}} = (40\,\mathrm{MeV})^4$, as this is a convenient number close to the midpoint of the bag-window. We see that for $\rho_B \lesssim 4\rho_0$, the two- and three-flavour bag pressures are almost identical. Hence, the strange quarks are not present for baryon number densities smaller than about four times the nuclear saturation density. However, they do increase the bag pressure significantly at high densities. This implies that three-flavour quark matter is bound tighter together than two-flavour quark matter. In Fig. 6.7 we see the quark and electron distributions as functions of the baryon number density. Here, $\rho_{\mathrm{tot}} \equiv \rho_u + \rho_d + \rho_s + \rho_e$ is the total number density. Indeed, we see that the strange quarks first appear at baryon number densities $\rho_B \approx 4\rho_0$. The density of the u quarks remains almost constant at $\rho_{\mathrm{tot}}/3$ in all baryon number density regimes. This is the exact density of the up quarks if there are no electrons present. In addition, we see that the electron density is very small (but not zero, see Fig. 6.8b) compared to ρ_{tot} for $\rho_B > 0$. Worth noticing is also the relation between the densities of the d and s quarks. Summed up, they always amount to about two-thirds of the total number density. This is expected from the equilibrium requirement (6.3c). At very high densities, the strange quark mass will be small compared to it's chemical potential μ_s. The three-flavour quark matter will then be composed of almost an equal amount of up, down and strange quarks. This describes the colour-flavour locked (CFL) phase [26], where no electrons are needed to maintain charge neutrality. If the strange quark matter hypothesis is true, the CFL phase will be absolutely stable. Strangelets may thus be formed in the high-density regions of a hybrid star and convert the entire star into a pure quark star, as discussed in section 6.2.2.

Fig. 6.8a shows the quark masses as functions of the baryon number density. The quark masses are given by eq. (6.52) with v_x and v_y replaced by $\bar{v}_x$ and $\bar{v}_y$ respectively. Therefore we also find a mass of the strange quark in the low-density region where the strange quarks do not exist. However, this will not affect any thermodynamical quantities as the contribution from the s quark in this region will be imaginary. The u and d quark
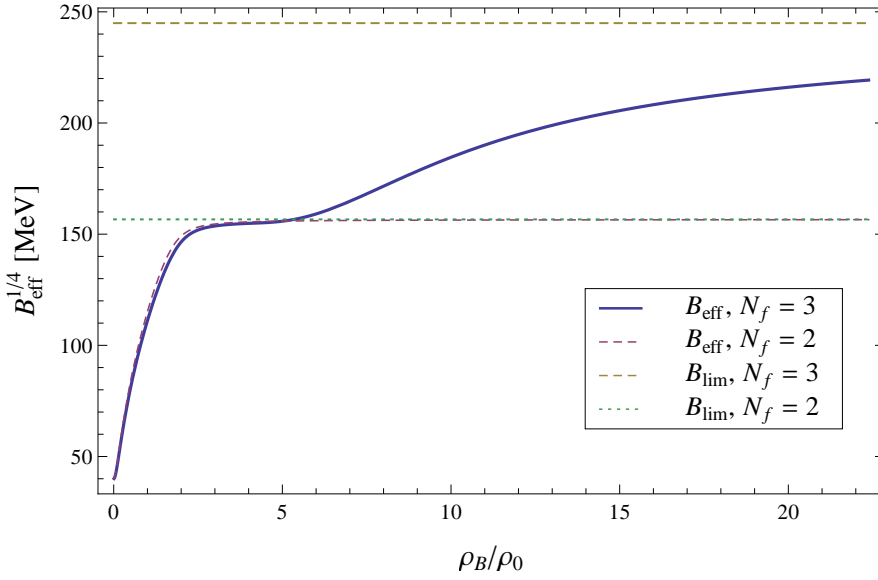
Figure 6.6: The effective bag pressures for two- and three-flavour quark matter as functions of the dimensionless baryon number density. The dotted and dashed lines are the asymptotes of $B_{\text{eff}}^{1/4}$ for two and three flavours respectively. To show the ultra high density regimes, we have included baryon chemical potentials up to $2.0\,\text{GeV}$.
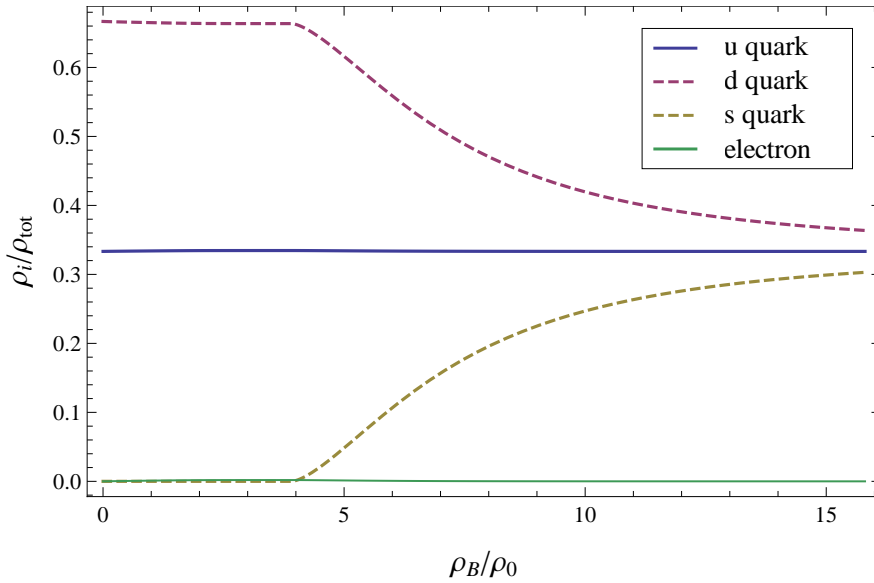
Figure 6.7: The quark and electron number densities as functions of the baryon number density.

masses decrease quite rapidly for low densities, and approaches zero as the density goes to infinity. Comparing Fig. 6.8a with 6.8b, we see that $m_q^2 \ll \mu_{u,d}^2$ for $\rho_B \gtrsim 5\rho_0$, implying that the u and d quarks appear approximately massless even for moderate densities. The strange quark mass will, however, never become negligible compared to μ_s in the density region covered in Fig. 6.8. Note that none of the quantities described in Figs. 6.7 and 6.8 depends on B_{eff}, so these plots are unaffected by the bag pressure.
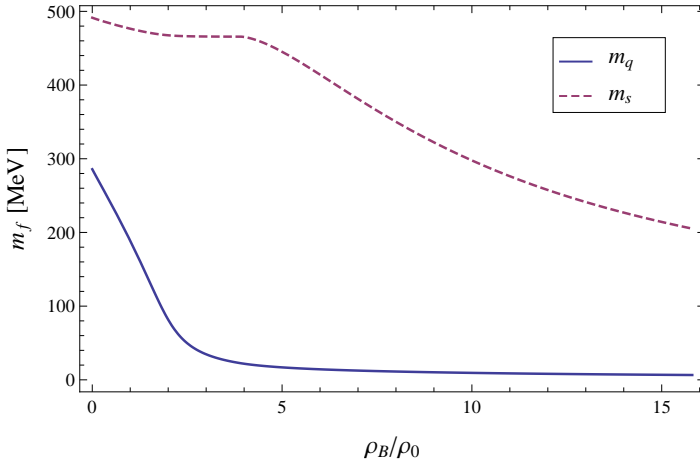
(a) The quark masses as functions of the baryon number density.
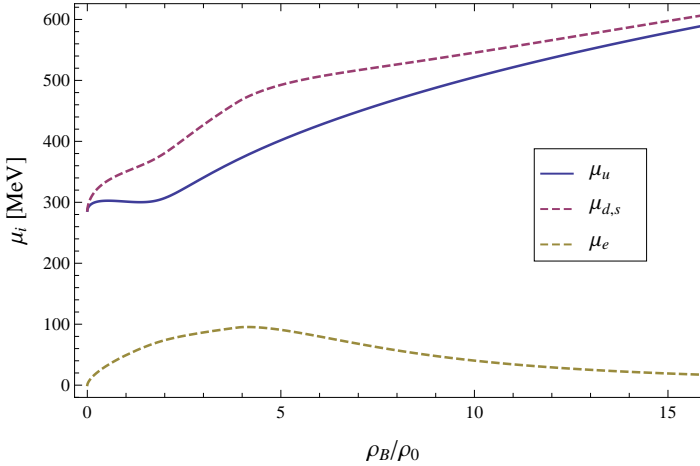
(b) The quark and electron chemical potentials as functions of the baryon number density.

Figure 6.8: The quark masses and chemical potentials as functions of the dimensionless baryon number density. The baryon chemical potential ranges from $860\,\mathrm{MeV}$ to $1800\,\mathrm{MeV}$.

Figure 6.9: The EoS for the quark-meson model and the MIT bag model compared. For the quark-meson model the bag-pressure is normalised to $40\,(\text{MeV})^4$ in the vacuum, while the MIT bag constant is the limiting value of B_{eff} as μ_B goes to infinity, $B_{\text{MIT}} = B_{\text{vac}} - B(f_\pi) \approx (156.7\,\text{MeV})^4$.

6.4.4 Mass-radius relation

The EoS we obtain for the three-flavour quark-meson model using an effective bag pressure is showed in Fig. 6.9. Due to the similar form of the two-flavour bag pressure and the three-fla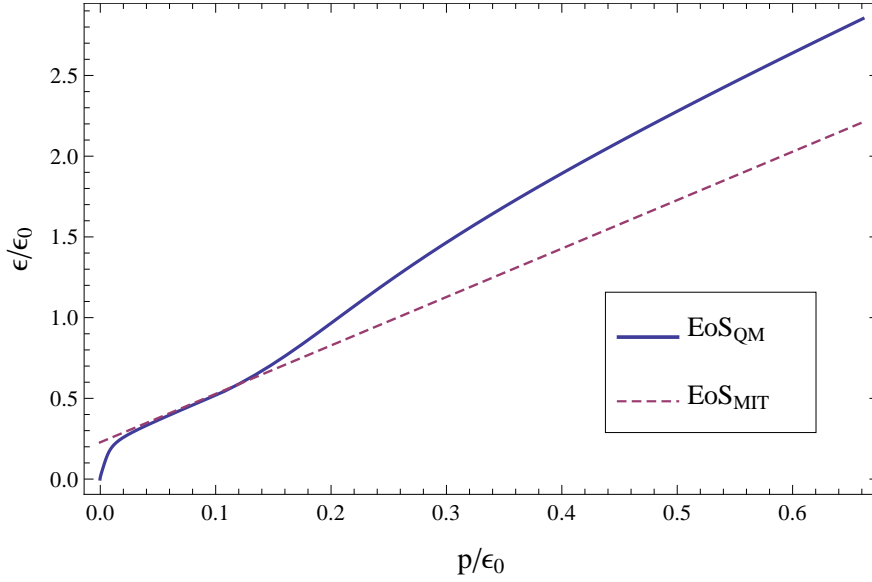vour bag-pressure for $\rho_B \lesssim 4\rho_0$, the three-flavour EoS is almost identical to the two-flavour EoS for $p \lesssim 0.1\epsilon_0$. Note the similarities between the EoS and the shape of the curve in Fig 6.6. This is expected since $\epsilon = \sum_f \epsilon_f + \epsilon_e + B_{\text{eff}}$ and $p = \sum_f p_f + p_e - B_{\text{eff}}$, where ϵ_e and p_e are the electron energy density and electron pressure respectively. The mass-radius relation obtained by using the three-flavour EoS in the TOV equation is shown in Fig. 6.10. The maximum masses with corresponding radii for the different normalisations of the bag pressure is written in Table 6.3. Comparing Table 6.2 with Table 6.3, we see that the maximum masses are just slightly larger for three flavours than for two flavours. The radii, however, are increased by over a km for these bag normalisations. It seems like the maximum mass and the corresponding radius varies slightly more with the bag normalisation for three flavours than for two flavours.

$B_{\text{vac}}^{1/4}$ [MeV]	$M_{\text{max}}\,[M_\odot]$	R [km]
28	1.79	13.1
35	1.78	12.5
48	1.76	11.6

Table 6.3: Maximum masses with corresponding radii for different values of B_{vac}
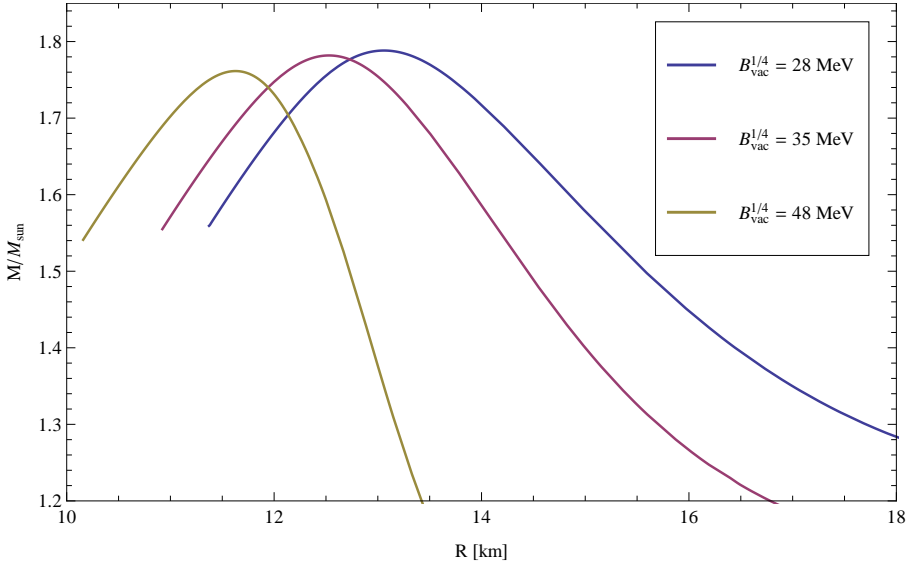
Figure 6.10: Various mass-radius relations using the three-flavour quark-meson EoS with different normalisations of the effective bag pressure. Maximum masses with corresponding radii are shown in Table 6.3.

Since we studied how some physical quantities in the three-flavour quark-meson model varied with the baryon number density in the previous section, it is interesting to see how the baryon number density varies with the distance from the center of the maximum mass star. This is shown for $B_{\mathrm{vac}} = (48\,\mathrm{MeV})^4$ in Fig. 6.11. For this star, the baryon number density ranges from $0.17\rho_0$ at the surface, $r = R = 11.6\,\mathrm{km}$, to $6.0\rho_0$ in the center. Since strange quarks appear at $\rho_B \gtrsim 4\rho_0$ in this model, the star will be made out of strange quark matter from the center of the star and about 4 km out from the center. For distances larger than 4 km from the center, the quark star described will be made of deconfined two-flavour quark matter. The importance of this result cannot be ignored: We find that the quark star is consists of two-flavour deconfined quark matter close to the surface of the star, even though we renormalised the bag pressure assuming that two-flavour deconfined quark matter is unstable at zero pressure, i.e. at the surface. Hence, we cannot describe a pure quark star by assuming that the strange quark matter hypothesis is true using the three-flavour quark-meson model with an effective bag pressure, as this results in a contradiction. Once again, this can be explained by the rapid increase of the effective bag pressure. Because B_{eff} increase so fast at low densities, the pressure from the quarks and electrons are counterbalanced by the bag pressure before ρ_B reach high enough densities for strange quarks to be made. In this way, both the upper and lower limits in the bag-window (6.40), are effectively found from two slightly different two-flavour models. The relatively large bag-window (which is roughly the same size as the bag-window found in the MIT bag model) might be explained by the impossibility of requiring that the minimum of the vacuum quark contribution to the thermodynamical potential should be located at
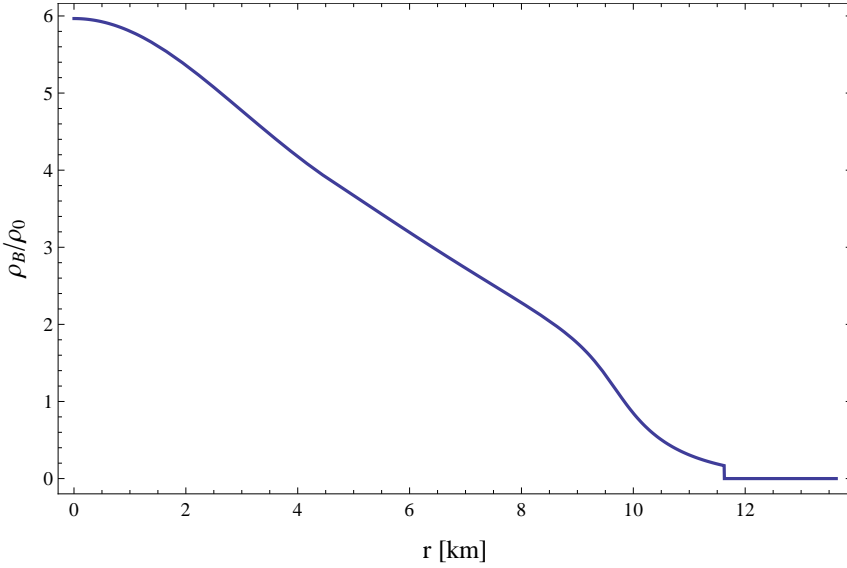
Figure 6.11: The baryon number density distribution inside the maximum mass star for $B_{\text{vac}}^{1/4} = 48\,\text{MeV}$. This quark star has a mass of $M = 1.76 M_{\odot}$ and a radius of $R = 11.6\,\text{km}$.

$v_x = \tilde{v}_x$ and $v_y = \tilde{v}_y$, discussed at the end of section 6.4.2. When the minimum of the potential is changed, so are all the physical quantities we study. Hence, changing the the minimum of the thermodynamical potential in the vacuum will e.g. also change the vacuum constituent quark mass $\tilde{m}_f$. From Fig. 6.8a we see that this is in fact the case. The light quark mass is only $286\,\text{MeV}$ for $\rho_B = 0$, where it should have been $300\,\text{MeV}$. Moreover, trying to fix this problem by setting $\tilde{m}_q = 286\,\text{MeV}$ and fixing the Yukawa coupling $g = 2\tilde{m}_q/\tilde{v}_x = 6.14$, will not solve anything, as this will in turn change the value for Λ, and thus change the minimum of the potential again. If this problem is fixable or not is hard to say, but *if* one could assign a different renormalisation scale for the light quarks and the s quark, i.e. using Λ_x in the vacuum term involving m_q, and using Λ_y in the vacuum term involving m_s, the potential would be minimised at $(\tilde{v}_x, \tilde{v}_y)$ and the problem would be fixed.

We show various mass-radius relations for bag pressure normalisations larger than what is required for the strange quark matter hypothesis to be true in Fig. 6.12. The maximum masses with corresponding radii are shown in Table 6.4 and the baryon number densities as functions of the radius for the maximum mass stars are showed in Fig. 6.13.

Another way to use the three-flavour quark-meson model to describe a quark star, is by swapping the effective bag pressure used up till now with a *constant* bag pressure, in analogy with the MIT bag model. We must then calculate a new interval of which the bag constant can take values from, assuming the strange quark matter hypothesis to be true. For this model, the bag-window becomes

$$30.4\,\text{MeV} < B^{1/4} < 70.6\,\text{MeV}. \tag{6.108}$$
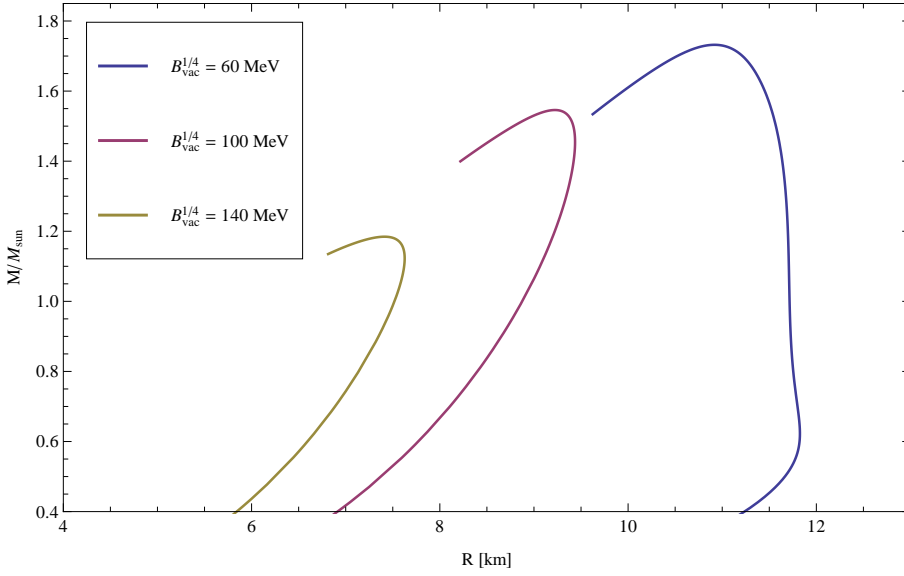
Figure 6.12: Various mass-radius relations using the three-flavour quark-meson EoS with normalisations of the effective bag pressure outside the bag-window (6.40). Maximum masses with corresponding radii are shown in Table 6.4.
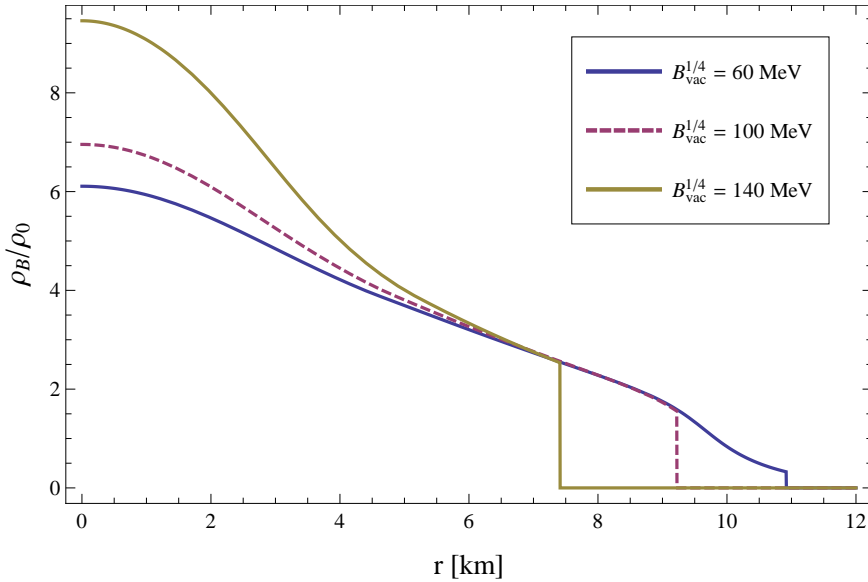
Figure 6.13: The baryon number density distribution inside the maximum mass stars found using various bag normalisations outside the bag-window. The maximum and minimum densities of each star is shown in Table 6.4 together with the mass and radius of the corresponding star.

$B_{\text{vac}}^{1/4}$ [MeV]	M_{max} [$M_\odot$]	R [km]	$\rho_B(R)$ [ρ_0]	$\rho_B(0)$ [ρ_0]
60	1.73	10.9	0.33	6.1
100	1.55	9.2	1.6	7.0
140	1.18	7.4	2.5	9.5

Table 6.4: Maximum masses with corresponding radii for values of B_{vac} outside the bag-window. The maximum and minimum baryon number densities for the corresponding maximum mass star are also included.
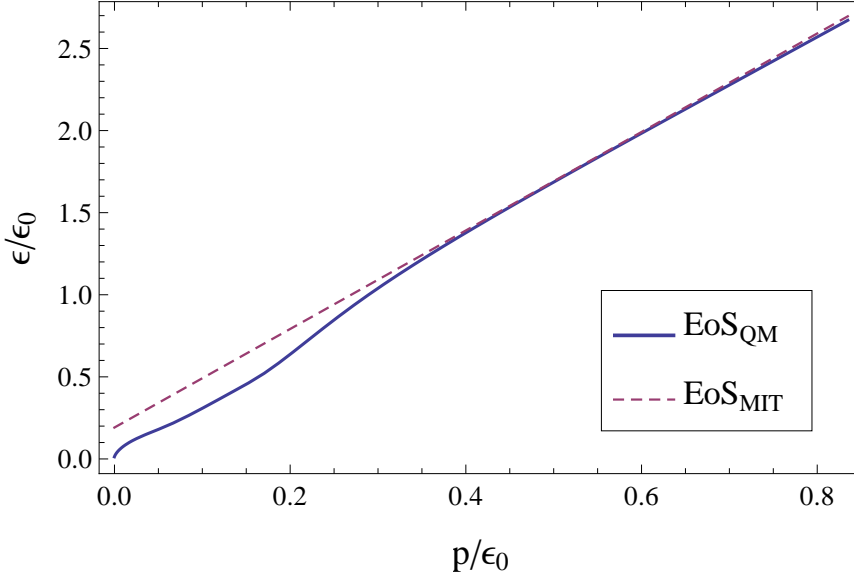
Figure 6.14: The EoS for the three-flavour quark-meson model and the MIT bag model compared. In both models the bag constant is $B^{1/4} = 50\,\text{MeV}$.

The EoS in this model is shown in Fig. 6.14. Maximum masses with corresponding radii and maximum and minimum baryon number densities are shown in Table 6.5 for various bag constant in the bag-window. We see that the maximum masses and radii become extremely large in this model. Moreover, the density inside the maximum mass stars never reaches values high enough for strange quarks to be made. Hence, this model cannot be used to describe quark stars.

$B_{\text{vac}}^{1/4}$ [MeV]	$M_{\max}$ [$M_\odot$]	R [km]	$\rho_B(R)$ [ρ_0]	$\rho_B(0)$ [ρ_0]
30.5	4.1	24.5	0.038	2.8
50	4.0	22.0	0.12	2.8
70.5	3.7	19.7	0.29	2.5

Table 6.5: Maximum masses with corresponding radii for various bag constants. The maximum and minimum baryon number densities for the corresponding maximum mass star are also included.

Chapter 7

Conclusion and outlook

7.1 Conclusion

In the first chapters of this thesis, we derived some of the thermodynamical functions needed to study quark stars, and in chapter 5 we derived the all-important TOV equation. Solving the TOV equation for the free Fermi gas EoS gave the unphysical result of unlimited radius and mass. When using the MIT bag model to mimic QCD interactions, we could predict quark stars with maximum masses ranging from $1.6M_\odot$ to $2.0M_\odot$, assuming that strange quark matter is absolutely stable at zero pressure. The corresponding radii of these maximum mass stars were estimated to be between $8.7\,\mathrm{km}$ to $11\,\mathrm{km}$.

Later we extracted a density dependent bag pressure from the two- and three-flavour linear sigma model with quark degrees of freedom, which we used as an alternative to the MIT bag constant. This resulted in the description of unphysical quark stars with deconfined two-flavour quark matter at the surface. For two flavours, the maximum masses of such stars were found to be slightly less than $1.8M_\odot$, and the corresponding radii ranged from $10.3\,\mathrm{km}$ to $11.1\,\mathrm{km}$. For three flavours, the maximum masses were also slightly less than $1.8M_\odot$, but the radii of the maximum mass stars now ranged from $11.6\,\mathrm{km}$ to $13.1\,\mathrm{km}$. We can conclude that using the EoS obtained by extracting an effective bag pressure from the two- and three-flavour quark-meson models are not fitted to describe pure quark stars. This is because we cannot achieve a stable strange quark matter at zero pressure using the bag pressure extracted from the three-flavour quark-meson model.

Swapping the effective, density dependent bag pressure with a constant bag pressure in the three-flavour quark-meson model neither gave a physical description of a quark star. The same problem arose for the constant bag pressure as with the density dependent bag pressure; the quark star which we assumed were made out of stable strange quark matter, did not have large enough densities at the surface for strange quarks to exist. Moreover, in the model with a constant bag pressure, the maximum mass stars did not even reach high enough densities in their center for strange quarks to exist.

We also studied some properties of the three-flavour quark-meson model and found that at very high densities, there is roughly the same number of u, d and s quarks. This is

known as the CFL phase, which is absolutely stable if the strange quark matter hypothesis is true. It might therefore be possible for quark stars to be formed if a hybrid star is dense enough in it's center for strangelets to be produced.

7.2 Outlook

Even though our final results were unphysical, the three-flavour quark-meson model with an extracted bag pressure can be used to describe deconfined quark matter inside of hybrid stars. The EoS obtained from the three-flavour model discussed in this thesis can be used in the inner regions of the star, where the density is high enough for quark matter to be deconfined. At which densities the phase transition from confined hadronic matter to deconfined quark matter occurs is still uncertain, but it occurs where the pressure of the quark phase (QP) and the hadronic phase (HP) are equal. Following a crude estimate by [26] and [22], we can find an approximation of the baryon number density at which the deconfinement may occur: The typical radius of a nucleon is $r_N \sim 1 \, \text{fm}$, which correspond to a volume of $V_N = 4\pi r_N^3/3$. Hence, the nuclei begin to touch at densities $\rho_B \sim \left(4\pi r_N^3/3\right)^{-1} \approx 0.24 \, (\text{fm})^{-3}$. This is less than twice the nuclear saturation density $\rho_0 = 0.16 \, (\text{fm})^{-3}$. From Figs. 6.11 and 6.13, we see that such densities are easily reached inside the unphysical quark stars described in these figures. One can also expect that a neutron star can reach such densities near the center. A simple model of a hybrid star could thus be made by using an EoS for the three-flavour quark-meson model with an effective, density-dependent bag pressure for baryon number densities higher than e.g. 2–3 times the nuclear saturation density, and for the lower density regions using an EoS describing hadronic matter. Schertler and Leupold modelled a hybrid star in a similar way, by using the Nambu-Jona-Lasinio (NJL) model instead of the quark-meson model [40]. These models (our and Scherler's) will, however, have a sharp interface between the QP and HP, because the pressure of the models can be parametrised by a single chemical potential, μ_B. Hence, the pressure of the QP and HP will be equal for one chemical potential only, excluding a mixed phase where both confined and deconfined quark matter could exist. This also imply that the density will be discontinuous at the interface, because the two phases have a different EoS. The exclusion of the mixed phase is a direct consequence of eq. 6.1, where we demand *local* charge neutrality instead of *global* charge neutrality. Quark stars must be globally charge neutral and not locally, so in reality we will have two independent chemical potentials, which implies that the pressures of the MP and HP will be equal in a range of chemical potentials. For a throughout discussion about the phase transition in neutron stars, see e.g. [22].

It would also be interesting to study the effects of rotation on the mass-radius relation of neutron stars. Several pulsars are known to rotate extremely fast, for example does the Crab pulsar rotate 30 times per second [22]. Since the TOV equation is derived under the assumption of spherically symmetric and static stars, one must then derive a new equation describing the structure of the star from a more general metric,

$$ds^2 = A(r,\theta)dt^2 - B(r,\theta)dr^2 - C(r,\theta)\left[r^2 d\theta^2 + r^2 \sin^2\theta(d\phi - \omega(r,\theta)dt)^2\right]. \quad (7.1)$$

In addition, we did not include the magnetic field in our calculations. How much a strong magnetic field affects our results would also be interesting to study.

Appendices

Analytical calculations

A.1 The periodicity of fields

The Green's function for fermions is defined as [10]

$$G_F(\mathbf{x}, \mathbf{y}; \tau_1, \tau_2) = \mathcal{Z}^{-1} \mathrm{Tr} \left\{ \mathrm{e}^{-\beta H} T_\tau \left[\hat{\psi}(\tau_1, \mathbf{x}) \hat{\psi}(\tau_2, \mathbf{y}) \right] \right\}, \tag{A.1}$$

where T_τ is the imaginary time ordering operator. For fermions T_τ is given by

$$\hat{\psi}(\tau_1, \mathbf{x}) \hat{\psi}(\tau_2, \mathbf{y}) \theta(\tau_1 - \tau_2) - \hat{\psi}(\tau_2, \mathbf{x}) \hat{\psi}(\tau_1, \mathbf{y}) \theta(\tau_2 - \tau_1). \tag{A.2}$$

As T_τ commutes with $\mathrm{e}^{-\beta H}$, we can manipulate the trace in eq. (A.1):

$$\begin{aligned} G_F(\mathbf{x}, \mathbf{y}; \tau, 0) &= \mathcal{Z}^{-1} \mathrm{Tr} \left\{ \mathrm{e}^{-\beta H} \hat{\psi}(\tau, \mathbf{x}) \hat{\psi}(0, \mathbf{y}) \right\} \\ &= \mathcal{Z}^{-1} \mathrm{Tr} \left\{ \hat{\psi}(0, \mathbf{y}) \mathrm{e}^{-\beta H} \hat{\psi}(\tau, \mathbf{x}) \right\} \\ &= \mathcal{Z}^{-1} \mathrm{Tr} \left\{ \mathrm{e}^{-\beta H} \mathrm{e}^{\beta H} \hat{\psi}(0, \mathbf{y}) \mathrm{e}^{-\beta H} \hat{\psi}(\tau, \mathbf{x}) \right\} \\ &= \mathcal{Z}^{-1} \mathrm{Tr} \left\{ \mathrm{e}^{-\beta H} \hat{\psi}(\beta, \mathbf{y}) \hat{\psi}(\tau, \mathbf{x}) \right\} \\ &= -\mathcal{Z}^{-1} \mathrm{Tr} \left\{ \mathrm{e}^{-\beta H} T_\tau \left[\hat{\psi}(\tau, \mathbf{x}) \hat{\psi}(\beta, \mathbf{y}) \right] \right\} \\ &= -G_F(\mathbf{x}, \mathbf{y}; \tau, \beta). \end{aligned} \tag{A.3}$$

In the third line we inserted a factor $1 = \mathrm{e}^{-\beta H} \mathrm{e}^{\beta H}$ and used the Heisenberg time evolution $\mathrm{e}^{\beta H} \hat{\psi}(0, \mathbf{y}) \mathrm{e}^{-\beta H} = \hat{\psi}(\beta, \mathbf{y})$. We also used the cyclic property of the trace and that $0 < \tau < \beta$. The result implies that fermionic fields are antiperiodic, i.e. that

$$\psi(0, \mathbf{x}) = -\psi(\beta, \mathbf{x}). \tag{A.4}$$

For bosons, the time ordering operator T_τ have a $(+)$ sign instead of a $(-)$ sign between the two terms, and following the same steps as in eq. (A.3) we find for bosonic fields $\phi(\tau, \mathbf{x})$

$$\phi(0, \mathbf{x}) = \phi(\beta, \mathbf{x}). \tag{A.5}$$

A.2 The contracted Christoffel symbol

The contracted Christoffel symbol is defined as $\Gamma^{\mu}_{\nu\mu}$. It can be rewritten using some matrix properties and by swapping indices. The components of a square matrix A wich have an inverse matrix B can be determined by the relation

$$A_{ij} = \frac{\partial \det B}{\partial B^{ij}} \det B. \tag{A.6}$$

As $g^{\mu\nu}$ is the inverse of the metric tensor $g_{\mu\nu}$, we thus have

$$g^{\mu\nu} = \frac{1}{g} \frac{\partial g}{\partial g_{\mu\nu}}, \tag{A.7}$$

where g is the determinant of $g_{\mu\nu}$. Now, multiplying both sides of this equation by $\frac{\partial g_{\mu\nu}}{\partial x^{\alpha}}$ we get

$$g^{\mu\nu} \partial_{\alpha} g_{\mu\nu} = \frac{1}{g} \partial_{\alpha} g = \partial_{\alpha} \ln |g| \tag{A.8}$$

The left hand side of this equation is on the same form as one of the terms in the contracted Christoffel symbol:

$$\Gamma^{\mu}_{\nu\mu} = \frac{1}{2} g^{\mu\alpha} (\partial_{\nu} g_{\mu\alpha} + \partial_{\mu} g_{\nu\alpha} - \partial_{\alpha} g_{\mu\nu}). \tag{A.9}$$

Since we sum over the indices μ and α, and therefore it does not matter what they are called, we can swap these indices in the last term. As the metric is diagonal, the two last terms will then cancel and we are left with

$$\begin{aligned} \Gamma^{\mu}_{\nu\mu} &= \frac{1}{2} g^{\mu\alpha} \partial_{\nu} g_{\mu\alpha} = \frac{1}{2} \partial_{\nu} \ln |g| \\ &= \frac{1}{\sqrt{-g}} \partial_{\nu} \sqrt{-g}. \end{aligned} \tag{A.10}$$

Note that $|g| = -g$ for a metric with signature -2.

A.3   The derivation of equation (5.19)

Our starting equation is

$$0 = -\partial_\mu \left(pg^{\mu\nu} \right) - \frac{pg^{\mu\nu}}{\sqrt{-g}} \partial_\mu \sqrt{-g} + \Gamma^\nu_{\alpha\mu} \left[(\epsilon + p)u^\mu u^\alpha - pg^{\mu\alpha} \right]. \tag{A.11}$$

As $p = p(r)$ is only a function of r, we have

$$-\partial_\mu \left(pg^{\mu\nu} \right) = \frac{1}{B} \left(p' - p\frac{B'}{B} \right) \delta^{\nu 1}. \tag{A.12}$$

The second term becomes

$$\begin{aligned}
\frac{-pg^{\mu\nu}}{\sqrt{-g}} \partial_\mu \sqrt{-g} &= \frac{-pg^{\mu\nu}}{-2g} \partial_\mu(-g) \\
&= \frac{p}{2BABr^4 \sin^2 \theta} (A'Br^4 + AB'r^4 + 4ABr^3) \sin^2 \theta \delta^{\nu 1} \\
&\quad + \frac{p}{2r^2 ABr^4 \sin^2 \theta} 2ABr^4 \sin\theta \cos\theta \delta^{\nu 2} \\
&= \frac{p}{2B} \left(\frac{A'}{A} + \frac{B'}{B} + \frac{4}{r} \right) \delta^{\nu 1} + \frac{p\cos\theta}{r^2 \sin\theta} \delta^{\nu 2}.
\end{aligned} \tag{A.13}$$

Furthermore, since only the zeroth component of u^μ is the only nonvanishing component, the third term reduces to

$$\begin{aligned}
\Gamma^\nu_{\alpha\mu}(\epsilon + p)u^\mu u^\alpha &= \Gamma^\nu_{00}(\epsilon + p)(g_{00})^{-1} \\
&= \frac{\epsilon + p}{2A} g^{\nu\beta}(2\partial_0 g_{\beta 0} - \partial_\beta g_0 0) \\
&= \frac{\epsilon + p}{2A} \frac{A'}{B} \delta^{\nu 1}.
\end{aligned} \tag{A.14}$$

Finally, the fourth and last term becomes

$$\begin{aligned}
-\Gamma^\nu_{\alpha\mu} pg^{\mu\alpha} &= \frac{-p}{2} g^{\nu\beta}(\partial_\alpha g_{\mu\beta} + \partial_\mu g_{\beta\alpha} - \partial_\beta g_{\mu\alpha})g^{\mu\alpha} \\
&= -pg^{\nu\beta}g^{\mu\alpha}(\partial_\alpha g_{\mu\beta} - \frac{1}{2}\partial_\beta g_{\mu\alpha}) \\
&= -pg^{\nu\beta} \left[\frac{B'}{B}\delta_{\beta 1} - \frac{1}{2} \left(\frac{A'}{A} + \frac{B'}{B} + \frac{4}{r} \right) \delta_{\beta 1} - \frac{\cos\theta}{\sin\theta}\delta_{\beta 2} \right] \\
&= \frac{p}{2B} \left[\left(\frac{B'}{B} - \frac{A'}{A} - \frac{4}{r} \right) \delta^{\nu 1} - 2\frac{B\cos\theta}{r^2 \sin\theta}\delta^{\nu 2} \right].
\end{aligned} \tag{A.15}$$

Now inserting eqs. (A.12) to (A.15), into eq. (A.11) and setting $\nu = 1$, we end up with

$$\begin{aligned}
-\frac{p'(r)}{B} &= \frac{p}{2B} \left(-2\frac{B'}{B} + \frac{A'}{A} + \frac{B'}{B} + \frac{4}{r} + \frac{B'}{B} - \frac{A'}{A} - \frac{4}{r} \right) + \frac{\epsilon + p}{2A} \frac{A'}{B} \\
&= \frac{\epsilon + p}{2A} \frac{A'}{B}.
\end{aligned} \tag{A.16}$$

Now, multiplying both sides with B, we end up with eq. (5.19),

$$p' = -\frac{1}{2}(p + \epsilon)\frac{A'}{A}. \tag{A.17}$$

A.4   The three-flavour meson potential

The meson potential written in terms of the field Φ is

$$U(\Phi^\dagger, \Phi) = m^2 \text{Tr}\left[\Phi^\dagger \Phi\right] + \lambda_1 \left[\text{Tr}\left(\Phi^\dagger \Phi\right)\right]^2 + \lambda_2 \text{Tr}\left[\left(\Phi^\dagger \Phi\right)^2\right] - \text{Tr}\left[H\left(\Phi^\dagger + \Phi\right)\right].$$

(A.18)

We will show how this can be written in terms of v_x and v_y as in eq. 6.55, but before we start, let us summarise some useful relations:

$$\Phi = T_a \Phi_a = T_a(\sigma_a + i\pi_a), \qquad \text{Tr}\left[T_a T_b\right] = \frac{1}{2}\delta_{ab}, \tag{A.19}$$

$$[T_a, T_b] = if_{abc}T_c, \qquad \{T_a, T_b\} = d_{abc}T_c, \tag{A.20}$$

$$f_{ab0} = 0, \qquad d_{ab0} = \sqrt{\frac{2}{3}}\delta_{ab}, \tag{A.21}$$

$$v_0 = \frac{1}{\sqrt{3}}(\sqrt{2}v_x + v_y), \qquad v_8 = \frac{1}{\sqrt{3}}(v_x - \sqrt{2}v_y), \tag{A.22}$$

$$\left\langle\Phi^\dagger\right\rangle = \left\langle\Phi\right\rangle = T_a \left\langle\sigma_a\right\rangle = T_0 v_0 + T_8 v_8. \tag{A.23}$$

The nonzero components of the structure constants are

$$f_{123} = 1, \qquad f_{458} = f_{678} = \frac{\sqrt{3}}{2}, \tag{A.24a}$$

$$f_{147} = -f_{156} = f_{246} = f_{257} = f_{345} = -f_{367} = \frac{1}{2}, \tag{A.24b}$$

$$d_{118} = d_{228} = d_{338} = -d_{888} = \frac{1}{\sqrt{3}}, \tag{A.24c}$$

$$d_{448} = d_{558} = d_{668} = d_{778} = -\frac{1}{2\sqrt{3}}, \tag{A.24d}$$

$$d_{146} = d_{157} = -d_{247} = d_{256} = d_{344} = d_{355} = -d_{366} = -d_{377} = \frac{1}{2}, \tag{A.24e}$$

where f_{ijk} and d_{ijk} are antisymmetric and symmetric under permutations of the indices ijk respectively. We will calculate each term in the potential one by one, starting with the first term, $m^2 \text{Tr}\left[\Phi^\dagger \Phi\right]$. For simplicity we will skip the parameters in front of the traces. We thus have

$$\begin{aligned}
\text{Tr}\left[\Phi^\dagger \Phi\right] &= \text{Tr}\left[(\sigma_a - i\pi_a)T_a T_b(\sigma_b + i\pi_b)\right] \\
&= (\sigma_a \sigma_b + i\sigma_a \pi_b - i\pi_a \sigma_b + \pi_a \pi_b) \cdot \frac{1}{2}\delta_{ab} \\
&= \frac{1}{2}\left(\sigma_a^2 + \pi_a^2\right).
\end{aligned} \tag{A.25}$$

By inserting the expectation values, we obtain

$$\begin{aligned}
\text{Tr}\left[\left\langle\Phi\right\rangle^2\right] &= \frac{1}{2}\left(v_0^2 + v_8^2\right) \\
&= \frac{1}{2}\left(v_x^2 + v_y^2\right).
\end{aligned} \tag{A.26}$$

Furthermore, we find

$$\left[\mathrm{Tr} \left(\Phi^\dagger \Phi \right) \right]^2 = \left[\frac{1}{2} \left(\sigma_a^2 + \pi_a^2 \right) \right]^2 , \tag{A.27}$$

which yields

$$\left[\mathrm{Tr} \left(\langle \Phi \rangle^2 \right) \right]^2 = \frac{1}{4} \left(v_x^2 + v_y^2 \right)^2 . \tag{A.28}$$

The most involved calculation is the calculation of $\mathrm{Tr} \left[\left(\Phi^\dagger \Phi \right)^2 \right]$, as this includes a product of four $SU(3)$ generators. Let us begin by calculating the trace of a product of three $SU(3)$ generators. Using eq. (A.20), we find

$$\begin{aligned}
\mathrm{Tr} \left[T_a T_b T_c \right] &= \mathrm{Tr} \left[(i f_{abe} T_e + T_b T_a) T_c \right] \\
&= i f_{abe} \frac{\delta_{ec}}{2} + \mathrm{Tr} \left[T_b (d_{acf} T_f - T_c T_a) \right] \\
&= i f_{abe} \frac{\delta_{ec}}{2} + d_{acf} \frac{\delta_{bf}}{2} - \mathrm{Tr} \left[T_a T_b T_c \right] .
\end{aligned} \tag{A.29}$$

We thus get

$$\mathrm{Tr} \left[T_a T_b T_c \right] = \frac{1}{4} (i f_{abc} + d_{abc}). \tag{A.30}$$

By using eq. (A.20) the product of four $SU(3)$ generators can be written as

$$\begin{aligned}
\mathrm{Tr} \left[T_a T_b T_c T_d \right] =& i f_{abe} \mathrm{Tr} \left[T_e T_c T_d \right] + i f_{acf} \mathrm{Tr} \left[T_b T_f T_d \right] \\
&+ d_{adg} \mathrm{Tr} \left[T_b T_c T_g \right] - \mathrm{Tr} \left[T_b T_c T_d T_a \right] ,
\end{aligned} \tag{A.31}$$

implying that

$$\begin{aligned}
\mathrm{Tr} \left[T_a T_b T_c T_d \right] = \frac{1}{8} \big[& i f_{abe} (i f_{cde} + d_{cde}) + i f_{ace} (-i f_{bde} + d_{bde}) \\
& + d_{ade} (i f_{bce} + d_{bce}) \big] .
\end{aligned} \tag{A.32}$$

Furthermore, by using

$$\begin{aligned}
\mathrm{Tr} \left[\left(\Phi^\dagger \Phi \right)^2 \right] &= \mathrm{Tr} \left[(\sigma_a - i \pi_a) T_a T_b (\sigma_b + i \pi_b) \right]^2 \\
&= (\sigma_a - i \pi_a)(\sigma_b + i \pi_b)(\sigma_c - i \pi_c)(\sigma_d + i \pi_d) \mathrm{Tr} \left[T_a T_b T_c T_d \right] ,
\end{aligned} \tag{A.33}$$

we find

$$\begin{aligned}
\mathrm{Tr} \left[\left(\Phi^\dagger \Phi \right)^2 \right] =& \frac{1}{8} (\sigma_a - i \pi_a)(\sigma_b + i \pi_b)(\sigma_c - i \pi_c)(\sigma_d + i \pi_d) \\
& \times \big[i f_{abe} (i f_{cde} + d_{cde}) + i f_{ace} (-i f_{bde} + d_{bde}) \\
& \quad + d_{ade} (i f_{bce} + d_{bce}) \big] .
\end{aligned} \tag{A.34}$$

Hence, by inserting the expectation values, we obtain

$$\text{Tr}\left[\left(\langle\Phi\rangle^2\right)^2\right] = \frac{1}{8}v_a v_b v_c v_d \left[if_{abe}(if_{cde} + d_{cde}) + if_{ace}(-if_{bde} + d_{bde})\right.$$
$$\left. + d_{ade}(if_{bce} + d_{bce})\right]. \tag{A.35}$$

The term $v_a v_b f_{abc}$ is nonzero only if $a \neq b$ and $a, b \neq 0$ in accordance with eqs. (A.21) and (A.24). However, as $v_i = 0$ for $i \neq 0, 8$ this is impossible. Thus, the only term in the [ ]-brackets contributing, is the term $d_{ade}d_{bce}$. Nevertheless, this term is very time-consuming to calculate. Therefore we will simply state the result and save the calculations for the especially interested reader. The surprisingly simple result is

$$\text{Tr}\left[\left(\langle\Phi\rangle^2\right)^2\right] = \frac{1}{8}\left(v_x^4 + 2v_y^4\right). \tag{A.36}$$

Luckily, the last term of eq. (A.18) is straightforward to calculate, since both h_a and v_a transform under the same orthogonal transformation. The general expression for this term is

$$\begin{aligned}
\text{Tr}\left[H\left(\Phi^\dagger + \Phi\right)\right] &= \text{Tr}\left[T_a h_a (T_b \sigma_b + \sigma_b T_b)\right] \\
&= 2h_a \sigma_b \frac{\delta_{ab}}{2} \\
&= h_a \sigma_a.
\end{aligned} \tag{A.37}$$

Inserting the expectation values, gives

$$\begin{aligned}
\text{Tr}\left[H\left(\langle\Phi\rangle^\dagger + \langle\Phi\rangle\right)\right] &= h_0 v_0 + h_8 v_8 \\
&= h_x v_x + h_y v_y.
\end{aligned} \tag{A.38}$$

By combining eqs. (A.26), (A.28), (A.36) and (A.38), we finally obtain

$$\begin{aligned}
U(v_x, v_y) =& \frac{1}{2}m^2\left(v_x^2 + v_y^2\right) + \frac{\lambda_1}{2}v_x^2 v_y^2 + \frac{1}{8}\left(2\lambda_1 + \lambda_2\right)v_x^4 \\
& + \frac{1}{8}(2\lambda_1 + 2\lambda_2)v_y^4 - h_x v_x - h_y v_y,
\end{aligned} \tag{A.39}$$

which is the tree-level meson potential in the three-flavour quark-meson model. The potential written in terms of the fields σ_a and π_a is

$$\begin{aligned}
U(\sigma_a, \pi_a) =& \frac{1}{2}m^2\left(\sigma_a^2 + \pi_a^2\right) + \frac{\lambda_1}{4}\left(\sigma_a^2 \sigma_b^2 + 2\sigma_a^2 \pi_b^2 + \pi_a^2 \pi_b^2\right) - h_a \sigma_a \\
& + \frac{\lambda_2}{8}(\sigma_a - i\pi_a)(\sigma_b + i\pi_b)(\sigma_c - i\pi_c)(\sigma_d + i\pi_d)\mathcal{F}_{abcd},
\end{aligned} \tag{A.40}$$

where we defined

$$\mathcal{F}_{abcd} \equiv \left[if_{abe}(if_{cde} + d_{cde}) + if_{ace}(-if_{bde} + d_{bde}) + d_{ade}(if_{bce} + d_{bce})\right]. \tag{A.41}$$

When calculating the pseudoscalar mass matrix, only terms proportional to $\pi_a \pi_b$ will contribute. The contributing terms proportional to λ_2 become

$$
\begin{aligned}
&\sigma_a \sigma_b \pi_c \pi_d (f_{ace} f_{bde} + d_{ade} d_{bce}) + \sigma_a \sigma_c \pi_b \pi_d (f_{abe} f_{cde} - d_{ade} d_{bce}) \\
&+ \sigma_a \sigma_d \pi_b \pi_c (-f_{abe} f_{cde} + f_{ace} f_{bde} + d_{ade} d_{bce}) \\
&+ \sigma_b \sigma_c \pi_a \pi_d (-f_{abe} f_{cde} + f_{ace} f_{bde} + d_{ade} d_{bce}) \\
&+ \sigma_b \sigma_d \pi_a \pi_c (f_{abe} f_{cde} - d_{ade} d_{bce}) + \sigma_c \sigma_d \pi_a \pi_b (f_{ace} f_{bde} + d_{ade} d_{bce}).
\end{aligned}
\tag{A.42}
$$

Since we sum over all indices, this can be rewritten as

$$
\begin{aligned}
\sigma_a \sigma_b \pi_c \pi_d (&f_{ace} f_{bde} + f_{ace} f_{bde} - f_{ade} f_{cbe} + f_{ace} f_{dbe} - f_{cbe} f_{ade} \\
&+ f_{cae} f_{bde} + f_{dbe} f_{cae} + f_{dbe} f_{cae} + d_{ade} d_{bce} - d_{ade} d_{cbe} \\
&+ d_{abe} d_{dce} + d_{cbe} d_{bae} - d_{dae} d_{bce} + d_{cbe} d_{dae}).
\end{aligned}
\tag{A.43}
$$

Thus, the contribution to the pseudoscalar mass matrix proportional to λ_2 is

$$
\frac{\lambda_2}{4} \sigma_a \sigma_b \pi_c \pi_d \mathcal{H}_{abcd},
\tag{A.44}
$$

where

$$
\mathcal{H}_{abcd} = f_{ace} f_{bde} + f_{ade} f_{bce} + d_{abe} d_{cde}.
\tag{A.45}
$$

We have now isolated the contributing terms to the pseudoscalar mass matrix, and discarded all terms that will vanish in the classical limit.

A.5 Calculation of the scalar and pseudoscalar mass matrices

We will in this section show how the terms proportional to λ_2 in eqs. (6.73) and (6.78) are calculated. The nonzero components of $\tilde{v}_a \tilde{v}_b \mathcal{G}_{abkl}$ in eq. (6.73) read

$$
\begin{aligned}
\tilde{v}_a \tilde{v}_b \mathcal{G}_{ab00} &= \tilde{v}_a \tilde{v}_b (d_{abe} d_{00e} + 2 d_{a0e} d_{b0e}) \\
&= \left(\frac{2}{3} + 2 \cdot \frac{2}{3} \right) \tilde{v}_0^2 + \left(\frac{2}{3} + 2 \cdot \frac{2}{3} \right) \tilde{v}_8^2 \\
&= 2 \left(\tilde{v}_0^2 + \tilde{v}_8^2 \right),
\end{aligned}
\tag{A.46a}
$$

$$
\begin{aligned}
\tilde{v}_a \tilde{v}_b \mathcal{G}_{ab11} &= \tilde{v}_a \tilde{v}_b (d_{abe} d_{11e} + 2 d_{a1e} d_{b1e}) \\
&= 2 \tilde{v}_0^2 + \left(\frac{2}{3} - \frac{1}{3} + 2 \cdot \frac{1}{3} \right) \tilde{v}_8^2 + 2 \left(\frac{\sqrt{2}}{3} + 2 \cdot \frac{\sqrt{2}}{3} \right) \tilde{v}_0 \tilde{v}_8 \\
&= 2 \tilde{v}_0^2 + \tilde{v}_8^2 + 2\sqrt{2} \tilde{v}_0 \tilde{v}_8 \\
&= \tilde{v}_a \tilde{v}_b \mathcal{G}_{ab22} = \tilde{v}_a \tilde{v}_b \mathcal{G}_{ab33},
\end{aligned}
\tag{A.46b}
$$

$$
\begin{aligned}
\tilde{v}_a \tilde{v}_b \mathcal{G}_{ab44} &= \tilde{v}_a \tilde{v}_b (d_{abe} d_{44e} + 2 d_{a4e} d_{b4e}) \\
&= 2 \tilde{v}_0^2 + \left(\frac{2}{3} + \frac{1}{6} + \frac{1}{6} \right) \tilde{v}_8^2 - 2 \left(\frac{\sqrt{2}}{6} + 2 \cdot \frac{\sqrt{2}}{6} \right) \tilde{v}_0 \tilde{v}_8 \\
&= 2 \tilde{v}_0^2 + \tilde{v}_8^2 - \sqrt{2} \tilde{v}_0 \tilde{v}_8 \\
&= \tilde{v}_a \tilde{v}_b \mathcal{G}_{ab55} = \tilde{v}_a \tilde{v}_b \mathcal{G}_{ab66} = \tilde{v}_a \tilde{v}_b \mathcal{G}_{ab77},
\end{aligned}
\tag{A.46c}
$$

$$
\begin{aligned}
\tilde{v}_a \tilde{v}_b \mathcal{G}_{ab88} &= \tilde{v}_a \tilde{v}_b (d_{abe} d_{88e} + 2 d_{a8e} d_{b8e}) \\
&= 2 \tilde{v}_0^2 + (1 + 2) \tilde{v}_8^2 - 2 \left(\frac{\sqrt{2}}{3} - 2 \cdot \frac{\sqrt{2}}{3} \right) \tilde{v}_0 \tilde{v}_8 \\
&= 2 \tilde{v}_0^2 + 3 \tilde{v}_8^2 - 2\sqrt{2} \tilde{v}_0 \tilde{v}_8,
\end{aligned}
\tag{A.46d}
$$

$$
\begin{aligned}
\tilde{v}_a \tilde{v}_b \mathcal{G}_{ab08} &= \tilde{v}_a \tilde{v}_b (d_{abe} d_{08e} + 2 d_{a0e} d_{b8e}) \\
&= 0 \cdot \tilde{v}_0^2 + \left(\frac{-\sqrt{2}}{3} - 2 \cdot \frac{\sqrt{2}}{3} \right) \tilde{v}_8^2 + 2 \left(\frac{2}{3} + 2 \cdot \frac{2}{3} \right) \tilde{v}_0 \tilde{v}_8 \\
&= -\sqrt{2} \tilde{v}_8^2 + 4 \tilde{v}_0 \tilde{v}_8 \\
&= \tilde{v}_a \tilde{v}_b \mathcal{G}_{ab80}.
\end{aligned}
\tag{A.46e}
$$

By multiplying these eqs. by $\lambda_2/2$, we get their contribution to the scalar mass matrix. We thus have

$$\left(M_\sigma^2\right)_{00} = m^2 + \lambda_1 \left(3\tilde{v}_0^2 + \tilde{v}_8^2\right) + \lambda_2 \left(\tilde{v}_0^2 + \tilde{v}_8^2\right), \tag{A.47a}$$

$$\left(M_\sigma^2\right)_{11} = \left(M_\sigma^2\right)_{22} = \left(M_\sigma^2\right)_{33}$$
$$= m^2 + \lambda_1 \left(\tilde{v}_0^2 + \tilde{v}_8^2\right) + \lambda_2 \left(\tilde{v}_0^2 + \frac{1}{2}\tilde{v}_8^2 + \sqrt{2}\tilde{v}_0\tilde{v}_8\right), \tag{A.47b}$$

$$\left(M_\sigma^2\right)_{44} = \left(M_\sigma^2\right)_{55} = \left(M_\sigma^2\right)_{66} = \left(M_\sigma^2\right)_{77}$$
$$= m^2 + \lambda_1 \left(\tilde{v}_0^2 + \tilde{v}_8^2\right) + \lambda_2 \left(\tilde{v}_0^2 + \frac{1}{2}\tilde{v}_8^2 - \frac{1}{\sqrt{2}}\tilde{v}_0\tilde{v}_8\right), \tag{A.47c}$$

$$\left(M_\sigma^2\right)_{88} = m^2 + \lambda_1 \left(\tilde{v}_0^2 + 3\tilde{v}_8^2\right) + \lambda_2 \left(\tilde{v}_0^2 + \frac{3}{2}\tilde{v}_8^2 - \sqrt{2}\tilde{v}_0\tilde{v}_8\right), \tag{A.47d}$$

$$\left(M_\sigma^2\right)_{08} = \left(M_\sigma^2\right)_{80} = 2\lambda_1\tilde{v}_0\tilde{v}_8 + \lambda_2 \left(-\frac{1}{\sqrt{2}}\tilde{v}_8^2 + 2\tilde{v}_0\tilde{v}_8\right). \tag{A.47e}$$

The nonzero components of $\tilde{v}_a \tilde{v}_b \mathcal{H}_{abkl}$ in eq. (6.78) read

$$\tilde{v}_a \tilde{v}_b \mathcal{H}_{ab00} = \tilde{v}_a \tilde{v}_b (2 f_{a0e} f_{b0e} + d_{abe} d_{00e})$$
$$= \frac{2}{3} \tilde{v}_0^2 + \frac{2}{3} \tilde{v}_8^2, \tag{A.48a}$$

$$\tilde{v}_a \tilde{v}_b \mathcal{H}_{ab11} = \tilde{v}_a \tilde{v}_b (2 f_{a1e} f_{b1e} + d_{abe} d_{11e})$$
$$= \frac{2}{3} \tilde{v}_0^2 + \left(\frac{2}{3} - \frac{1}{3} \right) \tilde{v}_8^2 + 2 \cdot \frac{\sqrt{2}}{3} \tilde{v}_0 \tilde{v}_8$$
$$= \frac{2}{3} \tilde{v}_0^2 + \frac{1}{3} \tilde{v}_8^2 + \frac{2\sqrt{2}}{3} \tilde{v}_0 \tilde{v}_8 \tag{A.48b}$$
$$= \tilde{v}_a \tilde{v}_b \mathcal{H}_{ab22} = \tilde{v}_a \tilde{v}_b \mathcal{H}_{ab33},$$

$$\tilde{v}_a \tilde{v}_b \mathcal{H}_{ab44} = \tilde{v}_a \tilde{v}_b (2 f_{a4e} f_{b4e} + d_{abe} d_{44e})$$
$$= \frac{2}{3} \tilde{v}_0^2 + \left(2 \cdot \frac{3}{4} + \frac{2}{3} + \frac{1}{6} \right) \tilde{v}_8^2 - 2 \cdot \frac{\sqrt{2}}{6} \tilde{v}_0 \tilde{v}_8$$
$$= \frac{2}{3} \tilde{v}_0^2 + \frac{7}{3} \tilde{v}_8^2 - \frac{\sqrt{2}}{3} \tilde{v}_0 \tilde{v}_8 \tag{A.48c}$$
$$= \tilde{v}_a \tilde{v}_b \mathcal{H}_{ab55} = \tilde{v}_a \tilde{v}_b \mathcal{H}_{ab66} = \tilde{v}_a \tilde{v}_b \mathcal{H}_{ab77},$$

$$\tilde{v}_a \tilde{v}_b \mathcal{H}_{ab88} = \tilde{v}_a \tilde{v}_b (2 f_{a8e} f_{b8e} + d_{abe} d_{88e})$$
$$= \frac{2}{3} \tilde{v}_0^2 + \left(\frac{2}{3} + \frac{1}{3} \right) \tilde{v}_8^2 - 2 \cdot \frac{\sqrt{2}}{3} \tilde{v}_0 \tilde{v}_8$$
$$= \frac{2}{3} \tilde{v}_0^2 + \tilde{v}_8^2 - \frac{2\sqrt{2}}{3} \tilde{v}_0 \tilde{v}_8, \tag{A.48d}$$

$$\tilde{v}_a \tilde{v}_b \mathcal{H}_{ab08} = \tilde{v}_a \tilde{v}_b (2 f_{a0e} f_{b8e} + d_{abe} d_{08e})$$
$$= -\frac{\sqrt{2}}{3} \tilde{v}_8^2 + \frac{4}{3} \tilde{v}_0 \tilde{v}_8 \tag{A.48e}$$
$$= \tilde{v}_a \tilde{v}_b \mathcal{H}_{ab80}.$$

Hence, the nonzero components of the pseudoscalar mass matrix, (6.78), are

$$\left(M_\pi^2 \right)_{00} = m^2 + \lambda_1 \left(\tilde{v}_0^2 + \tilde{v}_8^2 \right) + \frac{\lambda_2}{3} \left(\tilde{v}_0^2 + \tilde{v}_8^2 \right), \tag{A.49a}$$

$$\left(M_\pi^2 \right)_{11} = \left(M_\pi^2 \right)_{22} = \left(M_\pi^2 \right)_{33}$$
$$= m^2 + \lambda_1 \left(\tilde{v}_0^2 + \tilde{v}_8^2 \right) + \frac{\lambda_2}{3} \left(\tilde{v}_0^2 + \frac{1}{2} \tilde{v}_8^2 + \sqrt{2} \tilde{v}_0 \tilde{v}_8 \right), \tag{A.49b}$$

$$\left(M_\pi^2 \right)_{44} = \left(M_\pi^2 \right)_{55} = \left(M_\pi^2 \right)_{66} = \left(M_\pi^2 \right)_{77}$$
$$= m^2 + \lambda_1 \left(\tilde{v}_0^2 + \tilde{v}_8^2 \right) + \frac{\lambda_2}{3} \left(\tilde{v}_0^2 + \frac{7}{2} \tilde{v}_8^2 - \frac{\sqrt{2}}{2} \tilde{v}_0 \tilde{v}_8 \right), \tag{A.49c}$$

$$\left(M_\pi^2 \right)_{88} = m^2 + \lambda_1 \left(\tilde{v}_0^2 + \tilde{v}_8^2 \right) + \frac{\lambda_2}{3} \left(\tilde{v}_0^2 + \frac{3}{2} \tilde{v}_8^2 - \sqrt{2} \tilde{v}_0 \tilde{v}_8 \right), \tag{A.49d}$$

$$\left(M_\pi^2 \right)_{08} = \left(M_\pi^2 \right)_{80} = -\frac{\lambda_2}{3} \left(\tilde{v}_8^2 - 2 \tilde{v}_0 \tilde{v}_8 \right). \tag{A.49e}$$

Appendix B

Mathematica code

The first four pages contain the Mathematica code used to find the bag-window. The next five pages shows an example code of how to produce a mass-radius plot.

```
In[2253]:=  Clear["Global`*"]
            Needs["PlotLegends`"]
            (*PARAMETER FITTING*)
            mσ := 800;
            nc := 3;
            mquark := 300;
            fπ := 93;
            fK := 113;
            mπ := 138;
            mK := 496;
            v0 := 1 / Sqrt[6] (fπ + 2 fK);
            v8 := 2 / Sqrt[3] (fπ - fK);
            vx := fπ;
            vy := 1 / Sqrt[2] (2 fK - fπ);
            g := 2 mquark / vx;

            mq[x_] := g x / 2;
            ms[y_] := g y / Sqrt[2];
            VΛ[x_, y_] := (2 * 3 mq[x] ^ 4 (+ 3 / 4 + 1 / 2 Log[Λ ^ 2 / mq[x] ^ 2]) +
                  3 ms[y] ^ 4 (+ 3 / 4 + 1 / 2 Log[Λ ^ 2 / ms[y] ^ 2]));
            vDx[x_, y_] = D[VΛ[x, y], x];
            vDy[x_, y_] = D[VΛ[x, y], y];
            lambdax = Solve[vDx[vx, vy] == 0, Λ];
            lambday = Solve[vDy[vx, vy] == 0, Λ];
            Λx = Λ /. lambdax[[1]];
            Λy = Λ /. lambday[[1]];
            Λ = (2 Λx + Λy) / 3;

            ms00[m2_, λ1_, λ2_] := m2 + λ1 (3 v0 ^ 2 + v8 ^ 2) + λ2 (v0 ^ 2 + v8 ^ 2);
            ms88[m2_, λ1_, λ2_] := m2 + λ1 (v0 ^ 2 + 3 v8 ^ 2) + λ2 (v0 ^ 2 + 3 / 2 v8 ^ 2 - Sqrt[2] v0 v8);
            ms08[λ1_, λ2_] := 2 λ1 v0 v8 + λ2 (2 v0 v8 - 1 / Sqrt[2] v8 ^ 2);
            θs[λ1_, λ2_] := 1 / 2 ArcTan[ (2 ms08[λ1, λ2]) / (ms00[m2, λ1, λ2] - ms88[m2, λ1, λ2]) ];
            sol =
              Simplify[Solve[mπ ^ 2 == m2 + λ1 (v0 ^ 2 + v8 ^ 2) + λ2 / 3 (v0 ^ 2 + 1 / 2 v8 ^ 2 + Sqrt[2] v0 v8) &&
                  mK ^ 2 == m2 + λ1 (v0 ^ 2 + v8 ^ 2) + λ2 / 3 (v0 ^ 2 + 7 / 2 v8 ^ 2 - 1 / Sqrt[2] v0 v8),
                  {λ2, m2}]];
            λ2 = λ2 /. sol[[1]];
            m2 = m2 /. sol[[1]];

            sol2 = Solve[
                mσ ^ 2 == ms00[m2, λ1, λ2] Cos[θs[λ1, λ2]] ^ 2 + ms88[m2, λ1, λ2] Sin[θs[λ1, λ2]] ^ 2 +
                  2 ms08[λ1, λ2] Cos[θs[λ1, λ2]] Sin[θs[λ1, λ2]], λ1];
            λ1 = λ1 /. sol2[[1]];

            u[x_, y_] :=
              m2 / 2 (x ^ 2 + y ^ 2) + λ1 / 2 x ^ 2 y ^ 2 + 1 / 8 (2 λ1 + λ2) x ^ 4 + 1 / 8 (2 λ1 + 2 λ2) y ^ 4 - hx x - hy y;
            dux[x_, y_] = D[u[x, y], x];
            duy[x_, y_] = D[u[x, y], y];
            solx = Simplify[Solve[dux[vx, vy] == 0, hx]];
            soly = Simplify[Solve[duy[vx, vy] == 0, hy]];
            hx = hx /. solx[[1]];
            hy = hy /. soly[[1]];

In[2293]:=  (*Three flavours - finding maximum value of B_vac*)
            Clear[μb];
```

```
n := 300;
k := 1;
μbmin := 860;
μbmax := 1500;
ϕx := Array[fx, n];
ϕy := Array[fy, n];
ερ := Array[EP, {n, 2}];

mq[x_] := g x / 2;
ms[y_] := g y / Sqrt[2];
μu := μb / 3 - 2 μe / 3;
μd := μb / 3 + μe / 3;
μs := μb / 3 + μe / 3;

B0[x_, y_] := u[x, y] + nc / (8 Pi^2)
     (mq[x]^4 (3 / 2 + Log[Λ^2 / mq[x]^2]) + ms[y]^4 (3 / 4 + 1 / 2 Log[Λ^2 / ms[y]^2]));
p[x_, y_] := nc / (24 Pi^2) (Sum[(Re[μ (2 μ^2 - 5 mq[x]^2) (μ^2 - mq[x]^2)^(1 / 2) +
          3 mq[x]^4 (Log[1 / mq[x] ((μ^2 - mq[x]^2)^(1 / 2) + μ)])]),
       {μ, {μu, μd}}] + Re[μs (2 μs^2 - 5 ms[y]^2) (μs^2 - ms[y]^2)^(1 / 2) +

          3 ms[y]^4 (Log[1 / ms[y] ((μs^2 - ms[y]^2)^(1 / 2) + μs)])]) + μe^4 / (12 Pi^2);
exy[x_, y_] := -p[x, y] + nc / (3 Pi^2) (Sum[μ Re[(μ^2 - mq[x]^2)^(3 / 2)], {μ, {μu, μd}}] +

          μs Re[(μs^2 - ms[y]^2)^(3 / 2)]) + μe^4 / (3 Pi^2);
ρB[x_, y_] := nc / (9 Pi^2) (Sum[Re[(μ^2 - mq[x]^2)^(3 / 2)], {μ, {μu, μd}}] +
       Re[(μs^2 - ms[y]^2)^(3 / 2)]);
V1[x_, y_] := -nc / (24 Pi^2)
     (Sum[μ (2 μ^2 - 5 mq[x]^2) (μ^2 - mq[x]^2)^(1 / 2) + 3 mq[x]^4
          (Log[1 / mq[x] ((μ^2 - mq[x]^2)^(1 / 2) + μ)] - 3 / 4 - 1 / 2 Log[Λ^2 / mq[x]^2]),
       {μ, {μu, μd}}] + μs (2 μs^2 - 5 ms[y]^2) (μs^2 - ms[y]^2)^(1 / 2) +
        3 ms[y]^4 (Log[1 / ms[y] ((μs^2 - ms[y]^2)^(1 / 2) + μs)] -

          3 / 4 - 1 / 2 Log[Λ^2 / ms[y]^2])) - μe^4 / (12 Pi^2);
V[x_, y_] := u[x, y] + V1[x, y];

ClearAll[μb, μe, x, y]
dVx[x_, y_] = Re[D[V[x, y], x]];
dVy[x_, y_] = Re[D[V[x, y], y]];

μb := μbmin;
While[k ≤ n, Clear[μe];
 solμxy = FindRoot[{dVx[x, y] == 0, dVy[x, y] == 0,
     2 * UnitStep[μb / 3 - 2 μe / 3 - mq[x]] ((μb / 3 - 2 μe / 3)^2 - mq[x]^2)^(3 / 2) -
       UnitStep[μb / 3 + μe / 3 - mq[x]] ((μb / 3 + μe / 3)^2 - mq[x]^2)^(3 / 2) - UnitStep[
          μb / 3 + μe / 3 - ms[y]] ((μb / 3 + μe / 3)^2 - ms[y]^2)^(3 / 2) - (μe^2)^(3 / 2) == 0},
    {{x, 90, 0.001, 250}, {y, 100, 0.001, 250}, {μe, μb / 10, 0, μb}},
    MaxIterations → 500, AccuracyGoal → 6, PrecisionGoal → 6];
 μe = Re[μe /. solμxy];
 fx[k] = Re[x /. solμxy];
 fy[k] = Re[y /. solμxy];
 EP[k, 1] = ((p[fx[k], fy[k]] - B0[fx[k], fy[k]] + B0[fx[1], fy[1]]))^(1 / 4);
 EP[k, 2] = (exy[fx[k], fy[k]] + p[fx[k], fy[k]]) / (ρB[fx[k], fy[k]]);
 μb += (μbmax - μbmin) / (n - 1); k += 1]
ερint = Interpolation[ερ];
FindRoot[ερint[s] == 930, {s, 50}]
```

Out[2318]= {s → 48.1607}

In[2319]:= (*Two flavours - finding minimum value of B_vac *)
ClearAll[μe, μb]
k = 1;
μbmin := 900;
μbmax := 2000;
m2 := 1 / 2 (3 mπ^2 - mσ^2);
λ := 3 * (mσ^2 - mπ^2) / fπ^2;
g := 3.2258;
nf := 2;
Λ := 182;
h := mπ^2 fπ;
μu := 1 / 3 μb - 2 / 3 μe;
μd := 1 / 3 μb + 1 / 3 μe;
ερ2 := Array[EP2, {n, 2}];
mq[v_] := g v;

B0[ϕ_] :=
  1 / 2 m2 ϕ^2 + λ / 24 ϕ^4 - h ϕ + nc nf / (16 Pi^2) mq[ϕ]^4 (3 / 2 + Log[Λ^2 / mq[ϕ]^2]);
p[v_] := nc / (24 Pi^2) Sum[(Re[μ (2 μ^2 - 5 mq[v]^2) (μ^2 - mq[v]^2)^(1 / 2) + 3 mq[v]^4

        Log[1 / mq[v] ((μ^2 - mq[v]^2)^(1 / 2) + μ)]]), {μ, {μu, μd}}] + (μe^4) / (12 Pi^2);

ev[v_] := -p[v] + nc / (3 Pi^2) Sum[μ Re[(μ^2 - mq[v]^2)^(3 / 2)], {μ, {μu, μd}}] +
    (μe^4) / (3 Pi^2);

ρB[v_] := nc / (9 Pi^2) Sum[Re[(μ^2 - mq[v]^2)^(3 / 2)], {μ, {μu, μd}}];
V0[v_] := (1 / 2 m2 v^2 + λ / 24 v^4 - h v);
V1[v_] := -nc / (24 Pi^2) Sum[μ (2 μ^2 - 5 mq[v]^2) (μ^2 - mq[v]^2)^(1 / 2) +
        3 mq[v]^4 (Log[1 / mq[v] ((μ^2 - mq[v]^2)^(1 / 2) + μ)] -

            3 / 4 - 1 / 2 Log[Λ^2 / mq[v]^2]), {μ, {μu, μd}}] - (μe^4) / (12 Pi^2);
cond = Limit[V1[v], v → 0];
V[v_] := V1[v] + V0[v] - cond;

ClearAll[μb, μe]
dV[v_] = Re[D[V[v], v]];

μb := μbmin;
While[k ≤ n, Clear[μe];
 solμv = Quiet[FindRoot[{dV[v] ⩵ 0, 2 * UnitStep[μu - mq[v]] (μu^2 - mq[v]^2)^(3 / 2) -
        UnitStep[μd - mq[v]] ((μd)^2 - mq[v]^2)^(3 / 2) - (μe^2)^(3 / 2) ⩵ 0},
     {{v, 90, 0.001, 250}, {μe, μb / 11, 0, μb}}]];
 f[k] = Re[v /. solμv];
 μe = Re[μe /. solμv];
 EP2[k, 1] = (p[f[k]] - B0[f[k]] + B0[f[1]])^(1 / 4);
 EP2[k, 2] = (ev[f[k]] + p[f[k]]) / ρB[f[k]];
 μb += (μbmax - μbmin) / (n - 1); k += 1]
ερint2 = Interpolation[ερ2];
FindRoot[ερint2[s] ⩵ 930, {s, 50}]

Out[2346]= {s → 27.1091}

In[2347]:= `(*Bag Window:*)`
`Print[(s /. FindRoot[ερint2[s] == 930, {s, 100}]) <`
`   B < (s /. FindRoot[ερint[s] == 930, {s, 100}])]`

27.1091 < B < 48.1607

```mathematica
In[207]:= Clear["Global`*"]
Needs["PlotLegends`"]
(*PARAMETER FITTING*)
r0 := 1.477;
α := 1 / (20 r0^3);
sunm := 1.9885*^30;
c := 2.99792458*^5;
ε :=  sunm c^2 α
     ───────────;
        4 Pi
ε0 := 4.79179*^-29 ε;
bmitmev := (40)^4;
mσ := 800;
nc := 3;
mquark := 300;
fπ := 93;
fK := 113;
mπ := 138;
mK := 496;
v0 := 1 / Sqrt[6] (fπ + 2 fK);
v8 := 2 / Sqrt[3] (fπ - fK);
vx := fπ;
vy := 1 / Sqrt[2] (2 fK - fπ);
g := 2 mquark / vx;

mq[x_] := g x / 2;
ms[y_] := g y / Sqrt[2];
VΛ[x_, y_] := (2 * 3 mq[x]^4 (+3 / 4 + 1 / 2 Log[Λ^2 / mq[x]^2]) +
    3 ms[y]^4 (+3 / 4 + 1 / 2 Log[Λ^2 / ms[y]^2]));
vDx[x_, y_] = D[VΛ[x, y], x];
vDy[x_, y_] = D[VΛ[x, y], y];
lambdax = Solve[vDx[vx, vy] == 0, Λ];
lambday = Solve[vDy[vx, vy] == 0, Λ];
Λx = Λ /. lambdax[[1]];
Λy = Λ /. lambday[[1]];
Λ = (2 Λx + Λy) / 3;

ms00[m2_, λ1_, λ2_] := m2 + λ1 (3 v0^2 + v8^2) + λ2 (v0^2 + v8^2);
ms88[m2_, λ1_, λ2_] := m2 + λ1 (v0^2 + 3 v8^2) + λ2 (v0^2 + 3 / 2 v8^2 - Sqrt[2] v0 v8);
ms08[λ1_, λ2_] := 2 λ1 v0 v8 + λ2 (2 v0 v8 - 1 / Sqrt[2] v8^2);
θs[λ1_, λ2_] := 1 / 2 ArcTan[         2 ms08[λ1, λ2]
                             ──────────────────────────────────────];
                             ms00[m2, λ1, λ2] - ms88[m2, λ1, λ2]
sol =
  Simplify[Solve[mπ^2 == m2 + λ1 (v0^2 + v8^2) + λ2 / 3 (v0^2 + 1 / 2 v8^2 + Sqrt[2] v0 v8) &&
      mK^2 == m2 + λ1 (v0^2 + v8^2) + λ2 / 3 (v0^2 + 7 / 2 v8^2 - 1 / Sqrt[2] v0 v8),
     {λ2, m2}]];
λ2 = λ2 /. sol[[1]];
m2 = m2 /. sol[[1]];

sol2 = Solve[
   mσ^2 == ms00[m2, λ1, λ2] Cos[θs[λ1, λ2]]^2 + ms88[m2, λ1, λ2] Sin[θs[λ1, λ2]]^2 +
     2 ms08[λ1, λ2] Cos[θs[λ1, λ2]] Sin[θs[λ1, λ2]], λ1];
λ1 = λ1 /. sol2[[1]];

u[x_, y_] :=
  m2 / 2 (x^2 + y^2) + λ1 / 2 x^2 y^2 + 1 / 8 (2 λ1 + λ2) x^4 + 1 / 8 (2 λ1 + 2 λ2) y^4 - hx x - hy y;
```

```
      dux[x_, y_] = D[u[x, y], x];
      duy[x_, y_] = D[u[x, y], y];
      solx = Simplify[Solve[dux[vx, vy] == 0, hx]];
      soly = Simplify[Solve[duy[vx, vy] == 0, hy]];
      hx = hx /. solx[[1]];
      hy = hy /. soly[[1]];
```

```
In[254]:= n := 500;
      k := 1;
      μbmin := 860;
      μbmax := 1800;

      ϕx := Array[fx, n];
      ϕy := Array[fy, n];
      ϵp := Array[E, {n, 2}];

      μu := μb / 3 - 2 μe / 3;
      μd := μb / 3 + μe / 3;
      μs := μb / 3 + μe / 3;

      B0[x_, y_] := u[x, y] / ϵ0 + nc / (8 ϵ0 Pi ^ 2)
          (mq[x] ^ 4 (3 / 2 + Log[Λ ^ 2 / mq[x] ^ 2]) + ms[y] ^ 4 (3 / 4 + 1 / 2 Log[Λ ^ 2 / ms[y] ^ 2]));

      p[x_, y_] :=
        nc / (24 ϵ0 Pi ^ 2) (Sum[(Re[μ (2 μ ^ 2 - 5 mq[x] ^ 2) (μ ^ 2 - mq[x] ^ 2) ^ (1 / 2) + 3 mq[x] ^ 4
                (Log[1 / mq[x] ((μ ^ 2 - mq[x] ^ 2) ^ (1 / 2) + μ)])]), {μ, {μu, μd}}] +
            Re[μs (2 μs ^ 2 - 5 ms[y] ^ 2) (μs ^ 2 - ms[y] ^ 2) ^ (1 / 2) + 3 ms[y] ^ 4

                (Log[1 / ms[y] ((μs ^ 2 - ms[y] ^ 2) ^ (1 / 2) + μs)])]) + μe ^ 4 / (12 ϵ0 Pi ^ 2);

      ϵxy[x_, y_] :=
        -p[x, y] + nc / (3 ϵ0 Pi ^ 2) (Sum[μ Re[(μ ^ 2 - mq[x] ^ 2) ^ (3 / 2)], {μ, {μu, μd}}] +
            μs Re[(μs ^ 2 - ms[y] ^ 2) ^ (3 / 2)]) + μe ^ 4 / (3 ϵ0 Pi ^ 2);

      V1[x_, y_] :=
        -nc / (24 Pi ^ 2) (Sum[μ (2 μ ^ 2 - 5 mq[x] ^ 2) (μ ^ 2 - mq[x] ^ 2) ^ (1 / 2) + 3 mq[x] ^ 4
                (Log[1 / mq[x] ((μ ^ 2 - mq[x] ^ 2) ^ (1 / 2) + μ)] - 3 / 4 - 1 / 2 Log[Λ ^ 2 / mq[x] ^ 2]),
            {μ, {μu, μd}}] + μs (2 μs ^ 2 - 5 ms[y] ^ 2) (μs ^ 2 - ms[y] ^ 2) ^ (1 / 2) +
            3 ms[y] ^ 4 (Log[1 / ms[y] ((μs ^ 2 - ms[y] ^ 2) ^ (1 / 2) + μs)] -
                3 / 4 - 1 / 2 Log[Λ ^ 2 / ms[y] ^ 2])) - μe ^ 4 / (12 Pi ^ 2);

      V[x_, y_] := u[x, y] + V1[x, y];

      ClearAll[μb, μe, x, y]
      dVx[x_, y_] = Re[D[V[x, y], x]];
      dVy[x_, y_] = Re[D[V[x, y], y]];


      μb := μbmin;

      bagvacuum := bmitmev / ϵ0;
      While[k ≤ n, Clear[μe];
       solμxy =
```

```
    Quiet[FindRoot[{dVx[x, y] == 0, dVy[x, y] == 0, 2 * UnitStep[μb / 3 - 2 μe / 3 - mq[x]]
            ((μb / 3 - 2 μe / 3) ^ 2 - mq[x] ^ 2) ^ (3 / 2) - UnitStep[μb / 3 + μe / 3 - mq[x]]
            ((μb / 3 + μe / 3) ^ 2 - mq[x] ^ 2) ^ (3 / 2) - UnitStep[μb / 3 + μe / 3 - ms[y]]
            ((μb / 3 + μe / 3) ^ 2 - ms[y] ^ 2) ^ (3 / 2) - (μe ^ 2) ^ (3 / 2) == 0},
        {{x, 90, 0.001, 250}, {y, 100, 0.001, 250}, {μe, μb / 11, 0, μb}}]];
  μe = Re[μe /. solμxy];
  fx[k] = Re[x /. solμxy];
  fy[k] = Re[y /. solμxy];
  E[k, 1] = p[fx[k], fy[k]] - B0[fx[k], fy[k]] + B0[fx[1], fy[1]] - bagvacuum;
  E[k, 2] = εxy[fx[k], fy[k]] + B0[fx[k], fy[k]] - B0[fx[1], fy[1]] + bagvacuum;
  μb += (μbmax - μbmin) / (n - 1); k += 1]
εint = Interpolation[εp];
pmin := E[1, 1];
pmax := E[n, 1];
```

In[278]:=
```
ShowLegend[Plot[{εint[p], 3 p + 4 * 156.654 ^ 4 / ε0}, {p, pmin, pmax}, PlotRange → All,
    Frame → True, PlotStyle → {{Thickness[0.004]}, {Dashed, Thickness[0.003]}},
    FrameLabel → {Text[Style["p/ε₀", FontSize → 16]],
      Text[Style["ε/ε₀", FontSize → 16]]}, FrameTicksStyle → Medium],
  {{{Graphics[{ColorData[1][1], Thickness[0.06], Line[{{0, 0}, {3, 0}}]}],
      Text[Style["EoS_QM", FontSize → 15]]},
    {Graphics[{ColorData[1][2], Thickness[0.035], Dashed, Line[{{0, 0}, {3, 0}}]}],
      Text[Style["EoS_MIT", FontSize → 15]]}},
    LegendPosition → {0.30, -0.3}, LegendSize → {0.45, 0.3}, LegendShadow → None}]
```

Out[278]=
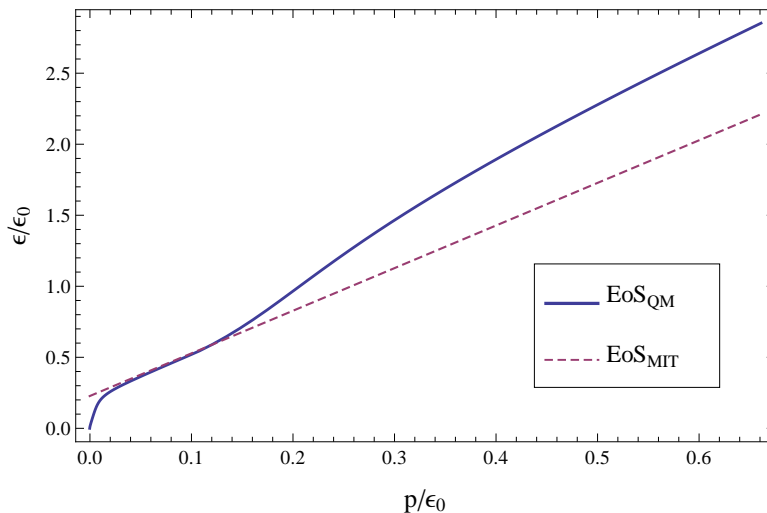
```
In[328]:= (* Solving the TOV equation with the obtained EoS *)
    ClearAll[pr, m, pc, r, bc, j]
    rmax := 50;
    n2 := 450;
    j := 1;
    massvec := Array[M, {n2, 2}];
    rvec := Array[Rv, {n2, 2}];
    er[r_] := With[{s = pr[r]}, ϵint[s]];

    diffeq[pc_] :=
     NDSolve[{pr'[r] == -UnitStep[-pr[r] + pmax] UnitStep[pr[r]] * r0 / r (pr[r] + er[r])
         (m[r] + α r^3 pr[r]) / (r - 2 r0 m[r]), m'[r] == α r^2 er[r], pr[10^-10] == pc,
        m[10^-10] == 10^-14}, {pr, m}, {r, 10^-12, rmax}, MaxSteps → 100 000]

    pressure[r_, pc_] := First[Re[pr[r] /. diffeq[pc]]];
    mass[r_, pc_] := First[Re[m[r] /. diffeq[pc]]];
    R[pc_] := Last[Last[FindRoot[pressure[r, pc], {r, .1, rmax}, Method → "Brent"]]];

    pcmin = 0.001;
    pcmax = pmax;
    pc = pcmin;

    While[j ≤ n2 / 3,
     Rv[j, 1] = pc;
     Rv[j, 2] = Quiet[R[pc]];
     M[j, 1] = pc;
     M[j, 2] = Quiet[mass[Rv[j, 2], pc]];
     pc += (pcmax - pcmin) / (9 n2); j++]
    While[j ≤ 2 n2 / 3,
     Rv[j, 1] = pc;
     Rv[j, 2] = Quiet[R[pc]];
     M[j, 1] = pc;
     M[j, 2] = Quiet[mass[Rv[j, 2], pc]];
     pc += (pcmax - pcmin) / n2; j++]
    While[j ≤ n2,
     Rv[j, 1] = pc;
     Rv[j, 2] = Quiet[R[pc]];
     M[j, 1] = pc;
     M[j, 2] = Quiet[mass[Rv[j, 2], pc]];
     pc += 17 (pcmax - pcmin) / (9 n2); j++]
    rint = Interpolation[rvec];
    mint = Interpolation[massvec];
    max = FindMaximum[{mint[x], pcmin < x < pcmax}, x];
```
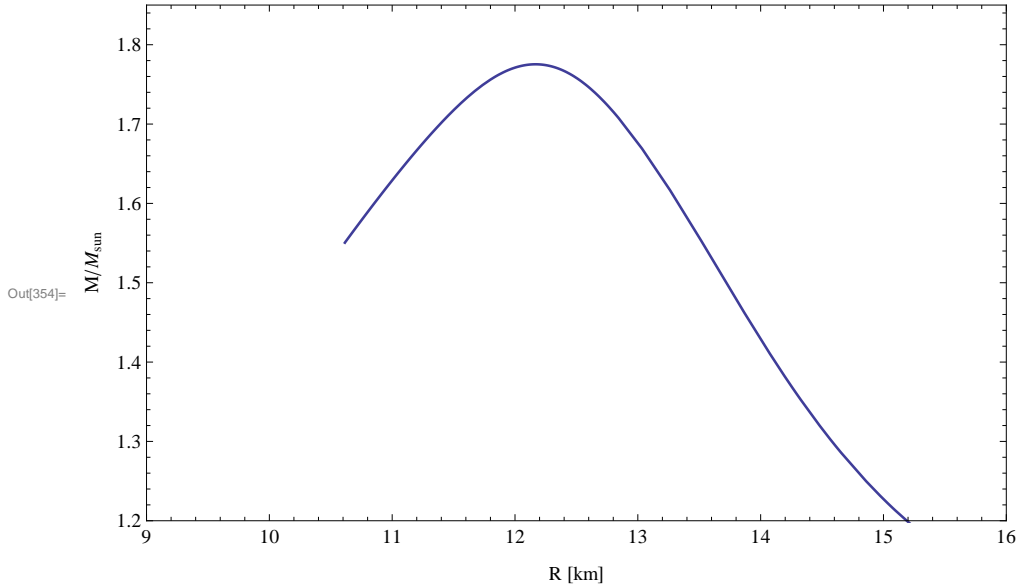
In[354]:= `ParametricPlot[{rint[pc], mint[pc]},`
`{pc, pcmin, pcmax}, PlotRange → {{9, 16}, {1.2, 1.85}},`
`AspectRatio → 0.6, PlotStyle → {Thickness[0.0030]}, FrameLabel →`
`{Text[Style["R [km]", FontSize → 12]], Text[Style["M/M`$_{sun}$`", FontSize → 12]]},`
`FrameTicksStyle → Medium, Frame → True]`
`Print["M`$_{maks}$` = " Text[max[[1]]], "  R = " Text[rint[x /. max[[2]]]]]`

Out[354]=

M_{maks} = 1.77535   R = 12.167

Bibliography

[1] A. Schmitt, *Dense matter in compact stars*. Lect. Notes Phys. 811, 1 (2010).

[2] J. Antoniadis et al., *A Massive Pulsar in a Compact Relativistic Binary*. Science, Vol. 340, Issue 6131 (2013).

[3] P. Demorest et al., *Shapiro delay measurement of a 2 solar mass neutron star*. Nature 467, 1081-1083 (2010).

[4] T. Klähn, R. Lastowiecki and D. Blaschke, *Implications of the measurement of pulsars with two solar masses for quark matter in compact stars and HIC. A NJL model case study*. [nucl-th/1307.6996] (2013).

[5] J. Wambach, *Neutron Star Matter*. [nucl-th/1307.6714] (2013).

[6] F. Weber and R. Negreiros, *QCD in neutron stars and strange stars*. [astro-ph/1101.5606] (2011).

[7] J. Myrheim, *Classical Theory of Fields*. Lect. Notes (2011).

[8] J. O. Andersen, *Introduction to Statistical Mechanics*. Akademisk forlag, 4th edition (2010).

[9] A. Zee, *Quantum Field Theory in a Nutshell*. Princeton University Press, 2nd edition (2010).

[10] J. I. Kapusta, *Finite-Temperature Field Theory Principles and Applications*. Cambridge University Press, 2nd edition (2006).

[11] C. M. Ho and R. J. Scherrer, *Anapole Dark Matter*. Phys. Lett. B 722, 341 (2013).

[12] A. Nieto, *Evaluating Sums Over the Matsubara Frequencies*. Comput. Phys. Commun. 92 54 (1995).

[13] S. Weinberg, *Gravitation and Cosmology*. John Wiley & Sons, Inc., 1st edition (1972).

[14] J. D. Walecka, *Introduction to General Relativity*. World Scientific Publishing Co. Pte. Ltd., 1st edition (2007).

[15] M. Kachelrieß, *Lecture Nots for FY3452 Gravitation and Cosmology*. (2013).

[16] Wolfram Mathematica 8, For Students

[17] M. A. Thomson, *Quantum Chromodynamics*. Lect. Notes in Particle Physics, (2009). `http://www.hep.phy.cam.ac.uk/~thomson/lectures/partIIIparticles/Handout8_2009.pdf`

[18] R. L. Delgado, C. Hidalgo-Duque, F. J. Llanes-Estrada, *To what extent is Gluon Confinement an empirial fact?*. [hep-ph/1106.2462] (2012).

[19] A. Chodos, R. L. Jaffe, K. Johnson, C. B. Thorn and V. F. Weisskopf, *New extended model of hadrons*. Phys. Rev. D 9, 3471 (1974).

[20] S. P. Adhya, P. K. Roy and A. K. Dutt-Mazumder, *Non-Fermi liquid correction to the neutrino mean free path and emissivity in neutron star beyond the leading order*. AIP Conf. Proc. 1524, pp. 263 (2013).

[21] C. Shen, U. Lombardo, N. Van Giai and W. Zuo, *Neutrino mean free path in neutron stars*. Phys. Rev. C 68 055802 (2003).

[22] N. K. Glendenning, *Compact Stars: Nuclear Physics, Particle Physics, and General Relativity*. Springer-Verlag New York, Inc., 2nd. edition (2000).

[23] A. R. Bodmer, *Collapsed Nuclei*. Phys. Rev. D 4, 1601 (1971).

[24] E. Witten, *Cosmic separation of phases*. Phys. Rev. D 30, 272 (1984).

[25] X.-D. Li, I. Bombaci, M. Dey, J. Dey and E. P. J. van den Heuvel, *Is SAX J1808.4-3658 A Strange Star?*. Phys. Rev. Lett. 83, 3776 (1999).

[26] F. Weber, *Strange Quark Matter and Compact Stars*. Porg. Part. Nucl. Phys. 54, 193 (2005).

[27] D. Gondek-Rosińska, W. Kluźniak and N. Stergioulas, *An unusually low mass of some "neutron" stars?*. [astro-ph/0206470] (2002).

[28] A. Bauswein et al., *Mass ejection by strange star mergers and observational implications*. Phys. Rev. Lett. 103, 011101 (2009)

[29] F. Weber, C. Schaab, M. K. Weigel and N. K. Glendenning, *Quark Matter, Massive Stars and Strange Planets*. [astro-ph/9604035] (1996).

[30] M. Gell-Mann and M. Lévy, *The Axial Vector Current in Beta Decay*. Nuovo Cim. 16 705 (1960).

[31] J. Beringer et al. (Particle Data Group), *Review of Particle Physics*. Phys. Rev. D 86, 010001 (2012).

[32] J. O. Andersen, R. Khan, *Chiral transition in a magnetic field and at finite baryon density*. Phys. Rev. D 85 065026 (2012).

[33] K. Fujii, H. Oike and T. Suzuki, *More on the Isomophism $SU(2) \otimes SU(2) \cong SO(4)$*. Int. J. Geom. Meth. Mod. Phys. 4, 471 (2007).

[34] J. Goldstone, A. Salam, S. Weinberg, *Broken Symmetries*. Phys. Rev. 127, 965 (1962).

[35] J. O. Andersen, R. Khan, L. T. Kyllingstad, *The chiral phase transition and the role of vacuum fluctuations*. [hep-ph/1102.2779] (2011).

[36] T. Maruyama et al., *Quantum Molecular Dynamics Approach to the Nuclear Matter Below the Saturation Density*. Phys. Rev. C 57, 655 (1998).

[37] B.-J. Schaefer and M. Wagner, *Three-flavour chiral phase structure in hot and dense QCD matter*. Phys. Rev. D 79, 014018 (2009).

[38] S. Gasiorowicz and D. A. Geffen, *Effective Lagrangians and Field Algebras with Chiral Symmetry*. Rev. Mod. Phys. 41, 531 (1969).

[39] J. T. Lenaghan, D. H. Rischke and J. Schaffner-Bielich, *Chiral Symmetry Restoration at Nonzero Temperature in the $SU(3)_r \times SU(3)_l$ Linear Sigma Model*. Phys. Rev. D 62, 085008 (2000).

[40] K. Schertler, S. Leupold and J. Schaffner-Bielich, *Neutron stars and quark phases in the NJL model*. Phys. Rev. C 60, 025801 (1999).